INVESTIGATION OF THE EFFECTS OF BIOFOULING ON THE HYDRAULIC PROPERTIES OF WELLS IN FRACTURED BEDROCK AQUIFERS

By

BRENDA ELIZABETH COOKE

A thesis submitted to the Department of Civil Engineering

in conformity with the requirements for

the degree of Master of Science (Engineering)

Queen's University

Kingston, Ontario, Canada

December, 2007

Abstract

The objective of this study is to improve the understanding of the effect of biofilm growth and biofouling on well performance in a fractured rock aquifer. The study was conducted by investigating biofouling in several recently drilled and much older wells. The study was conducted at three field sites using six groundwater wells in Perth, Portland and Cambridge Ontario. The well located in Perth was drilled in the spring of 2006 and after preliminary hydraulic testing; biofilm was grown in the well by the addition of nutrients (steel wool, Difco beef peptone and gelatin). The wells located in Portland and Cambridge are more than 10 years old and were already biofouled. In each case, the well was hydraulically tested using open- well pumping methods and via slug testing using a straddle packer system (1.7m spacing) in which measurements were obtained contiguously from the bottom to the top of the well. This provided distinct measurements of the hydraulic properties of the individual fracture zones along the length of each hole. The five older wells in Portland and Cambridge were cleaned following the initial testing using recirculation of hydrochloric acid followed by recirculation of 35% hydrogen peroxide. Once the cleaning was completed, the hydraulic testing was repeated. Each of the wells were videotaped using a downhole camera at various stages during the study. Samples were obtained on three occasions for bacterial typing using the BART™ system. Transmissivity data from the different states of fouling (drilled, fouled or cleaned) were compared and it was determined that fractures with low transmissivity values are more susceptible to the effects of biofouling than those with high transmissivity. The reduction in transmissivity was as much as 50% percent. Fractures with low transmissivity are of small apertures which are easily plugged by biofilm. The

cleaning process did not markedly improve total wellbore performance for those wells where a comparison was made following cleaning. The presence of any form of iron, (i.e. steel well casing or steel pump parts) in the well will contribute significantly to the biofouling, based on the results of the laboratory study.

Acknowledgements

A special thanks to John Miller, Valens Conservation Area and Bob Sneyd at the Center for Sustainable Watersheds for the use of their property and wells for this study.

A special thanks to McLelland Water Technology who provided the cleaning services at cost.

I would like to thank all those students who helped me throughout this project. Thanks to Titia Praamsma, Jana Levison, John Kozuskanich, Grace Yungwirth and Sean Speer who helped with field work and gave endless advice on completing this project. Thanks to those in Ellis 222 for all your help, advice and distractions when needed, especially Julie Burghart and Mike West.

Thank you to Matt Trousdale, Shawn Trimper for help in the field and keeping a smile on my face throughout all those hours of field work.

Thanks to Stan Prunster for all the help in the lab, for being there to bounce ideas back and forth and for helping to make those ideas reality.

Thanks to my advisor Kent Novakowski for helpful conversations, lots of guidance and visits to the field sites.

A great big thank you to my best friends Laura Knowles and Anna Larson for your endless encouragement, your support and for being my personal cheerleaders.

Thanks to my parents and family for their unyielding support, encouragement and advice throughout these past two years. I would not have been able to complete this without you!

Thank you to all who have been there throughout to answer questions, listen to complaints and frustrations, offering advice, distractions, support and encouragement.

Table of Contents

List of Tables

List of Figures

Chapter 1 : Introduction

Biofouling in groundwater wells is a practical problem that results in the degradation of well performance over time. Biofouling of a well occurs via the deposit of biofilm and calcium carbonate by bacteria along the wellbore and in the fractures, in a fractured rock aquifer (McLaughlan, 2002). In natural systems, such as porous and fractured rock aquifers, a large portion of resident bacteria live within biofilm environments which allow the bacteria to create a favorable environment to multiply (Klapper, 2004).

Biofilms are a collection of bacterial cells enclosed in a structured matrix of self secreted extracellular polymers attached to a surface, such as the wellbore (Costerton et al., 1995). Originally described as homogenous slabs of slime with randomly embedded bacterial cells, the understanding of the structure of biofilm has changed dramatically in recent years (Costerton et al., 1995; Stoodley et al., 2002). Biofilm structure is presently described as a series of complex structural support of the extracellular polymers secreted by the many different bacteria species contained in the bacterial microcolony (Costerton, 1995; de Beer et al., 1997; Costerton et al., 1999; Klapper, 2004). Water channels transport nutrients to the cells located deep within the biofilm, which would not be reached through diffusion, and remove waste products from these areas (Costerton et al., 1994).

Attachment of planktonic (free-floating) bacteria cells to a surface occurs in two stages: reversible attachment and irreversible attachment. Reversible attachment occurs where individual cells secret long, string-like polymers which weakly anchor the cell to the

surface (Costerton et al., 1995; Cullimore, 1999). Colonization of the surface occurs as the attached cells multiply and spread over the surface creating a conditioning film of minimal coverage allowing cells to detach from the surface (Characklis, 1990; Cullimore, 1999). Irreversible attachment occurs when the cells adhere and begin excreting extracellular polymeric substances, or exopolysaccharides (EPS) (Costerton et al., 1995). EPS is a long polymer chain made up of carbohydrates, proteins and lipids in long thread-like molecules that acts as the structural grid of the matrix (Wilderer and Characklis, 1989; Characklis, 1990; Costerton et al., 1995; Cullimore, 1999; Stoodley et al., 2002). EPS production creates permanent cellular attachment to the colonizing surface, overcoming even charge repulsion between the cells and substratum (Costerton et al., 1987; Characklis, 1990; Characklis et al., 1990; Becker et al., 2003). Once rigidly cemented to the surface, the EPS matrix is established, and the microcolony expands through cellular division and subsequent EPS production (Costerton et al., 1987; Stoodley et al., 2002).

Biofouling is the process whereby a natural or engineered process is affected by a biologically-produced substance (i.e. a bacterial community) (Mansuy et al., 1990; Cullimore, 1999; McLaughlan, 2002). The growth rate of biofouling is dependent on conditions such as available nutrients, temperature and pH (Cullimore, 1999).

Bacterial communities within the protective slime matrix are the most common form of well plugging, containing both organic and inorganic substances (McLaughlan, 2002). Other deleterious effects associated with biofouling include corrosion, gas generation,

bioaccumulation and biodegradation of equipment (Cullimore, 1999). The major effects of a biofouling deposit is measured in terms of the amount of plugging of both the aquifer and the pump components, corrosion of the pump components and changing the characteristics of water movement both to the well and inside the well (McLaughlan, 2002). Hindering of flow to a well is the main concern with biofouling (Cullimore, 1999; McLaughlan, 2002).

Biofilm growth in porous media influences porosity and pore geometry and thus the hydraulic conductivity and permeability (Shaw et al., 1985; Taylor and Jaffe, 1990; Taylor et al., 1990; Lappan and Folger, 1995). As a biofilm develops in porous media it is anchored on the particle grains and grows out into the pore throats (Kim and Folger, 2000). Through EPS production, the biofilm reduces and ultimately clogs the pore throats reducing permeability and flow paths by 10-30% (Kim and Folger, 2000). With the major flow paths sealed off the flow regime must change to paths with lower porosity and thus lower permeability (Ross and Bickerton, 2002). Sloughed off fragments of the biofilm are transported and can begin a new biofilm in an unaffected area or act as nutrients to attached cells in a nutrient poor area (Lappan and Folger, 1995).

The majority of the studies of biofilm in fractured rock have been conducted in the laboratory. The studies use fractures which were cut into a sample of rock or use two glass plates to simulate a fracture (Ross et al., 2001; Hill and Sleep, 2002; Ross and Bickerton 2002; Castegnier et al., 2006). These experiments show that it is possible to grow a biofilm to decrease the conductivity of the fracture. Higher hydraulic

conductivities in fractured rock aquifers compared to porous media cause biofilms to develop differently due to higher shear stresses of the passing fluid and due to transport differences (Ross et al., 2001).

How biofilm affects hydraulic characteristics of a well is not clearly understood. Hydraulic testing, including slug testing, constant head testing and pumping tests are conducted to determine the extent of the biofouling effect.

The overall objective of this study is to determine the influence of biofouling in a fractured bedrock aquifer. The specific purpose of this study is to improve our understanding of how bacteria-produced biofilm affects the hydraulic characteristics of fractures intersecting a well in a fractured rock aquifer. In this study we investigate how biofouling affects the surface of a well in a fractured bedrock aquifer, as well as determining whether the biofouling penetrates into fractures to a significant depth. Particular focus will be on determining the effect of fracture size on the degree of biofouling and whether biofilm growth into the fractures from nutrient addition in the wellbore is possible. Previously biofouled wells are investigated and one well is purposely biofouled.

A detailed literature review is presented in Chapter 2, the methodology and results are presented in Chapter 3, and general conclusions are presented in Chapter 4. The thesis is presented in manuscript format with Chapter 3 as the manuscript to be submitted to Hydrogeology Journal.

1.2 References

Castegnier, F., Ross, N., Chapuis, R. P., Deschenes, L., Samson, R., 2006, Long-Term Persistence of a Nutrient-Starved Biofilm in a Limestone Fracture, Water Research, (40):925-934

Costerton, J.W., Lewandowski, Z., Caldwell, D. E., Korber, D. R., Lappin-Scott, H. M. 1995. Microbial Biofilms, Annual Reviews of Microbiology. 49:711-745

Cullimore, R., 1999. Microbiology of Well Biofouling. Lewis Publishers. New York

Hill, D. D., Sleep, B. E., 2002, Effects of Biofilm Growth on Flow and Transport Through a Glass Parallel Plate Fracture, Journal of Contaminant Hydrology, 56:227-246

Kettles, I.M., 1992. Surficial geology, Perth, Ontario, Geological Survey of Canada, "A" Series Map, Report: 1800A.

Kim, D.-S., Fogler, H. S., 2000. Biomass Evolution in Porous Media and Its Effects on Permeability Under Starvation Conditions. Biotechnology and Bioengineering. 69(1): 47-56

Klapper, I., 2004. Effect of Heterogeneous Structure in Mechanically Unstressed Biofilms on Overall Growth. Bulletin of Mathematical Biology. 66:809-824

Lappan, R. E., Folger, H. S., 1995. Reduction of Porous Media Permeability from In Situ *Leuconostoc mesenteroides* Growth and Dextran Production. Biotechnology and Bioengineering. 50: 6-15.

McLaughlan, R., 2002. Managing Water Well Deterioration. International Contribution to Hydrogeologists. A.A. Balkema Publishers, LISSE

Reichart, T.M., 1992. Influence of Vertical Fractures in Horizontally Stratified Rock. Univeristy of Waterloo, Waterloo, Ontario

Ross, N., Villemur, R., Deschenes, L., Samson, R., 2001. Clogging of a Limestone Fracture by Stimulating Groundwater Microbes, Water Research, 35(8):2029-2037

Ross, N., Bickerton, G., 2002. Application of Biobarriers for Groundwater Containment at Fractured Bedrock Sites. Remediation 12(3): 5-21

Shaw, J. C., Bramhill, B., Wardlaw, N. C., Costerton, J. W., 1985. Bacterial Fouling in a Model Core System, Applied and Environmental Microbiology, 49(3): 693-701

Taylor, S. W., Milly, P. C. D., Jaffe, P. R., 1990. Biofilm Growth and the Related Changes in the Physical Properties of a Porous Medium 2) Permeability, Water Resources Research, 26(9):2126-2169

Taylor, S. W., Jaffe, P. R., 1990. Biofilm Growth and the Related Changes in the Physical Properties of a Porous Medium 1) Experimental Investigation, Water Resources Research, 26(9):2153-2159

Chapter 2 : Literature Review

Many studies have been completed on the topic of biofilm growth in porous media (e.g. Shaw et al., 1985; Cullimore, 1990; Kim and Fogler, 2000; Stewart and Folger, 2001) and the biofuling of water wells in porous aquifers (Cullimore, 1999). There are a limited number of studies on either topic for fractured bedrock setting (Ross et al., 2001; Hill and Sleep, 2002; Ross and Bickerton 2002; Castegnier et al., 2006). In the following chapter, the basis of biofilm growth, the impact in porous media and wells, and the potential impact in fractured media are reviewed.

Growth of biofilms in porous media begins by bacteria anchoring on the surface of grains (Kim and Folger, 2000; Taylor et al., 1990). Once anchored the bacteria begin producing extracellular polysaccharide matrix which progressively narrows the pore throats until some pore throats are completely clogged (Kim and Folger, 2000). In fractured bedrock the bacteria anchors to the rough surface of the fracture wall. As in porous media, the bacteria become anchored to the fracture surface and secrete the extracellular polysaccharide matrix, creating the biofilm. Hill and Sleep (2002) grew biofilm in a fracture made of two sand-blasted glass plates. The experiment showed that the bacterial biofilm initially attached to the fracture walls in discrete clusters and over time formed a continuous film (Hill and Sleep, 2002). This suggests the reduction of fracture aperture occurs almost uniformly over the whole footprint of the biofilm on the fracture wall, instead of cutting off the pathways. Multiple studies (Taylor and Jaffe, 1990; Hill and Sleep, 2002; Castegnier et al., 2006) have shown that biofilm development occurs close to the nutrient source, first cutting off the nutrient supply further down the flow path.

This could appear as an increase in the skin effect during hydraulic testing (see section 2.4.1). Regarding biofouled wells in porous media, Cullimore (1999) describes multiple examples. A main caution is that although dense growths may be seen in the wellbore the actual biofouling that causes the deterioration of the well performance is back in the porous media behind the well screen, and not visible (Cullimore, 1999). Examples from North Battlefield Saskatchewan, Montana, Atlantic Canada and Kneehill Alberta have been provided to demonstrate the deterioration of the water wells from bioclogging and the amelioration back towards the original productivity values (Cullimore, 1999).

2.1 Biofilms

A biofilm is defined as a collection of bacterial cells supported by a structured, hydrated, self-secreted extracellular polymer matrix which attaches to surfaces (Costerton et al., 1995; Costerton et al., 1999; Kim and Folger, 2000; Lewis, 2001; Klapper, 2004). The matrix creates a protected environment allowing the growth and survival of bacteria in hostile environments (Costerton et al., 1999). Biofilm growth rate is strongly influenced by exterior environmental factors such as the ratio of carbon, nitrogen, and phosphorus, temperature, redox potential and pH (Cullimore, 1999). Cell growth, biopolymer production and entrapment of cells and particles from the bulk fluid contribute to biofilm spreading and an increase in biofilm thickness (Characklis et al., 1990; Kim and Folger, 2000).

In the initial phase of biofilm growth the following processes take place: 1) the planktonic cells are distributed by flowing fluid, 2) the cells undergo binary division and

3) the planktonic cells are converted to attached cells (Stoodley et al., 2002). Planktonic cells are free floating bacteria present in the water flowing adjacent to a solid phase material (Prescott et al., 1999). A portion of the attached cells redistribute themselves on the solid phase material increasing the surface area of the biofilm. Next, binary division of cells occurs. As a cell divides, the daughter cells migrate away from the attached parent cell forming cell clusters (Stoodley et al., 2002). The third mechanism involves the conversion of planktonic cells to attached cells which increases the mass of the biofilm without the use of nutrients (Stoodley et al., 2002). Depending on the type of bacteria, the surface being colonized and the physical and chemical properties of the environment, one mechanism may dominate over the other at a given time (Stoodley et al., 2002).

Established biofilms are very difficult to remove completely by external means (Lewis, 2001). Erosion by flowing water continuously removes small particles off the surface of the biofilm mainly via shear stress (Rittmann, 1989). Sloughing may remove a larger patch of biologic material again by the shear stress imparted by flowing water (Rittmann, 1989; Kim and Folger, 2000).

2.1.1 Structure

Biofilms have a complex and varied structure due to fluid migration and bacterial content. Living biofilms have been shown to consist of a variable distribution of cells, extra cellular polymers, void spaces and water channels as seen in Figure 2-1 (Costerton et al., 1995). Biofilms were originally thought of as homogenous slabs of matrix material

with bacterial cells embedded randomly (Costerton et al., 1995; Stoodley et al., 2002). Currently biofilm structure is studied by the use of a scanning confocal laser microscope (SCLM) which enables the analysis of a biofilm in its natural living hydrated state (Costerton et al., 1995). Through the use of the SCLM, biofilms are now known to be complex structural networks with cell clusters, interstitial channels and voids filled with water contained within an exopolymer matrix (de Beer et al., 1997). Biofilms are not simply flat smooth layers of slime and bacterial cells, but may also contain mushroom like microcolonies growing out in to the bulk fluid (Costerton, 1995; Klapper, 2004). Contained within these microcolonies are very organized communities where many different species of bacteria co-exist and create exopolymeric substances (EPS) through cellular division and EPS production (Costerton et al., 1999). Production of the extracellular polymeric matrix largely determines the structure of the biofilm as it provides the structural support (Stoodley et al., 2002).

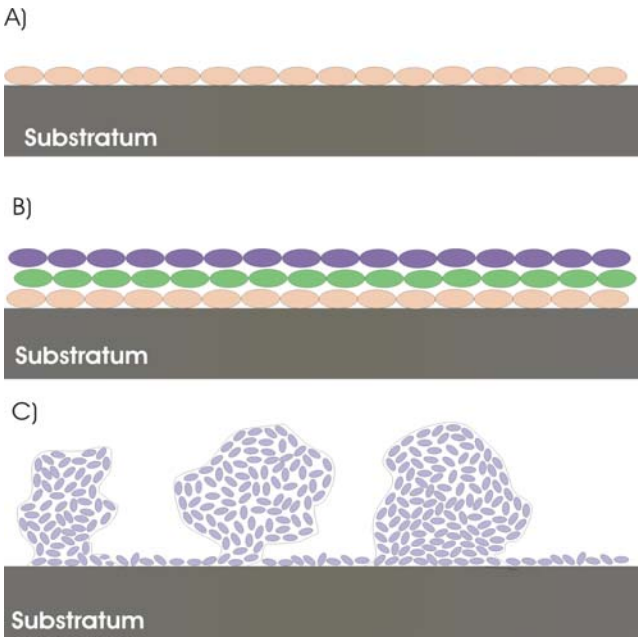

Figure 2-1: Three stages of the structure of biofilm. A) Single layer of attached cells. B) Multiple layers of bacteria cells attached to substratum. C) Complex communities of attached cells. Thicknesses of the layers in the biofilm are measured in micrometers, and can reach 400 µm. (Prescott et al. 1999).

The basic structure of a biofilm consists of the substratum, biofilm and bulk fluid. The substratum is the relatively impermeable, almost non-porous material, such as the walls of a fracture or a sand grain in an aquifer on which the bacteria colonize (Wilderer and Characklis, 1989). The biofilm consists of the extracellular polymer matrix and contained cells, water channels and voids. Lastly the bulk fluid is the groundwater that moves through the aquifer. A transitional area may be present between the biofilm and the bulk fluid, which is called the surface film, and is due to alternating water channels and microcolonies (Wilderer and Characklis, 1989; Klapper, 2004). In contrast, the uniform and densely structured base film has a distinct interface with the substratum (Wilderer and Characklis, 1989).

Water channels are common in all types of biofilms. A pure-culture biofilm contains a semi-regular grid of channels whereas the mixed species biofilm may have randomly placed channels (Costerton et al., 1995, Costerton et al., 1999). The water channels can be found anywhere from the biofilm-water interface to deep within the biofilm at the colonized surface (Costerton et al., 1995). An anastomosing network is often formed (Costerton et al., 1994; Costerton et al., 1995). These networks provide pathways allowing larger particles to reach the depths of the biofilm which they could not reach through diffusion. Water channels almost act as a primitive circulatory system to the cells within the biofilm, transporting nutrients to and removing waste from the cells (Costerton et al., 1994; Costerton et al., 1995). The exchange of nutrients between the cells and the water channels allows the biofilm to increase in thickness and complexity but still allows individual cells to remain within their optimal nutrient environment in any

location within the biofilm (Stoodley et al., 2002). de Beer et al. (1994) demonstrated that the water channels do increase the oxygen supply and the supply of other nutrients to bacteria in cell clusters within the biofilm relating the structure of the biofilm to the function. Water is directed into water channels where the nutrients and electron acceptors are delivered to the deep parts of the biofilm (Wilderer and Characklis, 1989; Stoodley et al., 2002). Although the water channels transport oxygen into the biofilm depths, the oxygen does not diffuse far into the matrix, explaining the anaerobic centers of the colonies (Costerton et al., 1994).

Some stratification can occur within the biofilm despite the water channels. An exposed aerobic layer can act as a protecting layer to the anaerobic layers underneath (Cullimore, 1999). These anaerobic layers produce hydrogen sulfide, organic acids and other organic products that overlying aerobic bacteria use as nutrients (Characklis et al., 1990; Cullimore, 1999). The matrix is typically composed of polysaccharides that are biologically produced by cells. The matrices are more densely concentrated around a colony of cells and less densely in the open spaces between colonies (Costerton et al., 1994).

2.1.2 Attachment to Surfaces

Since there are often many bacterial species within an aquifer it is important recognize that different bacteria attach differently to the substrata available (Characklis et al., 1990). Attachment of an organic film to the substratum in an aquifer occurs very quickly when cells are exposed to the substratum and change the wetting properties of the surface

(Characklis et al., 1990). With the large variety of species sometimes available within the groundwater, attached populations usually contain substantially more cells than the planktonic population in the surrounding fluid. The ability to attach to a solid surface within an aquifer varies from species to species (Costerton et al., 1994; Becker et al., 2003). Hydrophobicity of the cells surface and surface roughness are determining factors in cell attachment (Becker et al., 2003). A variety of surfaces available for colonization in an aquifer allows bacteria to colonize the most advantageous surface.

Bacterial cells transported adjacent to a rough surface have a greater chance of attachment. The cells sticking efficiency will be higher since the surface roughness creates sheltered spots from the main fluid flow where cells can attach (Wilderer and Characklis, 1989; Characklis et al., 1990).

At pH levels found in most natural systems, bacteria surfaces possess a net negative electrical charge creating a repulsion effect with a negative substratum surface, making it difficult to form even the weakest bonds to the substratum (Characklis et al., 1990; Becker et al., 2003). This charge repulsion is overcome by the extracellular proteins that can form strong enough bonds with the negative adsorption sites even though the proteins themselves have a net negative charge (Characklis et al., 1990).

The actual attachment of the bacteria occurs in two stages: reversible attachment and irreversible attachment. Reversible attachment occurs first with the individual cells excreting long, string-like polymers that connect with the substratum and weakly anchor

the cell to the surface (Costerton et al., 1995; Cullimore, 1999). As the cells begin to grow and multiply they colonize the substratum surface by rolling like a stone and spreading during reproduction, thus creating a conditioning film (Characklis et al., 1990; Cullimore, 1999). This conditioning film has minimal coverage of the surface but enables the cells to detach from the surface aided by external cell structures such as fimbriae to expand the colonization (Characklis et al., 1990). Once the bacteria adhere to the surface, the cells undergo a phenotypic change that encourages EPS synthesis (Costerton et al., 1995). Exopolysaccharide polymers initiate the irreversible adhesion of the cells to the surface of the substratum (Costerton et al., 1994). Irreversible adsorption is considered to be the permanent attachment of the cells to the substratum, usually done by extracellular polymers (Characklis et al., 1990). By producing extracellular substances the cells can overcome the charge repulsion by the substratum (Characklis et al., 1990; Becker at al., 2003). These interactions and bonding make the biofilm rigidly cemented to the surface of the substratum (Stoodley et al., 2002). Once the EPS matrix has been initiated, the bacteria cells begin to divide and multiply within the matrix, with the new cells also producing EPS, thus expanding the microcolony (Costerton et al., 1987). The main benefit of attaching to the substratum is that the bacteria can create microenvironments that are better suited to their survival (Characklis et al., 1990).

2.1.3 Extracellular Polymeric Substances

Extracellular polymeric substances, or exopolysaccharides, (EPS) put the film in biofilm. An exopolysaccharide is a long polymer chain produced by bacteria. The EPS of a microbial biofilm is made up of chemically diverse exopolysaccharides, proteins and

lipids consisting of long thin thread-like molecules to act as a grid structure which gives support to the bacteria cells (Wilderer and Characklis, 1989; Characklis et al., 1990; Costerton et al, 1995; Cullimore, 1999; Stoodley et al., 2002). With the crosslink bonding and hydration of biopolymers the strength of the biofilm will increase (Kim and Folger, 2000).

Indigenous microbial populations usually contain some EPS producers or contain species that have developed a switch to turn on EPS production in the right environment (Ross et al., 1998; Jefferson, 2004). The EPS production is driven by the common nutrient glucose which appears to be the substrate for EPS production (Jefferson, 2004). EPS is produced by the attached bacteria cells during initial population growth or under stressful conditions from nutrient deficiency or other external stresses (Cullimore, 1999).

Besides being just a protective layer the EPS aids in energy conservation by storing cellular energy within the network and concentrated nutrients from the bulk liquid to be used by the cells (Costerton et al., 1995; Cullimore, 1999; Characklis et al., 1990). As the EPS is produced by the bacteria it is concentrated near the cells and sparser farther away (Characklis et al., 1990).

2.1.4 Growth Curve

Bacteria growth within a biofilm is substantially different than planktonic bacteria growth (Costerton et al., 1995). Biofilm accumulation typically takes the form of a sigmoidal curve (Characklis et al., 1990). This curve represents the growth of the microorganisms

and can be divided into four phases: the lag phase, log or exponential phase, stationary phase, and death phase (Prescott et al., 1999). This is shown schematically in Figure 2-2 (Prescott et al., 1999).

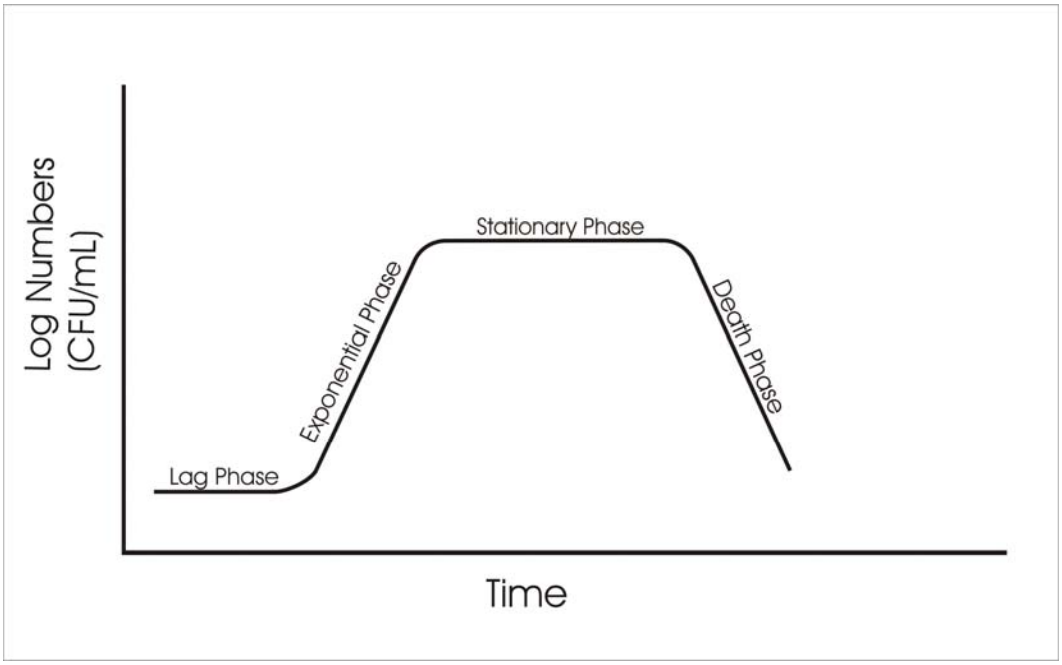

Figure 2-2: Typical bacterial growth curve in a closed system (modified from Prescott et al. 1999). The time scale is dependant on environmental conditions and bacteria type.

The lag phase is characterized by the lack of bacterial activity due to the bacterial adjustments required to adapt to the new environment and nutrients (Chappelle, 2001; Prescott et al., 1999). There is no increase in bacteria cell population, since no cell division is taking place as the bacteria determine how to process the new nutrients (Prescott et al., 1999).

Once the bacteria have adapted to the new nutrients they multiply at a rapid rate, increasing the population at the maximum rate possible in the log or exponential phase (Prescott, 1999; Chappelle, 2001).

As the nutrients begin to dwindle and the waste products begin to accumulate, the population stabilizes either as the growth rate equals the death rate or because the cells simply stop dividing and shift focus to survival limited by scarce nutrients (Prescott et al., 1999; Chapelle, 2001). The constant population with a horizontal growth curve is characteristic of the stationary phase (Chapelle, 2001).

Toxic wastes build up from metabolic activity and the population begins to die off entering the death phase of the growth curve (Prescott et al., 1999). The death phase may not be present in all growth curves, since it depends on limited nutrients. The cell population usually follows a logarithmic trend, as a certain fraction of cells perish in every time interval (Prescott et al., 1999). This can change however near the end of the death phase once the population has drastically decreased and the curve may be extended due to the survival of a few extra resistant cells (Prescott et al., 1999).

2.1.5 Growth in Fractured Rock Aquifers

The dominant microbial presence in groundwater aquifers is bacterial (Cullimore, 1990). Generally in the nutrient-poor environment that most fractured rock aquifers provide, the bacteria are predominantly dormant ultramicro-bacteria floating in the water or in EPS enclosed biofilms attached to the fracture walls (Costerton et al., 1995). Microbacteria are very small bacteria cells, 0.1-0.5 microns in size, are under starvation or environmental stress, and are transported in the bulk fluid phase (Cullimore, 1999). As ultramicrobacteria in the planktonic state, bacteria can survive a long time with very little

nutrients due to their dormancy. This planktonic mode is mostly for dissemination and persistence of the population in unfavorable environments (Costerton et al., 1995). During a decrease in nutrients the biofilms release ultramicro cells, a miniature version of themselves, to allow the population to re-establish when nutrients become available again (Characklis et al., 1990). The miniature cells have decreased metabolic activity that allows the cells to survive in a dormant state (Characklis et al., 1990). Once the planktonic cells are transported to a more favorable environment they are attracted to the organic nutrients concentrated on the surface of the fractures and attach to those surfaces (Costerton et al., 1995). This nutrient population relationship can be seen in Figure 2-3. Once attached with EPS, the bacteria multiply and increase in population creating a biofilm (Costerton et al., 1995).

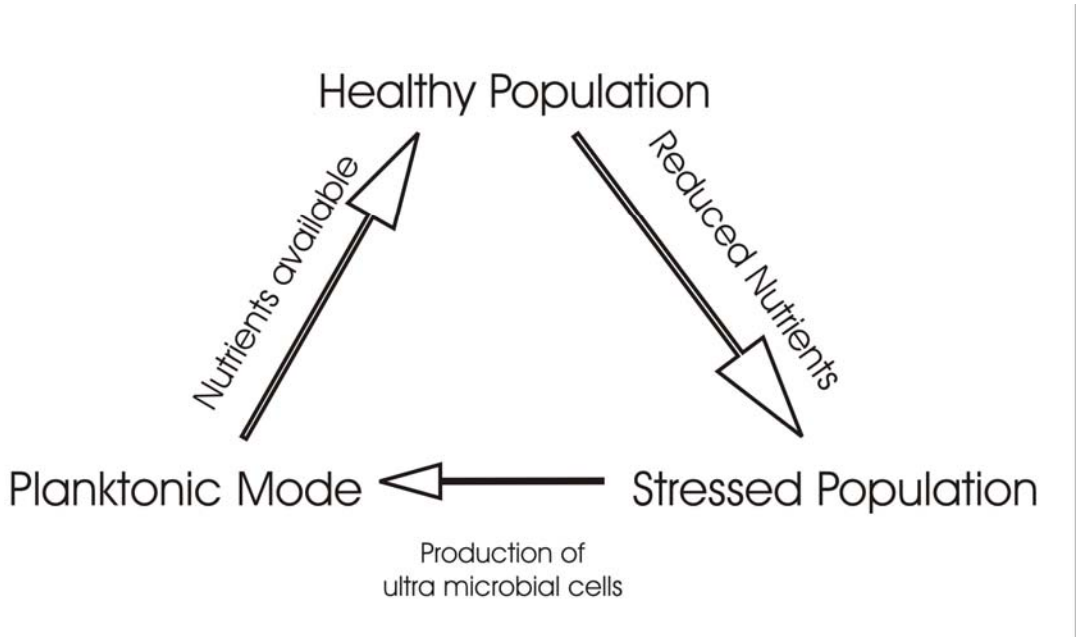

Figure 2-3: Relationship between available nutrients and the population of bacteria.

Groundwater temperature remains fairly constant throughout the year thus bacteria have adapted to survive within a narrow temperature range (Cullimore, 1990).

2.2 Biofouling

Biofouling is the effect of a biologically produced substance on a natural or engineered process (Cullimore, 1999). Although biofouling is not normally a health risk, effects include the plugging, corrosion, gas generation, bioaccumulation, biodegeneration and modifying the characteristics of water retention and water movement in an aquifer or pipes (Cullimore, 1999).

2.2.1 Microbial Processes in the Subsurface

The bacteria in the biofilm obtain soluble and particulate chemicals from the water flowing past by diffusion through the matrix (Cullimore, 1999; Klapper, 2004). These extracted chemicals are grouped into two categories: nutrients and bioaccumulates (Cullimore, 1995). Cell growth and reproduction use the electron donors, whereas the bioaccumulates build in the matrix of the biofilm and are not used by the cells (Cullimore, 1999). Bioaccumulates include non- degradable organics and metal ions, such as iron, manganese, aluminum, copper and zinc which prevent attack from scavenging microorganisms (Cullimore, 1999).

2.2.2 Microbial Resistance

Microbial resistance is the ability of the biofilm to withstand the effects of an elevated amount of an antimicrobial agent (Lewis, 2001). The mechanism for biofilm bacteria resistance to planktonic treatments remains unclear; the spatial distribution of cells at different physiological and metabolic states may be the integral factor guaranteeing survival under adverse conditions that the treatment causes (Costerton et al., 1995). Eng

et al. (1991) demonstrated that cells in the rapid growth stage were almost completely killed off by antimicrobial agents whereas the bacteria in the stationary phase were affected less by the agents (Costerton et al., 1995).

The 'resistance' of a biofilm is reported as the ability of the cells not to be killed in the presence of the antimicrobial agent (Lewis, 2001). Although not well understood, invulnerability to antimicrobial agents is thought to be due to specific characteristics of the biofilm such as slow growth, restricted penetration of antimicrobials into the biofilm and physiologic heterogeneity (Lewis, 2001; Jefferson, 2004).

Restricted penetration of the antimicrobial agents is due to the limited diffusion of the agents through the matrix (Costerton et al., 1999; Lewis, 2001). The EPS matrix also has the ability to bind antimicrobials within it thus preventing the agents from reaching the cells (Costerton et al., 1995; Lewis, 2001). EPS also allows different kinds of bacteria to grow in close proximity to each other, such as aerobic bacteria near the surface of the film and anaerobic bacteria deep within the film which increases the likelihood that some, but not all of the bacteria will be killed by the antimicrobial agents (Costerton et al., 1995). Within this stratified environment the bacteria are also present at many phases of development, including rapid growth and slower growth rates.

A decreased growth rate is generally due to nutrient limitation, which is common in many biofilms due to slow nutrient diffusion rates through the matrix (Costerton et al., 1999). With some cells growing at a slower rate, and antimicrobial agents generally killing

rapidly growing cells, some bacteria present in the biofilm will not be killed and can re-establish the population once the antimicrobial agents are gone (Costerton et al., 1999; Lewis, 2001). Thus, bacteria enclosed in a biofilm are protected from a decrease in available nutrients, changes in pH, fluctuations in oxygen levels and high levels of antimicrobial agents, all increasing their survival rate (Jefferson, 2004).

2.3 Well Fouling and Performance Degradation

2.3.1 Fouling

The fouling of a well occurs due to the creation of deposits in the well of particulate matter, mineral scale or biological deposits that lead to a decline in well performance (Sheikholeslami, 1999; McLaughlan, 2002). Types of fouling are often caused by changes in the well environment, for example, from an increase in flow through the aquifer, to chemical changes in the water, to the introduction of bacteria. Particulate fouling is caused by a change in the flow within the aquifer that allows fine sized particles to be transported from the aquifer to the well screen and deposited in the well (Characklis, 1981; McLaughlan, 2002). Mineral scale deposits result from chemical precipitation of minerals or scales due to changes in the groundwater chemistry (McLaughlan, 2002). Biofouling occurs when bacterial processes play a role in forming the deposit (Cullimore, 1999; McLaughlan, 2002).

2.3.1.1 Particulate Fouling

Particulate fouling occurs due to the transportation of assorted detrius from the aquifer into the well (Characklis, 1981; McLaughlan, 2002). The fouling involves an accumulation of fine particles close to the well that cause a reduction in aquifer porosity

(Sheikholeslami, 1999; McLaughlan, 2002). If the flow is constant, fines will be deposited into the wellbore and can cause pump corrosion or plugging (McLaughlan, 2002).

2.3.1.2 Mineral Scaling

Mineral scaling is caused by a number of factors but mostly the mixing of incompatible waters, or changes in groundwater temperature or pressure due to pumping (McLaughlan, 2002). A well can access different water chemistries in the different geological units the well passes through. The different waters mix within the borehole from the different geological units and if these waters are incompatible, a precipitate will form upon mixing and form a deposit on any available surface. An example of this would be carbonate rich water mixing with calcium rich water to precipitate calcium carbonate on the walls of the well (McLaughlan, 2002).

Mineral scales can also form due to a redox or pH change in the water (Mansuy et al., 1990; McLaughlan, 2002). Some chemical species that precipitate easily when redox changes occur in water include Fe^{3+}, Al^{3+}, S^{2-}, CO_3^{2-}, SO_4^{2-}, Ca^{2+}, and OH^- (hydroxide ions) (McLaughlan, 2002). When low pH waters are mixed with higher pH waters the solubility of some elements decreases and precipitate. Examples of this phenomenon are Fe^{2+} and Al^{3+}, which are more soluble in waters with low pH (McLaughlan, 2002). When water containing these ions mixes with waters of higher pH both ions precipitate out of solution (McLaughlan, 2002). The most common elements to precipitate during pH changes are iron and manganese, which are also the elements that are most prevalent in biofouling deposits (McLaughlan, 2002).

2.3.1.3 Biofouling

Biofouling occurs due to the presence of a biofilm-producing bacterial community and is the most common form of well plugging (Mansuy et al., 1990; McLaughlan, 2002). A biofilm, as described previously, contains both bacterial cells as well as inorganic concentrates that have been extracted from the adjacent water (McLaughlan, 2002). The inorganic components can be actively concentrated by organisms that use them for growth or passively concentrated in the EPS from the water (Mansuy et al., 1990; McLaughlan, 2002). How quickly the biofilm deposit accumulates is dependent on bacterial activity, availability of nutrient and inorganic particles in the water and the shear forces on the biofilm from the water (Cullimore, 1999; McLaughlan, 2002). The major effects of a biofouling deposit is measured in terms of the amount of plugging of both the aquifer and the pump components, corrosion of the pump components and changing the characteristics of water movement both to the well and inside the well (McLaughlan, 2002). It is the hindering of water flow to the well that is the main concern with the most common types of biofouling (Cullimore, 1999; McLaughlan, 2002).

If a well suddenly appears to become biofouled after a previously clean history, it is likely that iron bacteria have been introduced into the well (McLaughlan, 2002). It is not that the well has suddenly been fouled, only that the fouling has not been apparent until this point. The biofouling becomes apparent when there is a change in the well environment that encourages bacterial growth (McLaughlan, 2002). Many of the chemical reactions that take place in a well are controlled by bacteria (McLaughlan, 2002). Commonly it is not practical to try to determine if the conversion of aqueous iron

(Fe^{2+}) to the precipitated form of iron (Fe^{3+}) is abiotic or microbial since the bacteria responsible for this conversion usually live in the same environment where this conversion would naturally occur (McLaughlan, 2002).

The extent of biofouling in a specific system can be predicted with the metabolic activity of the bacteria and the availability of nutrients in the system (Costerton et al., 1995). When bacteria are metabolically active they can attach to a surface more easily especially wild cells in natural systems (Costerton et al., 1995). The amount of nutrient available controls both the growth rate of the population and the rate of EPS production thus controls the amount of biofilm accumulating on a surface (Costerton et al., 1995). The three most common bacteria groups associated with biofouling deposits are iron-related bacteria, slime-producing bacteria and sulfur-related bacteria (Mansuy et al. 1990). Iron related bacteria are nuisance bacteria that are associated with large deposits of iron and manganese oxide (Mansuy et al. 1990). Many iron-related bacteria also fit into the slime forming bacteria group that are commonly found in aquifers. Slime-forming bacteria produce copious amounts of EPS that increases the size of the biomass and holds chemical precipitates form by other bacteria (Mansuy et al. 1990). Sulfur-related bacteria are the anaerobic bacteria that usually live beneath the iron-related and slime-forming bacteria in an anaerobic layer. These bacteria are hard to detect by sampling the well water.

A new well installed in a fractured rock aquifer increases the oxygen content, increases the quantity of nutrients, and creates more rapid, more turbulent groundwater flow

(Cullimore, 1999). Oxygen diffuses from the oxygen-rich water standing in the well to the oxygen poor water in the aquifer. In contrast, the nutrients flow from the aquifer into the well, causing a diffusion front moving in the opposite direction. Where these two diffusion fronts meet, the greatest amount of microbial activity occurs (Cullimore, 1999).

2.4 Well Performance

Well performance is maximized by regular maintenance of all the components of the well (Dricoll, 1986). The performance of a well is usually determined after drilling by means of a pumping test to establish the maximum pumping rate the well can supply. This establishes a reference mark that later tests can be compared to in order to determine if some rehabilitation is necessary (Dricoll, 1986). Pumping tests are performed to obtain overall characteristics of the tested well, such as overall transmissivity and yield. Slug testing is performed to obtain a more detailed description of the vertical distribution of hydraulic characteristics. In the following section, a brief description of the standard methods for conducting and interpreting pumping and slug tests in fractured bedrock aquifers, is presented.

2.4.1 Pumping Tests

Pumping tests are frequently used to acquire the hydraulic properties of a well and aquifer including the specific capacity, the transmissivity, and the storativity (Dricoll, 1986; Silin and Tsang, 2002; Assaad et al., 2004). A pumping test is performed on a developed well occasionally with observation wells present at various distances to record the drawdown data during the test (Dricoll, 1986). Observation wells are used since

measuring drawdown accurately in the pumping well is often difficult due to turbulence generated by the pump (Dricoll, 1986).

A pumping test consists of pumping one well at a constant rate for a certain length of time with drawdown measurements taken periodically in the observation and pumping wells. The discharge rate is measured from the pumping well on a continuing basis (Dricoll, 1986; Clement et al., 1997; Silin and Tsang, 2002; Assaad et al., 2004). After pumping, drawdown recovery is measured as the water level in the well returns to pre-pumping levels (Dricoll, 1986; Goode, 1997; Assaad et al., 2004). The recovery allows for another set of data to check against the pumping results against since recovery curves are an inverted image of the drawdown curve (Assaad et al., 2004). The drawdown data are analyzed by plotting drawdown against time on a log-log scale from which transmissivity and storativity of the formation near the well can be determined (Dricoll, 1986; Gernand and Heidtman, 1997; Clement et al., 1997; Silin and Tsang, 2002). With these parameters known the performance of the aquifer and subsequently the well can be predicted for different pumping conditions (Dricoll, 1986).

A pumping test is also used to measure the specific capacity of a well which is then used as a measure of well yield (Assaad et al., 2004). The specific capacity is measured after the water level has stabilized under the pumping conditions and is expressed as liters per minute per meter of drawdown (Assaad et al., 2004).

Many fractured rock settings contain laterally extensive high permeability pathways that are usually horizontal fractures or bedding planes (Novakowski 1990). These fractures and fracture zones control the bulk permeability of the rock mass, being substantially higher than the conductivity of the rock matrix, especially in crystalline rock (Doe et al., 1987; Novakowski 1990). Fractured rock is a low-storativity media where the volume of water released from wellbore storage is much greater than the volume of water released from the formation due to storage during pumping (Earlougher, 1977; Dricoll, 1986; Kuchuk and Kabir, 1988; Novakowski, 1989; Silin and Tsang, 2002). This low storativity can be attributed to the fact that compression of both the matrix and fractures contribute only a minimal amount of water to ground water flow (Novakowski, 1990).

Wellbore storage effects pumping tests at early time and is detected by a unit slope on a log-log plot of drawdown with respect to time (Earlougher, 1977; Novakowski, 1990). Thus the appearance of a near unit slope on a plot will not give any information about the formation characteristics at all since the water is being pumped primarily from the well (Earlougher, 1977). Water begins to flow into the well from the surrounding formation as the water level in the wellbore falls (Dricoll, 1986). Over time the percentage yield coming from the aquifer increases (Earlougher, 1977; Dricoll, 1986). Wellbore storage effects will last longer in a large diameter well with low specific capacities than in a small diameter well with the same specific capacity (Dricoll, 1986). As the aquifer contributes more and more, the drawdown begins to plot below the line of unit slope and approach the curve of zero wellbore storage (Earlougher, 1977). If, however, the Theis curve is used to interpret the results and the linear slope portion is ignored, transmissivity

will be underestimated and storativity will be over estimated (Earlougher 1977; Novakowski, 1990).

Wellbore skin is defined as a region of altered hydraulic conductivity adjacent to the wellbore compared to the bulk aquifer (Chakrabarty and Enachescu, 1997; Yang and Gates, 1997; Henebry and Robbins, 2000; Silin and Tsang, 2002). This alteration may occur during drilling of the well and results in either a decrease or increase in hydraulic conductivity of this zone (Yang and Gates, 1997; Henebry and Robbins, 2000). During drilling in fractured rock aquifers the drilling mud or rock flour can penetrate fractures, clogging them (Novakowski, 1989; Novakowski, 1990).

The clogging of fractures by drilling mud or rock flour produces a region of lower permeability around the well, compared to the formation which is called a positive skin (Novakowski, 1990; Chakrabarty and Enachescu, 1997; Yang and Gates, 1997; Young, 1998). The reduction in permeability in the skin region is the most common of skin types (Novakowski, 1989). The effects of positive skin are reduced specific capacity values, lower transmissivity estimates and head losses which cause drawdown to be higher in the well than in the formation (Chakrabarty and Enachescu, 1997; Young, 1998).

Since the thickness of the disturbed region can be from millimeters to meters in scale, it must be considered when analyzing pumping tests as a separate region of flow connected with the radial flow in the formation (Novakowski, 1989). Skin effects can alter the magnitude of the calculated conductivity values of the formation from both pumping and

slug tests due to the reaction of the skin region varying from that of the formation (Henebry and Robbins, 2000).

Positive skin creates head losses and altered radial flow patterns during pumping tests and can produce significant errors in the analysis of a pumping test if they are not identified (Young, 1998). In the analysis of a pumping test conducted with a wellbore skin, the time versus dimensionless head type curves by Cooper et al (1967) are shifted horizontally depending on the conductivity of the skin although this shifting can lead to an inaccurate value of hydraulic conductivity of the formation (Yang and Gates, 1997).

In a fractured rock setting, a biofilm on the fracture walls would decrease the aperture of the fractures and thus decrease the permeability (Ross et al., 2001; Hill and Sleep, 2002; Ross and Bickerton 2002; Castegnier et al., 2006). If a well is biofouled with a large majority of the fractures intersecting the well clogged with biofilm, pumping test data would indicate a positive skin effect. To differentiate between biological and non-biological skin effects bacterial sampling of the well should be performed. If high concentrations of bacteria are present, the well has been developed properly, and has not shown skin effects before, the effect is probably caused by biofouling.

2.5 Characterization of the Hydraulic Properties of Fractured Rock

Detailed characterization of groundwater flow systems in fractured rock is usually conducted by isolating contiguous sections of the borehole that penetrated the aquifer. This is done to identify and characterize the specific fractures or fracture zones that

dominate the aquifer system. Pumping tests are not used for this process, as they are designed to integrate the measurement of hydraulic properties over the entire well depth. Rather smaller – scale tests are conducted using the methods described in the following section.

2.5.1. Straddle Packer Systems

Hydraulic testing in fractured rock is conducted using equipment to isolate an interval of the well thus reducing wellbore storage effects (Renard, 2005). Inflatable or mechanical packers are used to isolate the zone (Renard, 2005). Straddle packer systems consist of two packers separated by a perforated pipe. The section between the packers is the interval to be tested. Interference tests, pumping tests (rarely), constant head tests and slug tests can all be conducted using a packer system (Renard, 2005). These tests can be used to test a single section of the well, or can be used to test the entire length of the well in contiguous sections, thus obtaining a detailed profile of hydraulic characteristics of the well with respect to depth.

Constant head injection testing is often used to measure the transmissivity distribution in low conductivity media, such as fractured bedrock (Chang and Chen, 2002; Cardenas and Zlotnik, 2002; Novakowski 2002). This method of testing is most often used in highly variable media, such as fractured rock because of the wide range of detectable transmissivities, typically from 10^{-10} to $10^{-3}m^2/s$ (Novakowski, 2002). A hose is connected to a valve at the top of the packer system which is then connected to the constant head tank system at the surface. The hose ensures a closed system, since there is no free water surface, which essentially eliminates wellbore storage (Doe et al., 1987).

During the test, a constant head is maintained in the isolated interval with the injection rate recorded as a function of time (Mishra and Guyonnet, 1992; Nastev et al., 2000; Neville and Markle 2002). Interpretation is conducted using the flowrate measured at steady conditions and the values of the rise in hydraulic head induced by the injected fluid.

Slug tests can also be conducted using straddle packers to isolate an interval. With standpipe connected to the top of the packers leading to the surface, wellbore storage is used as an advantage (Doe et al., 1987). The test is conducted by the instantaneous addition or removal of a known volume of water and by observing the subsequent recovery of the water level with time (Papadopulos et al., 1973; Wylie and Magnuson, 1995; Chakrabarty and Enachescu, 1997; Clement et al., 1997; Novakowski and Bickerton, 1997; Assaad et al., 2004). By monitoring the response to this pressure increase in the isolated section, with the use of a pressure transducer, the hydraulic characteristics such as the storativity and transmissivity of the section can be calculated. This method has a narrower range of measurement, usually limited to a transmissivity between 10^{-7} to 10^{-3} m^2/s.

2.6 Summary

Indigenous bacteria have the ability, with increased nutrients added to the system, to produce a biofilm that can reduce the permeability of fractures in a well located in a fractured bedrock aquifer. Through hydraulic testing of the well, including pumping tests, slug tests and constant head injection tests, the hydraulic characteristics of the

aquifer can be determined. Pumping test and slug test data are susceptible to wellbore storage effects as well as positive skin effects which should be identified before well characteristics are calculated. Constant-head injection-testing can be affected by skin effects although since this type of testing is a closed system, wellbore storage is minimized. Biofouling of fractures in a well will show signs of positive skin effects, thus bacterial testing of the well is important. Biofilm growth in a fracture will occur close to the nutrient source, potentially cutting off nutrient supply to colonies further along the fracture and concentrating the biofilm near the wellbore fracture intersection.

Chapter 2 contains a detailed summary of biofilm properties and mechanisms, biofouling processes and hydraulic testing methods that can potentially detect biofouling in wells in fractured bedrock aquifers from current literature. Chapter 3 uses this information to conduct laboratory experiments and field hydraulic testing to determine how biofouling affects wells in a fractured bedrock aquifer.

2.5 References

Assaad, F., LaMoreaux, P. E., Hughes, T. H.(ed.), 2004. Field Methods for Geologists and Hydrogeologists, Springer, Berlin

Becker, M. W., Metge, D. W., Collins, S. A., Shapiro, A. M., Harvey, R. W., 2003. Bacterial Transport Experiments in Fractured Crystalline Bedrock, Ground Water, 41(5): 682-689

Cardenas, M.B., Zlotnik, V.A., 2002. A Simple Constant-Head Injection Test for Streambed Hydraulic Conductivity Estimation, GROUNDWATER, 41(6):

Castegnier, F., Ross, N., Chapuis, R. P., Deschenes, L., Samson, R., 2006, Long-Term Persistence of a Nutrient-Starved Biofilm in a Limestone Fracture, Water Research, (40):925-934

Chakrabarty, C., Enachescu, C., 1997. Using the Deconvolution Approach for Slug Test Analysis: Theory and Application, Ground Water, 35(5):

Chang, C.-C., Chen, C.-S., 2002. Field Experiment and Data Analysis of a Constant-Head Injection Test with Skin Effects in a Low-Transmissivity Aquifer, TAO, 13(1):15-38

Chappelle, F. H., 2000. Groundwater Microbiology and Geochemistry, 2nd ed, John Wiley and Sons, Inc. New York

Characklis, W. G., 1981. Bioengineering Report: Fouling Biofilm Development: A Process Analysis, Biotechnology and Bioengineering, 23:1923-1960

Characklis, W. G., Marshal, K. C., McFeters, G. A., 1990. The Microbial Cell, In: Biofilms, eds. Characklis, W.G., Marshall, K.G. John Wiley & Sons, Inc., Toronto

Characklis, W. G., McFeters, G. A., Marshal, K. C., 1990. Physiological Ecology in Biofilm Systems. In: Biofilms, eds. Characklis, W.G., Marshall, K.G., John Wiley & Sons, Inc. Toronto. 341-394

Clement, T. P., Truex, M. J., Hooker, B. S., 1997. Two-Well Test Method for Determining Hydraulic Properties of Aquifers. GROUNDWATER. 35(4)

Cooper, Jr., H.H., Bredehoeft, J.D., Papadopulos, I.S., 1967. Response of a Finite Diameter Well to an Instantaneous Charge of Water, Water Resources Research, 3(1):263-269

Costerton, J. W., Cheng, K.-J., Geesey, G. G., Ladd, T. I., Nickel, J. C., Dasgupta, M., Marrie, T. J., 1987. Bacterial Biofilms in Nature and Disease, Annual Reviews of Microbiology, 41:435-464

Costerton, J.W., Lewandowski, Z., DeBeer, D., Caldwell, D., Korber, D., James, G., 1994. Minireview: Biofilms, the Customized Microniche. Journal of Bacteriology 176(8):2137-2142

Costerton, J. W., Lewandowski, Z., Caldwell, D. E., Korber, D. R., Lappin-Scott, H. M., 1995. Microbial Biofilms, Annual Reviews of Microbiology 49:711-745

Costerton, J. W., Stewart, P. S, Greenberg, E. P., 1999. Bacteria Biofilms: A Common Cause of Persistent Infections. Science 284:1318-1322

Cullimore, D. R., 1990. An Evaluation of the Risk of Microbial Clogging and Corrosion in Boreholes, In: Water Wells, Monitoring, Maintenance, Rehabilitation, ed. Howsam, P., E.&F.N. Spoon, London

Cullimore, R., 1999. Microbiology of Well Biofouling, Lewis Publishers, New York

de Beer, D., Stoodley, P., Lewandowski, Z., 1997. Measurement of Local Diffusion Coefficients in Biofilms by Microinjection and Confocal Microscopy, Biotechnology and Bioengineering, 53:151-158

Doe, T., Oanes, J., Kanrick, M., Celar, J., Warner, S., 1987. Design of Well Testing Programs for Waste Disposal in Crystalline Rock, In: 6th Congress of the International Society for Rock Mechanics, Montreal Canada

Dricoll, F. G., 1986. Groundwater and Wells, 2nd ed., Johnson Filtration Systems Inc., St. Paul

Earlougher Jr., R. C., 1977. Advances in Well Test Analysis, Society of Petroleum Engineers of AIME, New York

Goode, D. J., 1997. Composite Recovery Type Curves in Normalized Time from Theis' Exact Solution, GROUNDWATER, 35(4)

Henebry, B. J., Robbins, G. A., 2000. Reducing the Influence of Skin Effects on Hydraulic Conductivity Determinations in Multilevel Samplers Installed with Direct Push Methods, Groundwater, 38(6)

Hill, D. D., Sleep, B. E., 2002, Effects of Biofilm Growth on Flow and Transport Through a Glass Parallel Plate Fracture, Journal of Contaminant Hydrology, 56:227-246

Jefferson, K. K., 2004. What drives bacteria to produce a biofilm? FEMS Microbiology Letters 236:163-173

Kim, D.-S., Fogler, H. S., 2000. Biomass Evolution in Porous Media and Its Effects on Permeability Under Starvation Conditions. Biotechnology and Bioengineering. 69(1): 47-56.

Klapper, I. 2004. Effect of Heterogeneous Structure in Mechanically unstressed Biofilms on Overall Growth. Bulletin of Mathematical Biology 66: 809-824

Kuchuk, F. J.; Kabir, S., 1988. Well Test Interpretation for Reservoirs with a Single Linear No-Flow Barrier, Journal of Petroleum Science and Engineering, 1:195-221

Lapcevic P. A., Novakowski, K. S., Sudicky, E. A., 1999. The Handbook of Groundwater Engineering, Delleur, Jacques W. (ed) Boca Raton, CRC Press

Lewis, K., 2001. Minireview of Riddle of Biofilm Resistance, Antimicrobial Agents and Chemotherapy, 45(4):999-1007

Mansuy, N., Nuzman, C., Cullimore, D. R., 1990. Well Problem Identification and Its Importance in Well Rehabilitation, In: Water Wells, Monitoring, Maintenance, Rehabilitation, ed. Howsam, P., E.&F.N. Spoon, London

McLaughlan, R., 2002. Managing Water Well Deterioration, International Contribution to Hydrogeologists, Vol. 22, A.A. Balkema Publishers, LISSE

Mishra, S., Guyonnet, D., 1992. Analysis of Observation-Well Response During Constant-Head Testing, GROUNDWATER, 30(4)

Nastev, M., Lapcevic, P., Girard, F., Etienne, M., Voralec, J., Savard, M.M., 2000. Hydraulic Characterization of Fractured Aquifers of St. Lawrence Lowlands in Southwestern Quebec, Proceedings of the 1st Joint IAH-CNC and CGS Groundwater Specialty Conference, Montreal, 53rd Conadian Geotechnical Conference, pp33-39

Neville, C. J., Markle, J. M, 2002. Interpretation of Constant-Head Tests: Rigorous and Approximate Analysis, Proceedings of the 1st Joint IAH-CNC and CGS Groundwater Specialty Conference, Montreal, 53rd Conadian Geotechnical Conference, pp359-366

Novakowski, K. S., 1989. A Composite Analytical Model for Analysis of Pumping Tests Affected by Well Bore Storage and Finite Thickness Skin, Water Resources Research, 25(9)

Novakowski, K. S., 1990. Analysis of Aquifer Tests Conducted in Fractured Rock: A Review of the Physical Background and the Design of a Computer Program for Generating Type Curves, Ground Water, 28(1)

Novakowski, K. S., 2002. Use of the Thiem Equation to Interpret Constant Head Tests Conducted in Boreholes, Technical Note, Water Resources Research

Novakowski, K. S., Bickerton, G. S., 1997. Borehole Measurement of the hydraulic properties of low permeability rock, Water Resources Research, 33(11)

Novakowski, K. S., Lapcevic, P., Oxtobee, J., Zanini, L., 2000. Groundwater Flow in the Lockport Formation Underlying the Smithville, Ontario Area, Proceedings of the 1st Joint IAH-CNC and CGS Groundwater Specialty Conference, Montreal, 53rd Conadian Geotechnical Conference, pp 49-54

Papadopulos, S. S., Bredehoeft J. D., Cooper H. H. Jr., 1973. On the Analysis of 'Slug Test' Data, Water Resources Research, 9(4):1087-1089

Peres, A. M. M, Onur, M., Reynolds, A.C., 1989. A New Analysis Procedure for Determining Aquifer Properties from Slug Test Data, Water Resources Research, 25(7):1591-1602

Prescott, L. M., Harley, J. P, Klein, D. A., 1999 Microbiology, 4th ed., McGraw-Hill, Boston

Renard, P., 2005. Chapter 151: Hydraulics of Wells and Well Testing, In: Encyclopedia of Hydrological Sciences, eds. Anderson, M. G., John Wiley & Son, Ltd

Rittmann, B. E., 1989. Detachment from Biofilms, In: Structure and Function of Biofilms, eds. Characklis, W. G., Wilderer P. A., John Wiley & Sons, Chichester

Rorabaugh, M. I., 1953. Graphical and Theoretical Analysis of Step-Drawdown Test of Artesian Well, Proceedings, American Society of Civil Engineers, 79

Ross, N., Bickerton, G., 2002. Application of Biobarriers for Groundwater Containment at Fractured Bedrock Sites, REMEDIATION

Ross, N., Villmeur, R., Dechenes, L., Samson, R., 2001. Clogging of a Limestone Fracture by Stimulating Groundwater Microbes, Water Research, 35(8):2029-2037

Shaw, J.C., Bramhill, B., Wardlaw, N.C., Costerton, J.W., 1985. Bacterial Fouling in a model core system, Applied Environmental Microbiology, 49:693-701

Sheikholeslami, R., Composite Fouling – Inorganic and Biological: A Review, Environmental Progress, 18(2):113-122

Silin, D. B., Tsang, C.-F., 2002. Estimation of Formation Hydraulic Properties Accounting for Pre-Test Injection or Production Operations, Journal of Hydrology, 265

Stewart, T.L., Folger, H.S., 2001. Biomass Plug Development and Propagation in Porous Media, Biotechnology and Bioengineering, 71(3)

Stoodley, P., Sauer, K., Davies, D. G., Costerton, J. W., 2002. Biofilms as Complex Differentiated Communities, Annual Review of Microbiology, 56:187-209

Taylor, S. W., Milly, P. C. D., Jaffe, P. R., 1990. Biofilm Growth and the Related Changes in the Physical Properties of a Porous Media 2) Permeability, Water Resources Research, 26(9):2126-2169

Taylor, S. W., Jaffe, P. R., 1990. Biofilm Growth and the Related Changes in the Physical Properties of a Porous Medium 1) Experimental Investigation, Water Resources Research, 26(9):2153-2159

Theis, C.V., 1935. The Lowering of the piezometric surface and the rate and discharge of a well using ground-water storage, Trans Am Geophys Union, 16:519-524

Walton, W. C., 1963. Efficiency of Wells, Mimeographed report of the Illinois State Water Survey Division, Urbana, Illinois

Wilderer, P. A., Characklis, W. G., 1989. Structure and Function of Biofilms, In: Structure and Function of Biofilms, eds. Characklis, W. G., Wilderer P. A., John Wiley & Sons, Chichester

Wylie, A., Magnuson, S., 1995. Spreadsheet Modeling of Slug Tests Using the van der Kamp Method, Ground Water, 33(2):326-329

Yang, Y. J., Gates, T. M., 1997. Wellbore Skin Effect in Slug-Test Data Analysis for Low- Permeability Geologic Materials, GROUNDWATER, 35(6)

Young, S. C., 1998. Impacts of Positive Skin Effects on Borehole Flowmeter Tests in a Heterogeneous Granular Aquifer, Ground Water, 36(1):67-75

Chapter 3 : Field Study

3.1 Introduction

In many aquifers, domestic well performance declines over time as a result of the accumulation of particulate matter, mineral scale deposits or biological deposits (Sheikholeslami, 1999; McLaughlan, 2002). In most settings, biofouling is the most prevalent process (Cullimore, 1999). Biofouling occurs through the development of biofilms which form through the growth of indigenous bacteria on the aquifer, well screen and pumping equipment (Cullimore, 1999; McLaughlan, 2002).

A biofilm is a collection of bacterial cells supported by a structured, hydrated, self-secreted, extracellular, polymer matrix that attaches to surfaces (Costerton et al., 1995; Costerton et al., 1999; Kim and Folger, 2000; Lewis, 2001; Klapper, 2004). Planktonic bacterial cells floating in the bulk fluid become attracted to the substratum surface and reversibly attach themselves to the rough surface (Costerton et al., 1995; Cullimore, 1999). The attachment becomes irreversible when the bacteria begin to produce exopolysaccharide polymers (EPS) that adhere to the surface and the bacteria become permanently attached (Characklis et al., 1990; Costerton et al., 1994). This is the beginning of biofilm growth. Once irreversible attachment occurs, the bacteria cells multiply and expand the biofilm.

Many studies have been completed on biofilm growth in porous media (e.g., Shaw et al 1985; Cullimore 1990; Taylor and Jaffe, 1990; Taylor et al., 1990; Lappan and Folger,

1995; Kim and Fogler 2000; Stewart and Folger 2001). These studies have shown that porous media cores can be plugged with bacteria through the injection of nutrients, such as combinations of glucose and fructose, phosphate-buffered saline solution with yeast extract, saccharose and black strap molasses, thus allowing the bacteria to grow and produce extracellular polymeric substances (EPS) that narrow and plug pore throats and channels. With the narrowing of pore throats and channels, the permeability of the samples can be reduced up to 3 orders of magnitude.

Biofilms have also been grown in fractures in a lab setting (e.g. Ross et al. 2001; Hill and Sleep 2002; Castegnier et al., 2006). Ross et al. (2001) demonstrated that in a fracture cut into limestone slabs, the hydraulic conductivity of the fracture was reduced by two orders of magnitude by the growth of bacteria from groundwater samples. Castegnier et al. (2006) also used a fracture cut into a limestone sample and again the hydraulic conductivity of the fracture was reduced by the growth of bacteria and the subsequent production of EPS. How biofilm growth might influence the hydraulic characteristics of a well intersecting a variety of fractures having different aperture width is poorly understood.

Biofilm thickness is not constant and varies considerably over a substratum (Characklis et al., 1990). Biofilm thickness has been measured between 10 and 1000 μm. Cunningham et al. (1991) measured biofilm thicknesses of 14, 40 and 63 μm in a laboratory experiment of biofilm growth in a variety of sand grain sizes. Bishop et al. (1995) measured biofilm thicknesses ranging between 52 and 1710 μm. The overall thickness

can vary as a result of variation in the thickness of different layers, from 300-400 μm each, which compose the biofilm (Characklis et al., 1990).

Fracture aperture also varies depending on the bedrock type. Raven (1986) measured fracture apertures in a fractured monzonite gneiss that ranged from 13 to 900 μm in four different fracture zones. Milloy (2007) measured fracture aperture ranging from 280 to 1120 μm in a granitic gneiss. Limestones and dolostones are known to have larger fracture aperture, particularly bedding plane fractures. Novakowski et al. (2006) determined a range of fracture aperture from 109 to >1500 μm in dolostones of the Lockport formation in southern Ontario. Conversely, Lapcevic et al. (1999) measured a range of 85 to 282 μm apertures in an Ordovician shale formation. Clearly, biofilm growth has the capacity to reduce, if not plug, many fractures in ideal conditions.

Well-performance is usually determined post-drilling by means of a pumping test to establish the maximum pumping rate that a well can sustain. This establishes a reference point that subsequent tests can be compared to in order to determine if well-rehabilitation is needed (Driscoll, 1986). Pumping tests conducted in a low-storativity medium, such as a fractured rock aquifer, are subject to wellbore storage effects and skin (Novakowski, 1989). Wellbore storage effects occur as a result of the greater volume of water released from the wellbore relative to that released from storage in the formation during initial pumping (Earlougher, 1977; Dricoll, 1986; Kuchuk and Kabir, 1988; Novakowski, 1989; Silin and Tsang, 2002). Wellbore storage effects can be identified as a linear slope on a log-log plot of drawdown with respect to time, in early time (Earlougher, 1977;

Novakowski, 1990). The portion of the graph with linear slope will not give any information about the characteristics of the well (Earlougher, 1977). As wellbore storage effects begin to diminish, the drawdown will follow a more typical Theis- like behaviour (Earlougher, 1977). If wellbore storage effects are ignored when compared to the Theis type curve, transmissivity will be underestimated and storativity will be overestimated (Theis, 1935; Earlougher, 1977; Novakowski, 1989; Moench, 1997).

A positive skin, the most common of wellbore skin types, is usually caused by the invasion of drilling rock flour, rock chips or drilling mud into the formation resulting in a zone surrounding the well having a lower permeability than the remainder of the formation (Novakowski, 1990; Chakrabarty and Enachescu, 1997; Yang and Gates, 1997; Young, 1998). Reduced specific capacity values, lower transmissivity estimates and head losses causing drawdown to be greater in the wellbore than in the formation are the common effects of a positive skin (Chakrabarty and Enachescu, 1997; Young, 1998). The presence of a biofilm could appear as a skin effect since the biofilm would only penetrate a short distance into the fracture before the reduced conductivity would limit the amount of nutrients available further along the fracture (i.e. Hill and Sleep, 2002).

For wells in fractured rock aquifers, more detailed testing can be conducted to identify the dominant fracture features (Renard, 2005). Inflatable packers separated by a perforated pipe are used to isolate contiguous intervals along the length of the well in order to obtain a more detailed profile of the hydraulic characteristics with respect to depth. The interval located between the packers is hydraulically tested using either

constant head injection methods (Chang and Chen, 2002; Cardenas and Zlotnik, 2002; Novakowski 2002) or a slug testing method (Papdopulous et al., 1973; Doe et al., 1987). Constant head injection testing can detect a range of transmissivities, from 10^{-10} to 10^{-3} m^2/s, and is often used in highly variable media such as fractured rock (Novakowski, 2002). Slug tests are limited to a narrower range of transmissivity, typically between 10^{-7} to 10^{-3} m^2/s.

The objective of the present study is to investigate the effect of biofouling on wells completed in typical sedimentary and crystalline rock terrain. More specifically, whether the biofilm penetrates into the fracture system is explored. The influence of the fracture aperture is also investigated using detailed hydraulic measurements. The study is conducted in fractured rock environments at three sites in Ontario. A comparison of hydraulic tests performed in several different stages of biofilm development in a total of six different wells was conducted. The three stages compared include freshly drilled (thus no biofilm), post-fouling, (with naturally-occurring biofilm present) and post commercial cleaning, which potentially removes all biofilm.

3.2 Methodology

The study was conducted in existing and new wells completed in bedrock aquifers located in the Cambridge, Perth and Portland areas of Ontario. The study sites are variously underlain by Silurian dolostone (Cambridge), granite gneiss (Perth) and a combination of Paleozoic and Precambrian rock (Portland). In order to assess the impact

of biofouling, each of the wells used in this study was characterized in detail, rehabilitated and re-characterized.

3.2.1 Wells

The Perth field site is located in a hay field in the Tay River Watershed in eastern Ontario. Located in the Frontenac Terrain of the central metasedimentary belt of the Grenville Province of the Precambrian Shield, the gently rolling topography is composed of less than two meters of well drained, glacial till derived from the granitic bedrock below (Kettles, 1992). The underlying bedrock is a Precambrian syenite-migmatite with abundant outcrop (Wilson, 1961). Rural farms and residential homes obtain water from the crystalline gneissic aquifer.

A new well, TW8, was drilled at the Perth site using air rotary percussion to a depth of 42 m with a 0.15 meters diameter. No overburden was present as the well was located directly on bedrock outcrop. The casing is 0.61 meters long, grouted with cement and topped with bentonite clay. Drilling chips were collected approximately every 3 meters for lithological identification. During drilling, approximate locations of fractures that produced a significant amount of water were noted, to later be compared to downhole video and hydraulic testing data. The well was located adjacent to an existing multi-level monitoring well of similar total depth (13 m away).

The Cambridge site is located in a 200 hectare conservation area, and has generally flat lying stratigraphy, which is forested with some grassy fields. A discontinuous till overburden varies in thickness from half a meter to two meters in depth (Reichart, 1992).

The bedrock consists of a layered sedimentary sequence of dolostone, sandstone and shales of Ordovician and Silurian age. The Guelph and Amabel submembers of the Middle Silurian Lockport dolostone comprise the bedrock in which the wells are completed (Reichart, 1992). The groundwater flow is primarily through bedding plane parting fractures, although sparse discontinuous vertical fractures with widely varying spacing are also present. The rural township of Puslinch draws its groundwater from this aquifer. Nine wells, of which three were used (MW7, MW8 and MW9) are located in the 200 ha property, and were drilled using NQ diamond drilling methods (Reichart, 1992). The three wells used are vertical in orientation and vary in depth from 25-30 m. The wells were initially tested using constant head methods following completion of drilling. A packer spacing of 1.6 m was used. Distance between the wells is given in Figure 3-1.

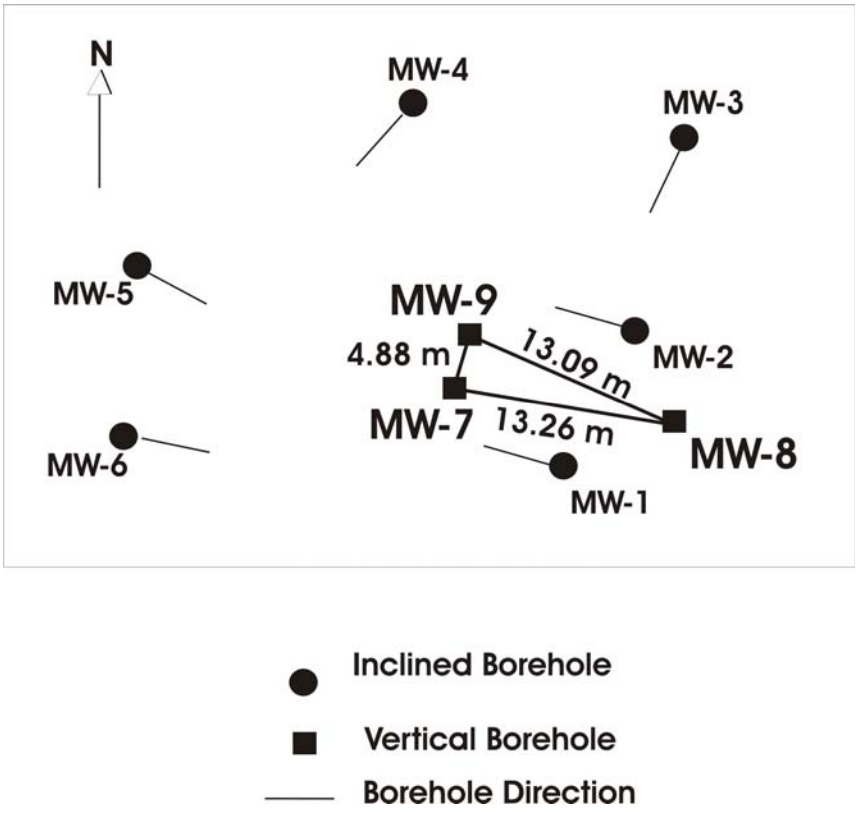

Figure 3-1: Schematic of well locations in Cambridge, On. (Reichart, 1992).

Portland Ontario is a rural residential community located on the shores of Rideau Lake. Depth of till overburden varies greatly throughout the town, from less than 1m to >10 m in areas transitioning through a boulder layer to the sandstone bedrock. The March and Nepean Formation sandstones unconformibly overlay Precambrian crystalline basement rocks at this location (Greggs and Gorman, 1976). Intrusions of marble are also found throughout the area (Greggs and Gorman, 1976). The Precambrian basement consists of granite gneisses, quartzite and quartzofeldspathic gneiss. Bedding plane fractures dominate the sandstones whereas the crystalline basement rock is sparsely fractured. Domestic water use is primarily from the bedrock aquifer.

Two water wells, WWFS and WWCH, located in the center of the town were used for this study. Each well is 0.15 meters in diameter with depths of 49 m and 43 m respectively. The wells were used in a heat pump configuration for a few years, but were then abandoned and left open. Distance between the wells is 33.5 m.

3.2.2 Well Characterization

In order to assess the impact of biofouling on the wells, pumping tests were performed on all six. The duration and flowrate of these tests depended on the yield of the well, which was estimated from previous data. Short term pumping tests varied between six and eight hours whereas the longer term pumping tests were conducted over 24 hours. Recovery data were also collected over 1-3 hours following cessation of pumping in each case. The purpose of the pumping tests was to investigate skin effects and provide a performance measure.

Short term pumping tests were conducted at both the Portland and Cambridge sites. Due to the proximity of residential wells in Portland, the pumping rate and duration of pumping were limited. Calculations prior to testing restrained the pumping rate to 15 L/minute using a 0.05 meter diameter stainless steel submersible pump. The duration of the two pumping tests were 6 hours for the fouled condition and 8 hours following cleaning. For both tests, three hours of recovery was recorded. Water level data were collected using pressure transducers which recorded every second at early time and every 15 minutes at late time.

Each pumping test conducted in Cambridge was 8 hours in length with a pumping rate of 20 L/min using a 0.05 meter diameter stainless steel submersible pump. Measurements of drawdown were taken with pressure transducers located in the pumped well and in each of the two observation wells. Readings were collected every 30 seconds at early time to once an hour near the end of the 8 hour test. Three hours of recovery data were collected in the same way.

Longer term pumping tests were conducted at the Tay River site in Perth. High transmissivity values obtained from initial slug testing indicated that only a high pumping rate would achieve measurable drawdown. Two pumping tests were conducted maintaining a pumping rate of 60 L/minute for 24 hours using a 0.10 meter stainless steel submersible pump. This was the maximum pumping rate the submersible pump could sustain. Drawdown measurements were recorded using pressure transducers in the

pumped well and in each of the levels in the completed observation well located at 13 m distance.

Slug testing was conducted using a straddle packer system consisting of two inflatable packers with an average spacing of 1.85 m lowered into the well on a cable using a hand winch. The packers were inflated with compressed nitrogen gas until they were well-seated against the wellbore, sealing the testing interval (an overpressure of 20-30 psi was used to ensure the seal). A pressure transducer was placed in the interval to record the waterlevel response to the slug. Slug testing was conducted in the wells at the Perth and Portland field sites and measurements were obtained contiguously over the entire length of each well.

Constant head testing was conducted using two inflatable packers with 1.6 m spacing at the Cambridge site. A one way valve was attached at the top of the straddle packer system to which the tubing leading to the constant head tanks and a pressure transducer were attached. Water was added to the well at a constant pressure from the pressurized tank system at surface. The tanks, ranging in diameter from 0.01m to 0.15 m, were pressurized using compressed nitrogen gas to maintain the constant pressure. Both the interval spacing and the locations corresponded to constant head testing performed by Reichart (1992).

Each well was videotaped with a downhole video camera before and after cleaning to identify areas of extensive biofouling which were later compared to the cleaned

conditions. For TW8 in Perth, videos were the main means for biofouling identification. A video was recorded right after drilling and during the biofilm growth process. During video recording depths were recorded at three meter intervals.

Another visual study was conducted through the use of biological activity reaction test (BART™) systems. Three systems were used to identify the most common types of bacteria found in groundwater environments: iron related bacteria (IRB), slime forming bacteria (SLYM) and sulfate reducing bacteria (SRB) (Mansuy et al., 1990). Groundwater samples were collected from each of the six wells, placed in the BART™ systems and observed daily. The first indication of a positive response specific to each type of BART™ system was noted as well as the lag time between groundwater addition and this first response.

Groundwater chemistry was also investigated to correlate with the BART™ system results. Groundwater samples were collected from wells P2 and P3 in Portland, MW7, MW8 and MW9 in Cambridge and TW7 in Perth. The wells sampled in both Portland and Perth are located near the tested wells. All the groundwater samples were analyzed for temperature, dissolved oxygen and pH. Samples from Cambridge and Perth were also analyzed for a suite of ions, including sodium, calcium, iron, magnesium, potassium and sulfur.

3.2.3 Cleaning of the Wells

Cleaning of the wells was performed by McLelland Water Technology. The first step in cleaning was the addition of hydrochloric acid. The wells were then pumped until the water ran clean by visual inspection. A 35% solution of hydrogen peroxide was then added. This served two purposes: 1) to neutralize the acid and 2) to react with any remaining biological matter present in the well. Peroxide was added and the well was pumped until the water had a reading of less than 5 ppm of hydrogen peroxide. Due to the proximity of residential wells to those being cleaned in Portland, and the lack of facility to pump off the remainder, hydrochloric acid was not used. The amounts of both HCl and hydrogen peroxide used varied between all the wells depending on the diameter of the well, the amount of biofouling present and the well yield. From this cleaning method there may be a difference in the degree of cleaning between the wells, which cannot be quantified.

3.2.4 Laboratory Study

In order to more completely understand the biofouling mechanism for the new Tay River well, a laboratory study was undertaken. The objective of the study was to determine the species present naturally in the groundwater and to determine under what conditions biofilm growth (i.e. biofouling) might occur. Using this information, the new well was purposefully biofouled so as to accelerate the natural process.

Samples of groundwater were obtained from the freshly drilled well and placed in commercial Biological Activity Reaction Test™ (BART) chambers. These tests have a series of different environments within each vial that allow specific bacteria to flourish.

BART™ chambers were employed for iron-related bacteria (IRB), slime-related bacteria (SLYM), and sulfur-reducing bacteria (SRB). BART™ systems are qualitative tools that can yield quantitative results, where the amount of time it takes for the first appearance of a positive result (growth of bacteria) can give an estimate of the amount of bacteria present in the sample water (see Appendix A). When positive results were observed, elapsed time was noted for each chamber.

Following the completion of the bacterial-typing, seven microcosm experiments were conducted to investigate the acceleration of biofouling with the identified bacterial population. High density polyethylene (HDPE) bottles were autoclaved at 140°C for 30 minutes for sterilization to ensure the only microbes present were those found in the groundwater samples. Each solution was added to a 250 mL HDPE bottle with screw caps. The caps were placed on top to limit but still allow oxygen to enter the sample in an attempt to duplicate field conditions. Several different nutrient packages were added to the sample water in order to determine which most encouraged biofilm growth. Three rounds of experiments were conducted, in each case varying the nutrient combination.

In the first round dextrose and Difco beef peptone were used in approximately 1 g/L solution with 200 mL of groundwater from TW7. Iron filings were also used at a concentration of 2.5 g/L again with 200 mL of groundwater in each sample. A control set was also used, containing groundwater with no nutrients added. Four glass slides measuring 15x25 mm were placed in the bottom of each bottle to act as a removable surface on which biofilm growth could be identified. The bottles were placed on a

rotating table set at 45 RPM to enable the movement of the solution over the slides in order to deliver nutrients and move wastes away from the biofilm. Movement of the solution over the slides could introduce a shear stress over the glass slide which could prevent biofilm attachment. However, the necessity of the delivery of nutrients and the removal of wastes from the glass slides was more important than the potential shear stress that could not be measured, so the microcosms were rotated. The glass slides were removed periodically to be analyzed with a modified Dubois et al. (1956) method for the amount of glucose present as an indicator of bacterial growth (Appendix B).

The second round of experiments were prepared to determine if a different combination of nutrients would produce more biofilm growth. Groundwater was taken from TW8 at the end of the second 24 hour pumping test and was used in the solutions. Two 250 mL 1 g/L solutions were prepared of each nutrient (Beef peptone and LB Broth) and then placed in 500 mL Mason jars. Iron filings were added to one jar of each nutrient, at a concentration of 2.5 g/L. Iron filings were sprinkled over the bottom of the jars to ensure even distribution and to encourage growth of IRB. Five glass slides were placed on the bottom of each jar with as little overlap as possible. A control jar with just groundwater also received five glass slides. As with the previous round, these slides were removed and analyzed using the modified Dubois et al (1956) method to determine the amount of glucose present.

A third round of experiments was prepared using the beef peptone and steel wool. Two control jars were prepared, one with strictly groundwater and no nutrients added, and a

second with just the beef peptone nutrient mixture, and no iron added. The concentration of nutrient was increased to 2 g/L beef peptone solution. Steel wool was measured into approximately 1.5 gram bundles. These bundles were placed in the 2 g/L beef peptone solutions, suspended around the middle of the solution to allow bacteria to surround the iron source. Steel wool was used since installation in the well is easier than with the iron filings. Photos of the glass jars containing the growing biofilm are shown in Figure 3-2.

Figure 3-2: Photo of 3 jars containing nutrient and steel wool, and the one control jar.

In order to promote and accelerate biofouling, steel wool bundles were placed in the well at approximately 19.5 m, 31.5 m and 38.5 m below top of casing. These depths correspond to low transmissivity zones detected during hydraulic testing. An example of these bundles is shown in Figure 3-3. Low transmissivity zones were targeted to promote growth of biofilm in areas that could be visually monitored with downwell video. These steel bundles were replenished periodically from October 2006 until August 2007. In early August 2007, nutrient packets were made using approximately 0.5 g of beef peptone nutrient and approximately 9 g of gelatin dissolved in 200 mL of water. These were allowed to cure for 12 hours in the refrigerator. Two nutrient packets were hung in

the well along with a bundle of steel wool at the three depths, as shown in Figure 3-3. Biofilm growth was monitored using well videos.

Figure 3-3: Photo of steel wool and nutrient bundles before being put down well.

3.4 Results and Discussion

In the following sections, the results of the well characterization and video inspection are presented for the conditions prior to and post rehabilitation. The results for the new well in which biofilm growth was accelerated are presented separately at the end of this section.

3.4.1 Prior to Well Rehabilitation

The extent of biofouling in each wellbore was clearly visible with the use of the downwell camera. These observations were used as a first indication of biofouling in the wells. Screen captures from these videos are shown in Figure 3-4 and Appendix C to illustrate the extent of biofouling and the effect of cleaning.

Sitting open for 15 years allowed extensive biofouling to develop in the wells at the Cambridge field site. The following screen captures from down well video, (Figure 3-4), shows the extent of biofouling present in wells MW7, MW8 and MW9. The feathery appearance of the biofilm growing out of the fractures into the wellbore, allowed sloughing off of parts of the biofilm which was incidentally collected with the groundwater obtained for analysis with the BART™ system. Comparative screen captures of all downwell video from the three field sites between biofouled and cleaned wells are presented in Appendix C.

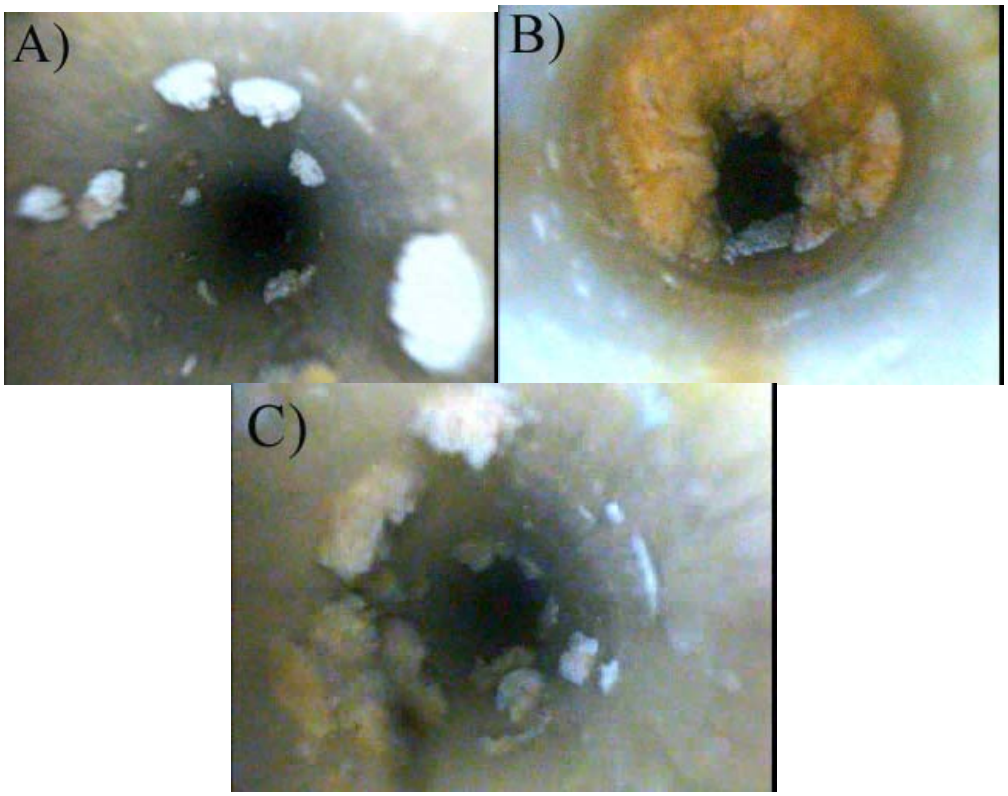

Figure 3-4: Biofouling present at the Cambridge field site in the wellbores of: A) MW7 at 10.7 meters below top of casing (mbtoc), B) MW8 at 9.14 mbtoc, C) MW9 at 10.7 mbtoc.

Left open for 10 years, wells WWCH and WWFS at the Portland site had also become fouled. A screen capture from downwell video of WWFS shows biofilm covering the entire surface of the wellbore (Figure 3-5), in contrast to the feathery appearance of

biofilm in the wells in Cambridge. The more uniform appearance of the biofilm could be mistaken for mineral scale, although the floating particles indicate bacterial biofilm.

Figure 3-5: Biofilm present all over the wellbore at 29.3 meters below top of casing in WWFS.

The uniform appearance of the biofilm in WWCH and WWFS is potentially due to the flow in the well as it was used in a heat pump configuration. The flow of water through the wells would promote biofilm growth close to the surface, not extending out into the bulk fluid. The wells in Cambridge, MW7, MW8 and MW9, were not disturbed during the 15 years they were left open. The feathery appearance of the biofilm growth out into the bulk fluid indicates very little flow in the wellbore, since the feathery part of the biofilm is easily sloughed off.

As groundwater samples were collected, sloughed off parts of the biofilm were also collected due to the shear forces induced by pumping, and placed in BART systems. Groundwater samples were collected from MW9 and placed in the IRB, SLYM and SRB BART™ systems for a representative sample of the groundwater from the Cambridge site. Positive reactions, and the lag time in days from the addition of groundwater sample

to the positive reaction are shown in Appendix D. Sloughed off parts of the biofilm contained large amounts of bacteria compared to the sample water, thus positive reactions occurred more rapidly. The smaller the lag time the larger the population of bacteria present in the sample water. Approximate populations according to lag time are shown in Appendix A. The type of positive reaction can also indicate the general type of bacteria present in the groundwater sample. Positive reactions from the Cambridge groundwater sample are summarized in Table 3-1.

Table 3-1: Correlation between type of positive reaction and general type of bacteria present in groundwater sample from Cambridge Field Site.

Groundwater Sample Location	Positive Reaction Observed	Bacteria Present
Cambridge	IRB- foam around ball - reddish slime - dark brown at bottom SLYM- white ring around ball - dark at bottom SRB- black on ball - black on bottom of vial	IRB- Mixed anaerobic and IRB with some aerobic slime forming bacteria SLYM- dominant aerobic slime forming bacteria, such as *Micrococcus* SRB- aerobic slime formers with SRB incorporated into community, ability to habituate anaerobic environments

Groundwater samples from Cambridge were sent to SiRem Laboratories in Guelph, Ontario to be analyzed and hetertrophic populations of 23, 8 and 51 cfu/mL for MW7, MW8 and MW9 respectively, were measured.

Samples were taken from both WWCH and WWFS at the Portland field site and placed in IRB, SLYM and SRB BART™ systems. Although the uniform appearance of the biofilm indicates sloughing is more difficult to achieve, particulate bacteria present in the wellbore could be collected in the groundwater samples and present positive reactions in the BART™ systems. Positive reactions and lag time are shown in Appendix D, the corresponding general types of bacteria and an estimate of bacteria populations are

summarized in Table 3-2 and Table 3-3 based on the tabulated approximations found in Appendix A. This sampling method does have a bias towards the sloughed off pieces of biofilm which would give faster positive reactions than the positive reactions from particulate bacterial cells.

Table 3-2: Bacteria most likely present and a population estimate in the WWCH sample water from the Portland field site (Cullimore, 1999).

	Positive Reaction Observed	Bacteria Present	Time Lag (days)	Population Estimate
IRB	- foam and brown ring around ball	-mixed anaerobic bacteria with aerobic slime forming bacteria	3	10 000 cfu/mL
SLYM	- slime ring around ball	-aerobic slime forming bacteria	5	5 000 cfu/mL
SRB	-black on bottom of ball -black on bottom of vial	-aerobic slime formers incorporate SRB and are able to colonize anaerobic conditions	5	5 000 cfu/mL

Table 3-3: Bacteria most likely present and a population estimate in the WWFS sample water from the Portland field site (Cullimore, 1999).

	Positive Reaction Observed	Bacteria Present	Time Lag (days)	Population Estimate
IRB	-foam and brown ring around ball, reddish cloud under ball	-mixed anaerobic and aerobic slime-forming bacteria	3	10 000 cfu/mL
SLYM	-white ring around ball	- dominant aerobic slime forming bacteria, such as *Micrococcus*	3	50 000 cfu/mL
SRB	-black on bottom of ball -black on bottom of vial	-aerobic slime formers with SRB incorporated into community	2	100 000 cfu/mL

These results show that the dominant bacteria in well WWCH are iron-related and the dominant bacteria in well WWFS are sulfate-reducing bacteria followed closely by slime-forming bacteria. Sulfate reducing bacteria do not produce slime in the same quantities as either the slime-forming or iron-related bacteria, thus the fractures would be less plugged (Cullimore, 1999). The dominant bacteria in WWCH being IRB, which can produce quantities of slime, more fracture plugging would be expected.

The results of the analysis of groundwater chemistry are summarized in Appendix D. The pH at both the Cambridge and Portland field sites is approximately neutral and both sites contain dissolved oxygen. The temperature range in Portland is greater, from 4.2-11.4 °C whereas the Cambridge groundwater temperature ranges from 7.7 – 9.1 °C. These are typical low total dissolved solid environments with good quality potable water.

3.4.2 Hydraulic Testing Results

Short term pumping tests were performed on wells MW7, MW8, MW9, and drawdown curves can be found in Appendix E. Each drawdown curve was analyzed with the Moench (1997) solution in the commercial program AQTESOLV. Theis was used as a preliminary analysis to obtain an approximation of the overall characteristics of the well, despite the likely presence of wellbore storage and skin. The Moench (1997) solution accounts for wellbore storage in an unconfined aquifer, which better describes the conditions for wells MW7, MW8 and MW9. Transmissivity estimates obtained from the Moench (1997) solution are 2.8×10^{-5}, 3.3×10^{-6} and 4.1×10^{-5} m^2/s for MW7, MW8 and MW9 respectively. Diagrams of the type curve fits of the Moench (1997) solution are presented in Appendix E.

Recovery data were interpreted using the Theis (1935) residual recovery method. Transmissivity values obtained from the recovery data, using AQTESOLV, and data obtained from pumping data analysis are displayed in Table 3-4. Graphs used to obtain the transmissivity values are shown in Appendix E.

Table 3-4: Summary of transmissivity values obtained through recovery data analysis from the wells at the Cambridge field site.

Well Identification	Moench (1997) Transmissivity values from Pumping Data (m^2/s)	AQTESOLV Transmissivity values from Recovery data (m^2/s)
MW7	2.8×10^{-5}	3.5×10^{-5}
MW8	3.3×10^{-6}	4.2×10^{-5}
MW9	4.1×10^{-5}	5.2×10^{-5}

Upon comparison, the transmissivity values obtained from the recovery data are similar in order of magnitude to the pumping data, although slightly less for wells MW7 and MW9, but slightly more for well MW8. The slight variation could be due to the assumptions used for Theis recovery solution where it is assumed that the aquifer is homogenous and wellbore storage effects are not present.

Results of the Moench (1997) analysis for the transmissivity values from WWCH in Portland is 3.4×10^{-5} m^2/s. Curve matching using the Moench (1997) solution in AQTESOLV is presented in Appendix F. Matching of the Moench (1997) solution to the drawdown data collected from the pumping test conducted on WWCH located at the Portland field site is presented in Figure 3-6. The recovery data does match that predicted, showing signs of limited skin effects, however the early pumping data does not match at all. The sharp increase in drawdown at early time does not have a linear slope, thus is not a wellbore storage effect. The sharp increase in drawdown can be potentially attributed to dewatering of the upper fractures in the well. The match is not perfect as the specific yield (Sy) is approximately two orders of magnitude too high, showing that the drawdown data are insensitive to the specific yield. This insensitivity is attributed to the short time duration of the pumping test. A pre- cleaning pumping test was not conducted on well WWFS.

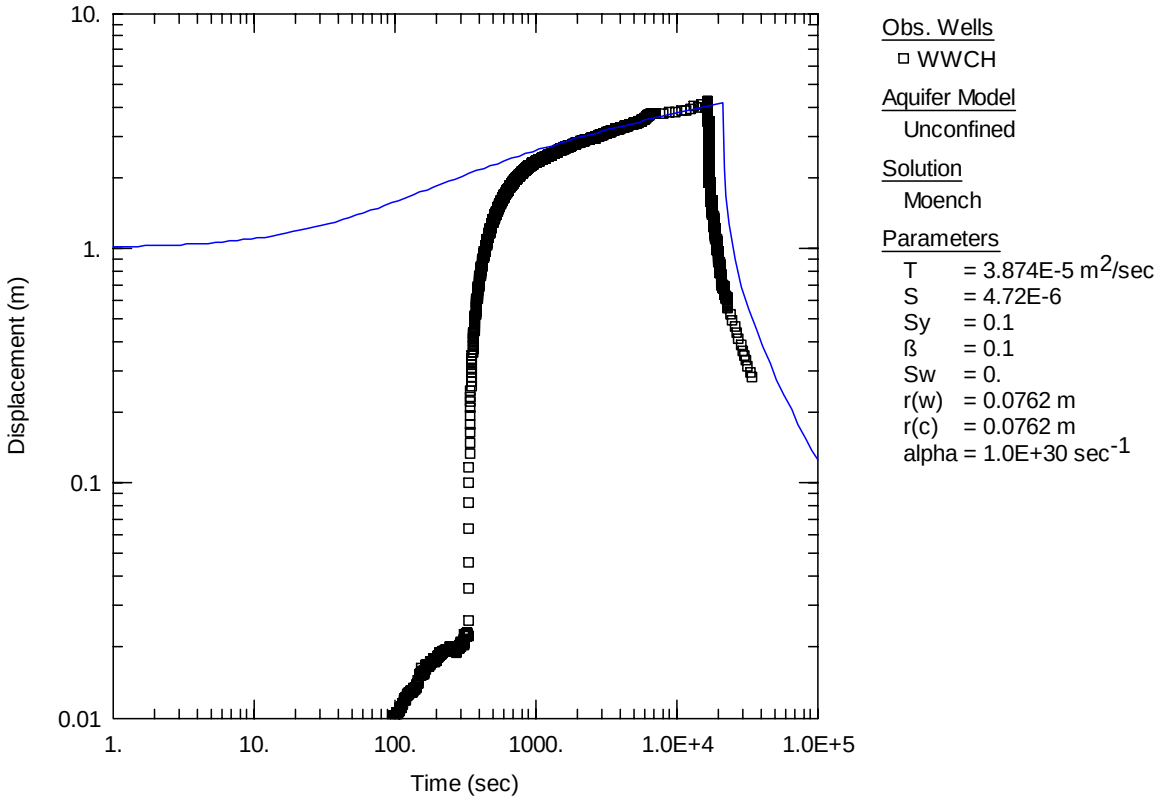

Figure 3-6: Curve matching solution of Moench (1997) to WWCH biofouled pumping test drawdown data. The theoretical curve is represented by a thin line and the collected data is represented by the data points.

Pumping tests for the cleaned wells in Cambridge were not conducted due to a concern of dewatering upper fractures during previous pumping tests.

Pumping tests were conducted on both WWCH and WWFS after cleaning at the Portland field site. The graphs showing the curve matching of the pumping test data to both the Theis (1935) solution and the Moench (1997) solution are presented in Appendix F. These graphs show a deviation from the Moench (1997) solution at early pumping time and during recovery, as shown in Figure 3-7 for well WWFS.

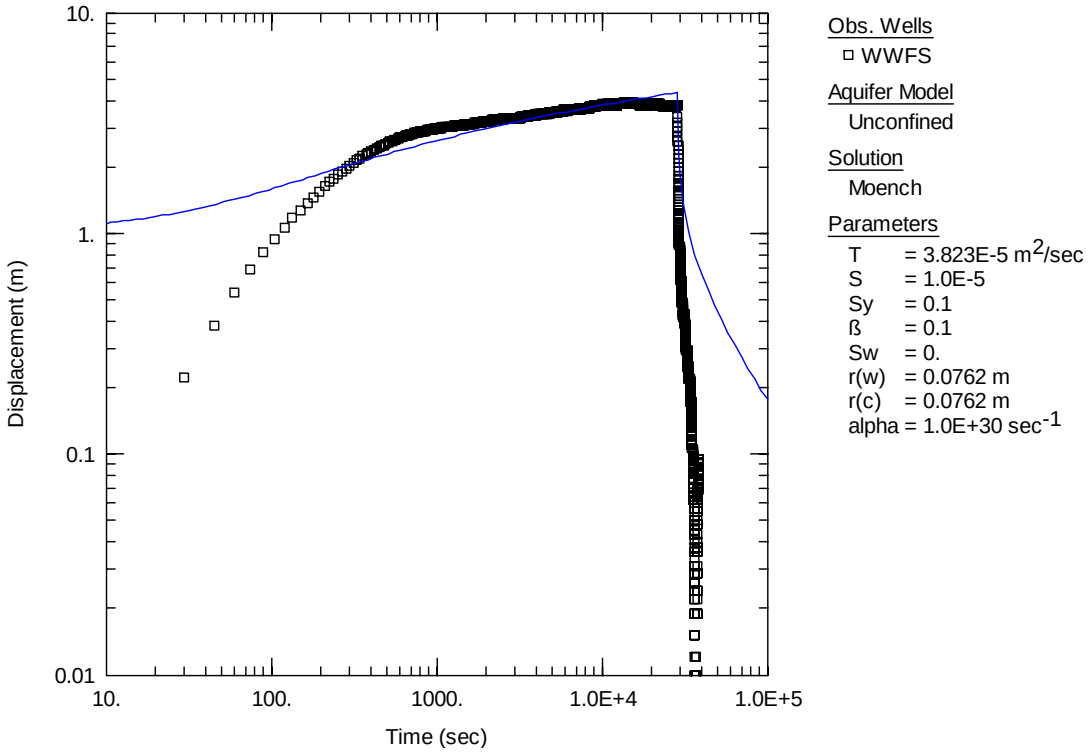

Figure 3-7: Curve matching of WWFS cleaned pumping data to Moench (1997) solution after well rehabilitation. The theoretical curve is represented by a thin line and the collected data is represented by the data points.

The deviation from the Moench (1997) solution in the recovery data shows strong evidence of skin effects in this well as the recovery data has significantly more vertical decline than predicted. This indicates that the fractures containing biofilm are not being effectively cleaned out by the cleaning method. The skin effects observed in the biofouled condition for well WWCH were unchanged after cleaning.

Pumping tests conducted on WWCH in the cleaned state show a decrease in the overall transmissivity relative to the biofouled state. The biofilm could have merely shrunk due to dehydration when hydrogen peroxide was added and returned to its regular state once the stress had passed. Also with the hydrogen peroxide, any dissolved iron in the water

would become oxidized and precipitate out of solution. This precipitate could become incorporated into the biofilm and potentially increase the plugging mechanism which is a shortcoming of the cleaning process used at the Portland field site.

The pumping tests show a range from limited to significant skin effects are present in the biofouled pumping test, from both Cambridge and Portland and remain present in the cleaned pumping test data for the Portland well. This suggests that the cleaning only eradicates the surface biofilm, as seen in the downwell videos, but does not penetrate into the fractures that have been clogged with biofilm.

The Theim equation was used to analyze the results of the constant head injection tests (Novakowski, 2002). In the analysis of the constant head testing data, using the Theim equation, the main assumption that steady state flow is achieved and that the aquifer is homogenous are sources of error in the calculations of transmissivity that cannot be exactly quantified nor eradicated (Novakowski, 2002). The error associated with the estimation of the radius of influence, however, can be reduced. The radius of influence, as used in the Theim equation, can be assumed to be a fixed value or the assumed value can be used in an iterative calculation process. The iterative calculations are performed until constant values for both transmissivity and radius of influence are obtained (Novakowski, 2002). This iterative process can improve the accuracy of the calculations by as much as an order of magnitude (Novakowski, 2002). Error associated with pressure measurement is approximately half a millimeter, which is insignificant, compared to other sources of error.

Constant head injection testing was conducted in the wells of the Cambridge field site to enable a comparison to previously measured values. The Hvorslev method and Vander Kamp method were used to calculate the transmissivities from slug testing in wells WWFS and WWCH of the Portland field site in the fouled state. After the wells underwent cleaning, hydraulic testing was conducted again on the new conditions. Constant head injection testing was again conducted on wells MW7, MW8 and MW9 in the cleaned states. Transmissivity-depth profiles for each of the wells were plotted to compare transmissivity distribution along the depth of the well for each stage of the biofouling process. The transmissivity profile of MW7 is shown in Figure 3-8, and the transmissivity profiles of MW8 and MW9 are presented in Appendix G. Each profile contains transmissivity measurements from hydraulic testing performed at the two stages of biofouling in this study: biofouled (grey lines) and cleaned (black lines).

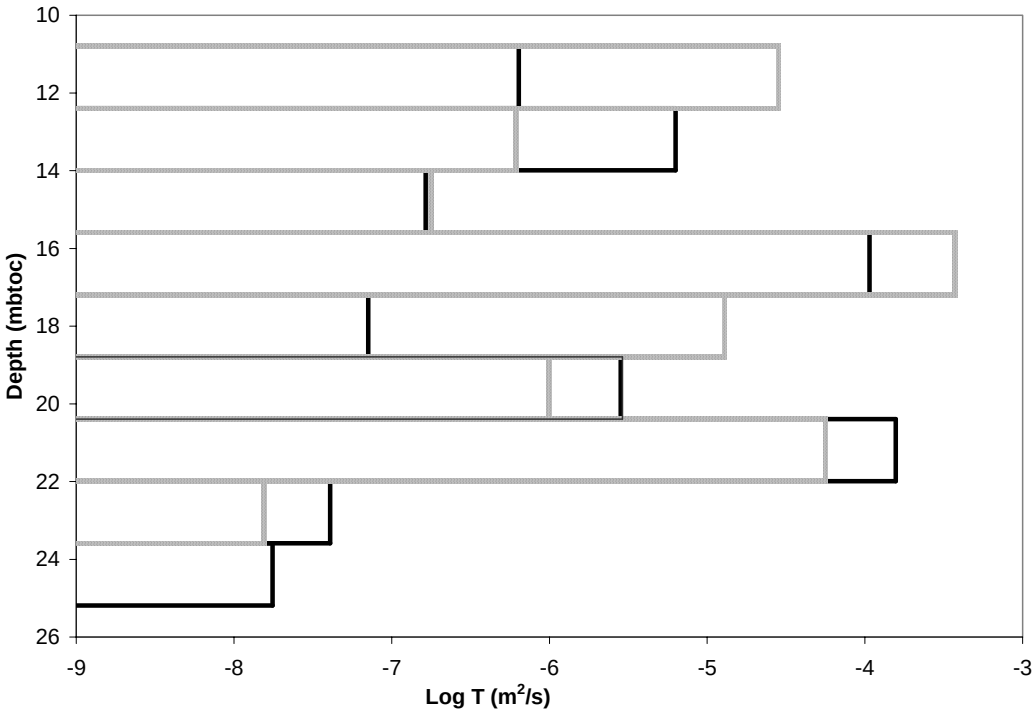

Figure 3-8: Transmissivity- depth profile of MW7. Grey lines represent biofouled values and black lines represent cleaned values.

Through constant head injection testing the transmissivity of certain intervals in the well had more significant changes in transmissivity than others. Some intervals that had low transmissivity values in the biofouled states contained improvement in transmissivity values in the cleaned states.

The wells located at the Portland field site were retested using the same slug testing methods as with the biofouled conditions. Care was taken to match the testing sections of the first round of slug testing although a perfect match was not made. Transmissivity-depth profiles for WWCH and WWFS in the fouled and cleaned states are presented in Appendix G. The comparison between the fouled and cleaned states shows an improving trend in transmissivity, as illustrated in Figure 3-9.

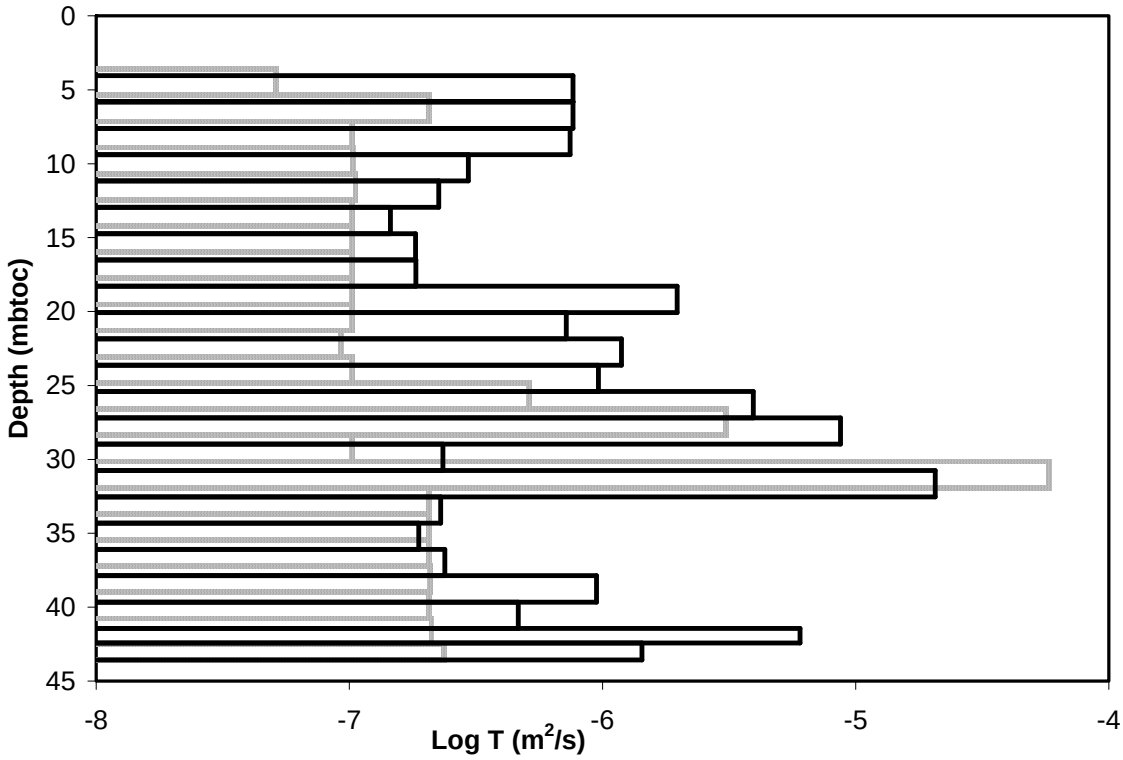

Figure 3-9: Comparative plot of transmissivity-depth profile of WWFS. Grey lines represent biofouled conditions and black lines represent cleaned conditions.

Although there is some overlap in the sections from the fouled data collection, the majority of the cleaned transmissivity values are greater than those from the fouled well, as seen in Figure 3-9. This could be due to smaller fractures occurring in this fractured rock aquifer that biofouling would clog more easily. For each of the transmissivity profiles (Figure 3-9) the low transmissivity zones tend to show a larger change between the biofouled and cleaned profiles. This could indicate that the biofilm more easily clogs the small fractures with low flow compared to the larger fractures carrying more flow to the well.

The pumping test results show that the biofilm is penetrating into the rock, seen as the skin effect present in the cleaned pumping test data of WWCH. The downwell videos

show that the biofilm present on the wellbore surface is removed following cleaning, and the slug testing shows an improvement in the transmissivity of the small aperture fractures after cleaning.

The conflicting results can be explained by the size of fracture aperture. With the pumping tests, the larger fracture features most likely dominate flow. These are more difficult for the bacteria to form a biofilm in due to higher shear stresses acting against attachment. However, these larger aperture fractures most likely have biofilm present further into the formation since the nutrient can penetrate farther due to the thin biofilm at the intersection of the fracture and the well. The smaller aperture fractures do not contribute as much flow during a pumping test. These small apertures can be plugged more easily by biofilm due to lower shear stresses and a smaller space to occupy. However the mouth of the fracture at the intersection of the well will most likely become significantly reduced in aperture very quickly, thus limiting the amount of nutrient available to penetrate into the fracture. The small fractures, therefore, have a plug of sorts at the wellbore, that can be removed through cleaning, and thus the significant improvement in slug testing results. In contrast, the large fractures have a film along the walls of the fracture farther into the formation having little effect on the pumping test results.

In order to quantify the hydraulic testing results, the geometric mean was calculated for each well in the two different states, biofouled and cleaned. A geometric mean was also calculated for the low transmissivity values, determined by inspection of histograms

(Appendix H). A summary of both geometric means for the 5 wells examined in this study is presented in Table 3-5.

Table 3-5: Summary of the calculated geometric means of transmissivity of the entire well in the biofouled and cleaned states. For TW8 the cleaned state title represents the freshly drilled state.

Well Identification	Geometric Mean of All T Measurements (m^2/s)		Geometric Mean of Low T Measurements (m^2/s)	
	Biofouled	Cleaned	Biofouled	Cleaned
MW7	3.3×10^{-6}	1.1×10^{-6}	1.7×10^{-6}	2.3×10^{-7}
MW8	5.2×10^{-7}	1.1×10^{-6}	2.7×10^{-7}	4.4×10^{-7}
MW9	1.1×10^{-6}	8.9×10^{-7}	1.9×10^{-7}	3.2×10^{-7}
WWCH	3.9×10^{-7}	8.6×10^{-7}	2.6×10^{-7}	5.9×10^{-7}
WWFS	2.1×10^{-7}	7.5×10^{-7}	1.6×10^{-7}	6.5×10^{-7}

Based on the results shown in Table 3-5 an improvement is made in transmissivity between the biofouled and cleaned states in 3 of the 5 wells (MW8, WWCH and WWFS). Error in the positioning of the packers over the large fractures could be responsible for the decrease in transmissivity between biofouled and cleaned states in wells MW7 and MW9. Well MW9, however, does show an increase in the low transmissivity geometric mean, indicating that the small aperture fractures were more affected by the biofouling. Geometric mean calculations of the low transmissivity measurements show greater improvements between the biofouled and cleaned states, on average a two-fold increase. This larger increase indicates that the small fractures are most influenced during the biofouling process. The increase in transmissivity is smaller when the geometric mean of low transmissivity values are examined, which suggests error around the large fractures.

3.4.3 New Well

BART™ analysis was used to identify the general type of bacteria on which the laboratory exercise would be focused. Sample water taken from adjacent well TW7 shows a positive reaction first to iron related bacteria (IRB), slime producing bacteria (SLYM) and a small but still positive reaction to sulfate reducing bacteria (SRB). Samples from TW8 were also placed in the same three BART™ systems and had similar results. The positive results from the BART™ systems can be seen in Appendix D. The type of bacteria present in TW8 and the approximate populations based on the time lag of these bacteria are summarized in Table 3-6.

Table 3-6: Bacteria most likely present and a population estimate in the TW8 sample water.

	Positive Reaction Observed	Bacteria Present	Time Lag (days)	Population Estimate
IRB	-Foam around ball -Brownish red ring around ball -Dark color in column	Mixed anaerobic and iron related bacteria with some aerobic slime forming bacteria	3	10 000 cfu/mL
SLYM	-slime around ball -cloudiness in water column	Dominant aerobic slime forming bacteria, such as *Micrococcus*, with some adaptable anaerobes	6	1 000 cfu/mL
SRB	-black forming on bottom of vial	Deep seated anaerobic bacteria dominated by *Desulfovibrio*	11	<100 cfu/mL

Groundwater chemistry data were collected from TW7, 15m away from TW8, and results are presented in Appendix D. The groundwater is of neutral pH, contains dissolved oxygen and had a temperature of 7.4°C. This groundwater environment has low total dissolved solids and is a potable groundwater source.

Based on the laboratory results (Appendix I), steel wool was hung in the well at depths matching low transmissivity zones from the pumping test. In the well, there was some

indication of biofilm growth from just the addition of steel wool, however the biofilm grew more rapidly when a combination of steel wool and nutrient-gelatin packets were placed in the well. These nutrient-gelatin packets were made to release the nutrients slowly into the surrounding water so a higher steady amount of nutrients would be available for the bacteria. This encouraged biofilm growth and resulted in positive identification of biofilm on the wellbore.

The new well has a steel well casing at the top which does not come in contact with the water surface. If the casing did contact the water surface, the addition of iron from the well casing could increase the biofilm growth in the well. In other drilled wells at the Tay river site minor biofouling has occurred without the addition of nutrients. The presence of steel wire suspending instrumentation in the wells and the well casing are the sources of iron and bacterial slime has been found on the wire. Drilled wells increase the amount of oxygen present in the system, encouraging aerobic bacteria to grow, although the addition of nutrients is often needed for biofilm growth to occur.

During the process of encouraging biofilm growth in well TW8, downwell videos were used as a visual indicator of biofilm growth. Some indication of biofilm growth can be seen in Figure 3-10.

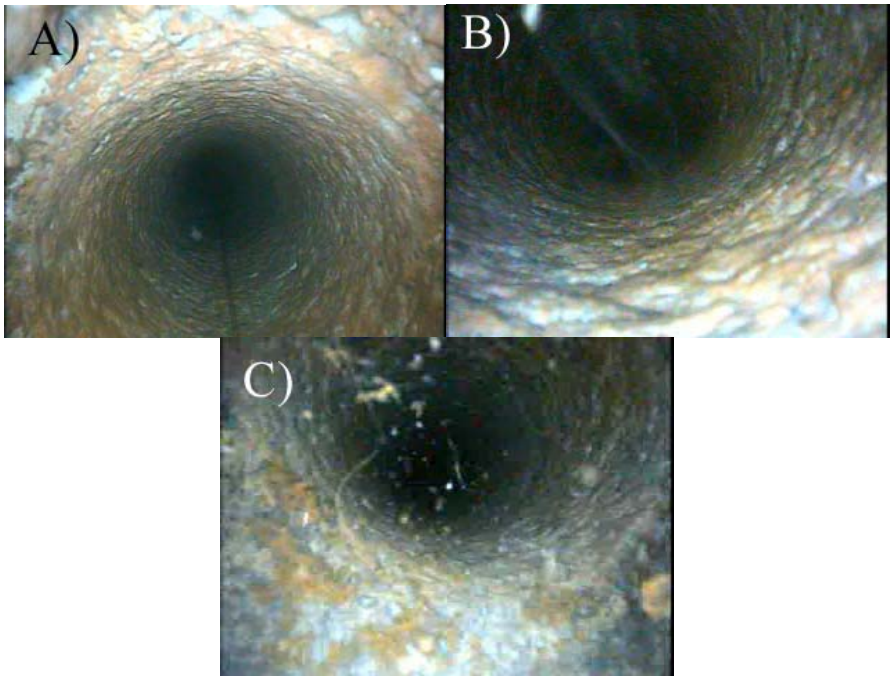

Figure 3-10: Screen capture of potential biofilm growth at varying depths in TW8. A) 10.7 meters below top of casing (mbtoc) B) 19 m btoc and C) 35 m btoc.

Two 24-hr pumping tests were performed on TW8 at the Perth field site. The first pumping test, at a flow rate of 60 L/min, showed signs of recharge. The fluctuations at later time indicated recovery during pumping, caused by severe ponding located approximately 10 meters from the pumped well, located over a recharge point to the aquifer.

A second pumping test was conducted with a longer discharge hose to prevent ponding in the recharge spot identified in the first pumping test. A 24 hour test at the same flow rate was conducted.

The two pumping tests were analyzed using the Moench (1997) curve matching (Appendix). Values of transmissivity are summarized in Table 3-7. Note that this well produces a very large amount of water. The Theis solution for pumping test #1 was not

included in this calculation since the storativity associated with the transmissivity value is unrealistic. The geometric mean of the storativity values is 2.7×10^{-5}. The pumping test results do not show the presence of skin effects.

Table 3-7: Summary of transmissivity values obtained from Theis(1935) and Moench (1997) curve matching analysis of TW8 pumping test #1 and pumping test #2.

	Pumping Test #1		Pumping Test #2	
	Moench (1997) Solution		Moench (1997) Solution	
	T (m^2/s)	S	T (m^2/s)	S
TW8	0.0015	1.48E-5	0.0015	8.22E-5

Slug testing was conducted on TW8 both in the cleaned state and in the purposefully biofouled state, and results indicate that biofilm growth did affect transmissivity. The transmissivity-depth profile comparing the drilled and biofouled slug test results is shown in Figure 3-11. Lower transmissivity is associated with small fracture aperture which is supported with no fractures present in the downwell video in the intervals with low transmissivity. Some low transmissivity zones show the largest decrease in transmissivity due to biofouling compared to the freshly drilled state, such as the interval located at 17.5-15.6 mbtoc that decreased from 5.2×10^{-6} to 7.4×10^{-7} m^2/s, or the interval at 19.3-17.4 mbtoc that decreased from 1.3×10^{-6} to 7.2×10^{-7} m^2/s. Therefore, as with the wells discussed previously, biofouling appears to target the small aperture fractures since there is less flow through these fractures. In this case, attachment can occur more readily and the young biofilm with a weak attachment can resist the minimal shear forces acted upon it, whereas with a young biofilm in a larger fracture it would be more difficult to attach and a weakly attached biofilm could be sloughed off by the higher shear forces.

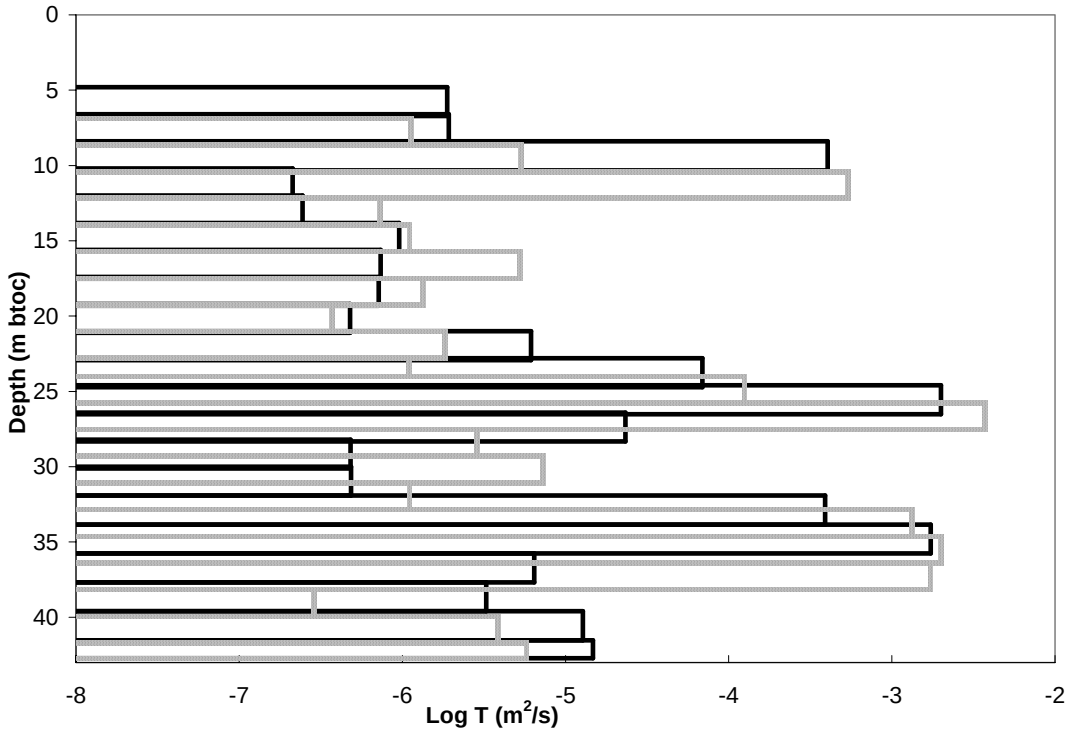

Figure 3-11: Transmissivity-depth profile for TW8 located at the Perth field site. Grey lines represent freshly drilled values, black lines represent biofouled values.

The transmissivity range does decrease slightly in the biofouled state when compared to the freshly drilled state, as evidenced by the decline of the geometric mean of the entire transmissivity for the well from 1.1 x 10^{-5} to 6.7 x 10^{-6} m^2/s. For the low transmissivity sections the geometric mean does show a slight decrease as well, from 1.6 x 10^{-6} to 1.0 x 10^{-6} m^2/s. TW8 was drilled and purposefully biofouled during this project. The overall geometric mean indicates about a two fold increase in transmissivity between the drilled and biofouled states which is not what was expected. This is attributed to double counting large fracture features and error in the placement of the packers around these features.

Upon closer inspection of downwell videos for TW8 it appeared that two major fracture zones, at 25 meters and 35 meters below the top of casing, provide the majority of the water for the pumping test. The fracture located at 25 mbtoc was slightly affected by the growth of biofilm, whereas the fracture located at 35 mbtoc was not at all affected by biofilm growth, as demonstrated in the slug test results presented in Figure 3-11.

3.4.3.1 Laboratory Results

Three rounds of nutrient-addition experiments in the laboratory were conducted to determine the combination of nutrients best suited for biofilm growth in sample groundwater from TW8. Glucose concentrations, representing biofilm growth, on glass slides removed from the bottom of each microcosm experiment determined which combination of nutrients would be installed in TW8 at the Perth field site.

Combinations of beef peptone (a yeast extract), dextrose, iron filings, LB broth and commercial steel wool were used. Resulting glucose concentrations of the three rounds of experimentation are shown in Appendix . The combination that produced the greatest amount of biofilm growth, indicated by the highest concentration of glucose at more than 200 µg/mL, was the beef peptone and coarse grained steel wool.

Based on the laboratory results,Appendix , steel wool was hung in the well at depths matching low transmissivity zones from the pumping test. In the well, there was some indication of biofilm growth from just the addition of steel wool; however the biofilm grew more rapidly when a combination of steel wool and nutrient-gelatin packets were

placed in the well. These nutrient-gelatin packets were made to release the nutrients slowly into the surrounding water so a higher steady amount of nutrients would be available for the bacteria. This encouraged biofilm growth and resulted in positive identification of biofilm on the wellbore.

3.4.4 Summary of Project

A summary of the field site geology, testing methods used and results are presented in Table 3-8.

Table 3-8: A summary of the three field sites geology, testing methods and results.

Site Location	Identification of Wells	Geology	Testing Methods	Results
Perth, Ontario	TW8	-<2 meters of well drained glacial till -abundant outcrop -Frontenac terrain of central metasedimentary belt of Grenville Province -bedrock composed of crystalline Precambrian syenite-migmatite	-down well videos - BART™ system analysis -long term pumping tests in drilled condition -slug testing in drilled and biofouled conditions	-patchy biofilm growth on wellbore after nutrient bundle addition -IRB most populous in well, targeted for biofilm growth -long term pumping tests dominated by several large fracture features -slug testing showed slight decrease in over all T -slight increase in geometric mean of T (1.0 x 10-6 to 1.6 x 10-6) of the small fractures
Portland, Ontario	WWFS WWCH	-varying depth of till overburden -transition through boulder layer to sandstone bedrock of Nepean and March formations -unconformity between sandstone and Precambrian crystalline basement rock composed of granite gneisses, quartzite and quartzofeldspathic gneisses	-down well videos - BART™ system analysis -short term pumping tests in biofouled and cleaned conditions -slug testing in biofouled and cleaned conditions	-biofilm growth is close to and uniform over wellbore surface -IRB consistent in both wells -SRB presence in WWFS -skin effects present in both biofouled and cleaned conditions for WWCH -skin effects present in recovery data for WWFS in cleaned condition -an approximate two fold increase in the geometric mean of the low T zones

Site Location	Identification of Wells	Geology	Testing Methods	Results
Cambridge, Ontario	MW7 MW8 MW9	-discontinuous till overburden -layered sedimentary sequence of dolotsones, sandstones and shales -wells completed in Guelph and Amabel submembers of Lockport dolostone sequence	-down well videos -BART™ system analysis -short term pumping tests in biofouled condition -constant head injection tests in biofouled and cleaned conditions	-biofilm growing out of fractures in to wellbore -positive result from all three systems (IRB, SLYM, SRB) -dewatering of upper fractures during pumping tests -skin effect present in recovery data -mixed results in geometric mean of T -MW8 was only well to show improvement after cleaning was performed, two fold increase

3.6 Conclusions

Biofouling was investigated in bedrock wells located at three sites located in carbonate rock (Cambridge, Ontario), gneissic terrain (Perth, Ontario) and a sandstone/Precambrian terrain (Portland, Ontario). Through the use of BART™ systems it was determined that the bacterial growth was dominated by iron-related and slime-forming bacteria with some sulfate reducing bacteria present at all three sites.

Visual inspection of wells at the Cambridge site showed biofilm growth, which occurred prior to this study, protruding out of fractures into the wellbore. The wells located in Portland conversely, were fouled by a biofilm that uniformly covered the wellbore surface. The biofilm grown in the Perth well showed both surficial biofilm and the development of columnar, feathery structure from fractures. Despite the physical difference in biofilm appearance, the effects on the reduction of transmissivity were similar.

The wells WWCH and WWFS are considered to best represent typical residential wells. WWCH and WWFS were used in a heat pump configuration and are considered to have been under the same conditions as the other residential wells in the area. The four other wells, MW7, MW8, MW9 and TW8 were not used over an extended period of time with fluctuations in water level due to pumping. Thus these wells do not exactly duplicate the residential well conditions.

Hydraulic testing of all of the wells investigated in this study determined that the smaller fractures were influenced more by biofilm plugging than the larger fractures. For example, the lower transmissivity zones consistently showed a greater decrease in transmissivity than sections with higher initial transmissivity as a result of biofouling as seen in the geometric means. These low transmissivity zones have small fractures, so it can be concluded that biofilm growth preferentially affects the small fractures in a fracture distribution to a greater extent. As the transmissivity of a given well is often dominated by the largest aperture fractures, well rehabilitation in these setting is unlikely to have a significant impact.

Pumping tests conducted before well rehabilitation show the presence of wellbore skin in some cases, which may be attributed to biofouled conditions. The cleaning process did not markedly improve total wellbore performance for those wells where a comparison was made following cleaning, and skin was not improved following cleaning according to the results of the pumping tests.

Based on the results of the laboratory study the presence of a steel well casing, or steel pump parts placed in the well could contribute significantly to biofouling of wells. As only the small fractures appear to be influenced, wells that have the large dominant fractures would be unaffected. Conversely, wells that are low to marginal producers (i.e. < 5gpm) may plug up rapidly. These types of wells are very common in granitic terrains. Continuous maintenance and cleaning of these wells will be necessary to maintain performance.

3.7 References

Cullimore, R., 1999. Microbiology of Well Biofouling, Lewis Publishers, New York

Domozych, D.S., Kort, S., Benton, S., Yu, T. 2005. The extracellular polymeric substances of the green alga *Penium margaritaceum* and its role in biofilm formation. Biofilms, 2:129-144.

Dubois, M., Gilles, K.A., Hamilton, J.K., Rebers, P.A., 1956. Colorimetric Method for Determination of Sugars and Related Substances. Analytical Chemistry. 28(3):350-353.

Greggs, R. G., Gorman, W. A. 1976. Geology of the Thousand Islands, Parks Canada.

Kettles, I.M., 1992. Surficial geology, Perth, Ontario, Geological Survey of Canada, "A" Series Map, Report: 1800A.

Kim, D.-S., Fogler, H. S., 2000. Biomass Evolution in Porous Media and Its Effects on Permeability Under Starvation Conditions, Biotechnology and Bioengineering, Vol. 69, No. 1

Lapcevic, P. A., Novakowski, K. S., Sudicky, E. A., 1999. The interpretation of a Tracer Experiment Conducted in a Single Fracture Under Natural Groundwater Flow, Water Resources Research, 35(8):2301-2312

Mansuy, N., Nuzman, C., Cullimore, D. R., 1990. Well Problem Identification and Its Importance in Well Rehabilitation, In: Water Wells, Monitoring, Maintenance, Rehabilitation, ed. Howsam, P., E.&F.N. Spoon, London

Milloy, C. A., 2007. Measurement of Hydraulic Head for the Evaluation of Groundwater Recharge to Discrete Fracture Zones in a Crystalline Bedrock Aquifer, Queen's University, Kingston, Ontario

Moench, A. F., (1997) Flow to a Well of Finite Diameter in a Homogenous, Anisotropic Water Table Aquifer, Water Resources Research, 33(6):1397-1407

Novakowski, K. S., 2002. Use of the Thiem Equation to Interpret Constant Head Tests Conducted in Boreholes, Technical Note, Water Resources Research

Novakowski, K., Bickerton, G., Lapcevic, P., Voralek, J., Ross, N., 2006. Measurements of Groundwater Velocity in Discrete Rock Fractures, Journal of Contaminant Hydrology, 82:44-60

Raven, K. G., 1986. Hydraulic Characterization of a Small Groundwater Flow System in Fractured Monzonitic Geniss, National Hydrology Research Institute, 30:1-133

Reichart, T.M, 1992. Influence of Vertical Fractures in Horizontally Stratified Rock, Univeristy of Waterloo, Waterloo, Ontario.

Ross, N., Bickerton, G., 2002. Application of Biobarriers for Groundwater Containment at Fractured Bedrock Sites, REMEDIATION

Shaw, J.C., Bramhill, B., Wardlaw, N.C., Costerton, J.W., 1985. Bacterial Fouling in a model core system, Applied Environmental Microbiology, 49:693-701

Stewart, T.L., Folger, H.S., 2001. Biomass Plug Development and Propagation in Porous Media, Biotechnology and Bioengineering, 71(3)

Theis, C.V., 1935. The Lowering of the piezometric surface and the rate and discharge of a well using ground-water storage, Trans Am Geophys Union, 16:519-524

Wilson, M.E., 1961. Geology, Perth-Lanark and Leeds counties, Ontario, Canada Geological Survey Map 1089 A.

Chapter 4: Conclusions and Recommendations

An investigation of biofouling in bedrock wells was under taken at three sites located in carbonate rock (Cambridge, Ontario), gneissic terrain (Perth, Ontario) and a sandstone/Precambrian terrain (Portland, Ontario). At all three sites it was determined, through the use of BART™ systems, the bacterial growth was dominated by iron-related and slime-forming bacteria with some sulfate reducing bacteria.

Biofilm growth, which occurred prior to this study, was identified through visual inspection as protruding out of the fractures into the wellbore. Conversely, the wells located in Portland were fouled by a biofilm that uniformly covered the wellbore surface. The well located in Perth showed a combination of both surficial and the beginnings of feathery structures from fractures. The biofilm effects on the reduction of transmissivity were similar, despite the physical difference in biofilm appearance.

Through hydraulic testing of the wells this study identified that the smaller fractures are affected more by biofilm plugging than the larger fractures. Demonstrating this are the lower transsmissive zones that show consistently greater decrease in transmissivity when compared to zones with higher initial transmissivity values due to biofouling. Small fractures are characteristic of these low transmissivity zones, thus biofilm growth preferentially affects the small aperture fractures in a fracture distribution. The largest aperture fractures typically dominate the transmissivity of a given well so rehabilitation is less likely to have a significant impact in these settings.

Pumping tests conducted before well rehabilitation show the presence of wellbore skin in some cases, which may be attributed to biofouled conditions. The cleaning process did not markedly improve total wellbore performance for those wells where a comparison was made following cleaning, and skin was not improved following cleaning according to the results of the pumping tests.

The presence of any form of iron, such as a steel well casing or steel pump parts, in the well contribute significantly to the biofouling of the well, based on the results of a laboratory study.

The next step would be to attempt to encourage growth in specific fractures of varying aperture to determine if aperture is a determining factor in the effect of biofilm on transmissivity.

Encouragement of the growth of slime forming bacteria would potentially have a greater effect on transmissivity due to the increase in slime. Targeting a nutrient to encourage slime forming bacteria growth would be recommended.

Laboratory experiments on the removal of biofilm would also be beneficial in determining the most effective method of removing the biofilm from the rock surface.

Appendix A

Connection between time lag and bacteria population tables from Cullimore (1999).

Table A - 1: Relationship between time lag and population for Iron related bacteria.

Time Lag (days)	Population cfu/ml (log)
1	1 000 000 (6.0)
2	100 000 (5.0)
3	10 000 (4.0)
4	5 000 (3.6)
5	1 000 (3.0)
6	100 (2.0)
7	100 (2.0)
8	100 (2.0)

Table A - 2: Relationship between time lag and population for sulfate reducing bacteria.

Time Lag (days)	Population cfu/ml (log)
1	1 000 000 (6.0)
2	100 000 (5.0)
3	50 000 (4.6)
4	10 000 (4.0)
5	5 000 (3.6)
6	1 000 (3.0)
7	100 (2.0)
8	100 (2.0)

Table A - 3: Relationship between time lag and population for slime forming bacteria.

Time Lag (days)	Population cfu/ml (log)
1	5 000 000 (6.6)
2	500 000 (5.6)
3	50 000 (4.6)
4	10 000 (4.0)
5	5 000 (3.6)
6	1 000 (3.0)
7	1 000 (3.0)

Appendix B

Modified Dubois et al (1956) Method, used in laboratory experiment to determine glucose increase on glass slides, thus indicating biofilm growth on glass slides.

Preparation of Solutions

Glucose Standards

Add 0.02g of dextrose to a 200mL volumetric flask and fill with deionized water to get a standard solution of 100ug/mL. Perform serial dilution from the 100ug/mL standard to get the next 3 standards using 50mL volumetric flasks. The required volume of solution to be added for each standard is shown in Table B- 1.

Table B- 1: Required volumes of glucose solution to be added to flask for serial dilution.

Standard (ug/mL)	Volume of 100ug/mL solution added (mL)
50	25
10	5
5	2.5

Obtain the remaining two standards by dilutions of the 10ug/mL standard in 50mL volumetric flasks. The required volume of solution to be added for each standard is shown in Table B- 2

Table B- 2: Required volume of glucose solution to prepare standard solutions.

Standard (ug/mL)	Volume of 10ug/mL solution added (mL)
1	5
0.5	2.5

Mix standards by inverting at least three times. Transfer solutions to vials with black caps for later use.

Phenol Solution

Add 10g of phenol to 100mL of deionized water. When sufficiently mixed, the solution should have a white appearance.

Procedure for Testing

Prepare trays of labeled vials for glucose standards, controls and samples, (there should be twelve vials in total). Transfer glass slides into labeled vials, holding them by the edges with tongs. Rinse tongs with deionized water after each slide is transferred. Place caps on vials.

Using a pipette, add 1mL of deionized water to the Blank, DIC, GWC, GW1, GW2 and GW3 vials. Add 1mL of glucose standard to the appropriate vials, moving from low concentration to high concentration. Glucose standards should be inverted three times before use in order to ensure proper mixing. Change the tip on the pipette. Add 1mL of the phenol solution to each vial, shaking it regularly to maintain a white appearance.

Under the fume hood, quickly add 5mL of sulfuric acid to each tube using a pump and directing the stream against the liquid surface. Immediately after delivering acid, cap and seal the vial and shake three times. Before adding acid to vials, it should be verified that there is no air remaining in the pump. When working with the acid, safety goggles and nitrile gloves should be worn. The reaction of the acid is highly exothermic, so a rapid temperature increase should be expected. A summary of each solution is shown in Table B- 3.

Table B- 3: Modified Dubois *et al* (1956) Solutions

Solution	Contents
Standards	1mL standard 1mL 10% phenol solution 5mL sulphuric acid
Slide solutions	Glass slide 1mL deionized water 1mL 10% phenol solution 5mL sulphuric acid
Blank	1mL deionized water 1mL 10% phenol solution 5mL sulphuric acid

Allow the solutions to stand for a minimum of 10 minutes. Glass slides should be submerged in solution during this period. This can be achieved by propping up the tray of vials such that each tube rests at an angle. Set solutions in a 25^{o}C-30^{o}C water bath for an additional 10-20 minutes before transferring them into labeled Hach tubes.

Zero the Hach machine using the blank, then read the absorbance of each solution three times at 490nm. Before each reading, tubes should be wiped clean.

Procedure for Cleaning Glassware

All solutions can be discarded in COD waste. Rinse all tubes, vials and caps with deionized water into the waste container under the fume hood. Soak glassware and caps in soapy detergent water for around 10 minutes. Scrub glassware with a test tube brush and rinse three times with tap water. Soak for an additional 10 minutes in 20% sulfuric acid solution. Remove into a beaker and rinse three times with deionized water. Place glassware in the drying oven and set caps to dry on paper towel on the lab bench. In the oven, vials can be placed directly on the rack, while Hach tubes should be placed upside-down in a beaker.

Presentation of Results

To analyze the growth of biofilm, the modified Dubois et al. (1956) calorimetric method of glucose quantification was used. This method assesses the amount of carbohydrate deposited on the glass slides which corresponds to the amount of biofilm on the slides. The slides are be removed from the solutions, exposed to phenol and rapid sulfuric acid addition which produces a color change detectable by spectrophotographic analysis. Spectrophotographically analyze the samples and compare to prepared glucose standards to obtain the amount of biofilm present. The glucose concentration is plotted as a function of the number of days since growth began to give concentration curves which can identify if the concentration is increasing, thus growth of a biofilm.

Appendix C

Comparative screen captures of MW7, MW8, MW9, and WWCH between biofouled and cleaned conditions. Comparative screen captures of TW8 between freshly drilled and biofouling indication.

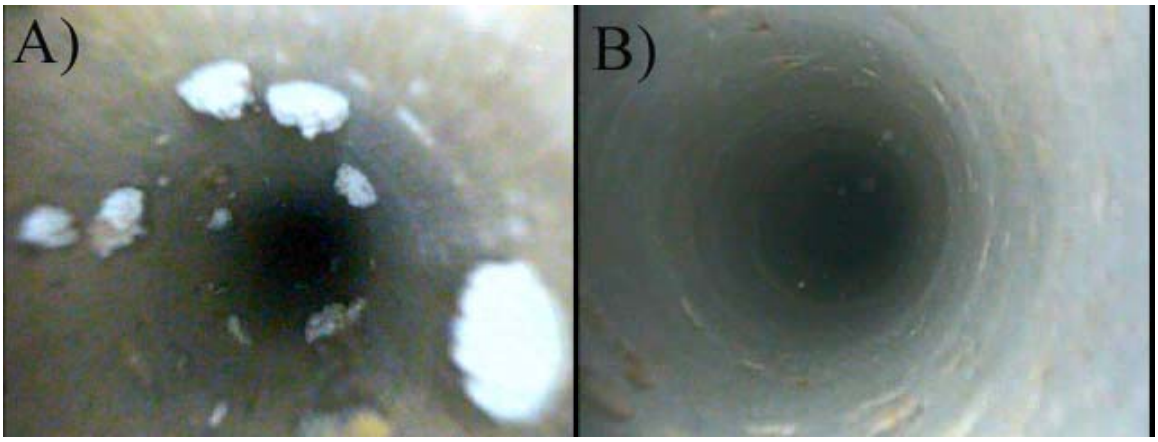

Figure C- 1: Screen captures of MW7. A) Biofouling at 10.7mbtoc, B) Cleaned at 10.7mbtoc.

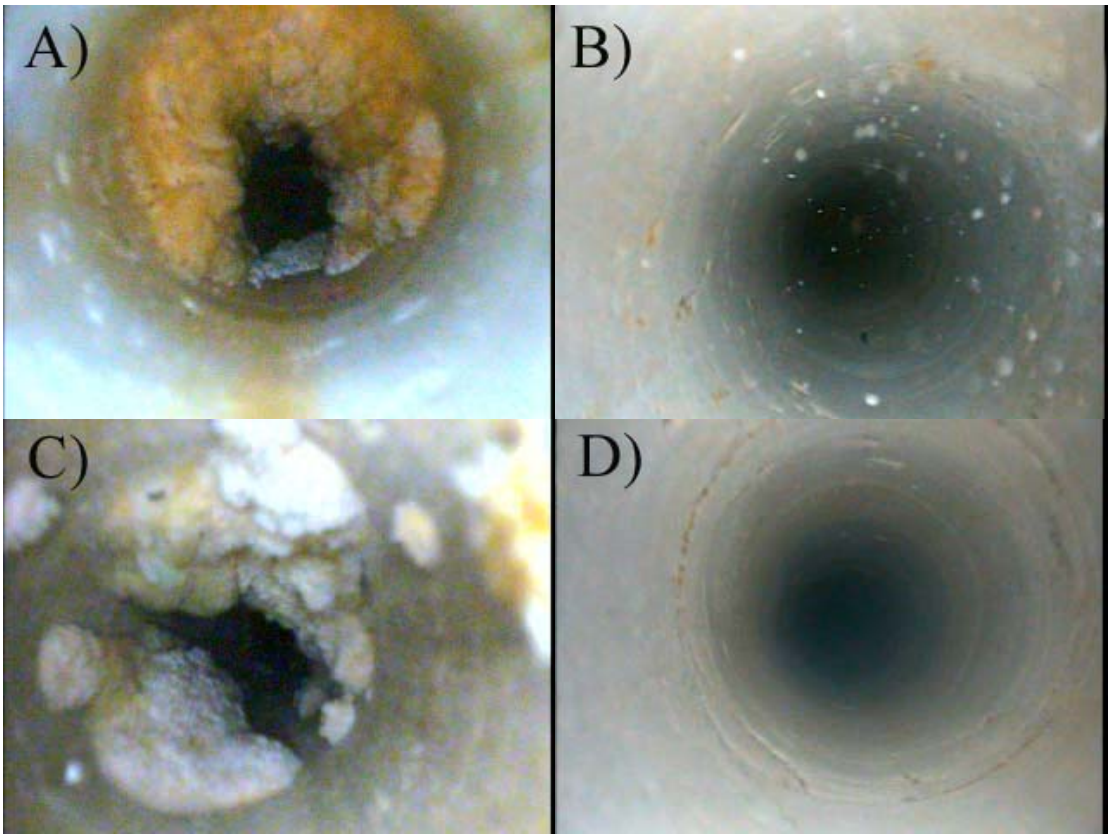

Figure C- 2: Screen captures of MW8. A) Biofouling at 9.14 mbtoc, B) Cleaned at 9.14 mbtoc, C) Biofouled at 10.7 mbtoc, D) Cleaned at 10.7 mbtoc.

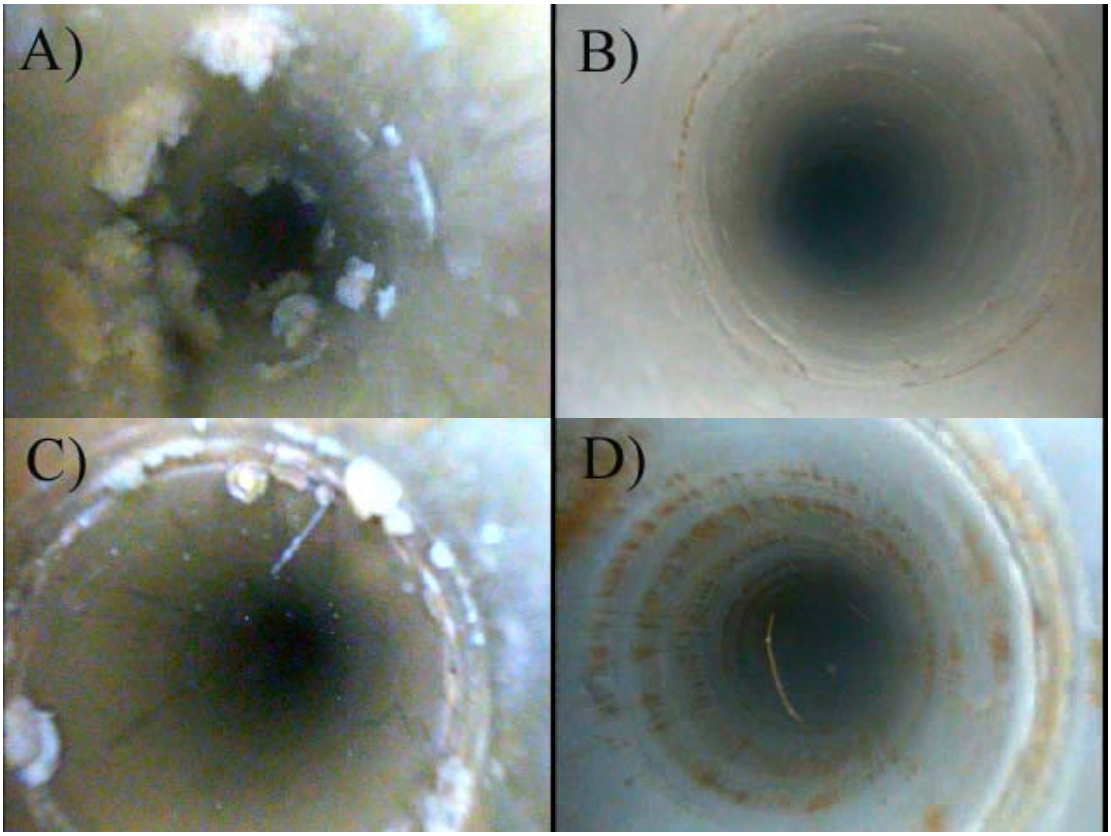

Figure C- 3: Screen captures of MW9. A) Biofouling at 10.7 mbtoc, B) cleaned at 10.7 mbtoc, C) Biofouled at 16.8 mbtoc, D) Cleaned at 16.8 mbtoc.

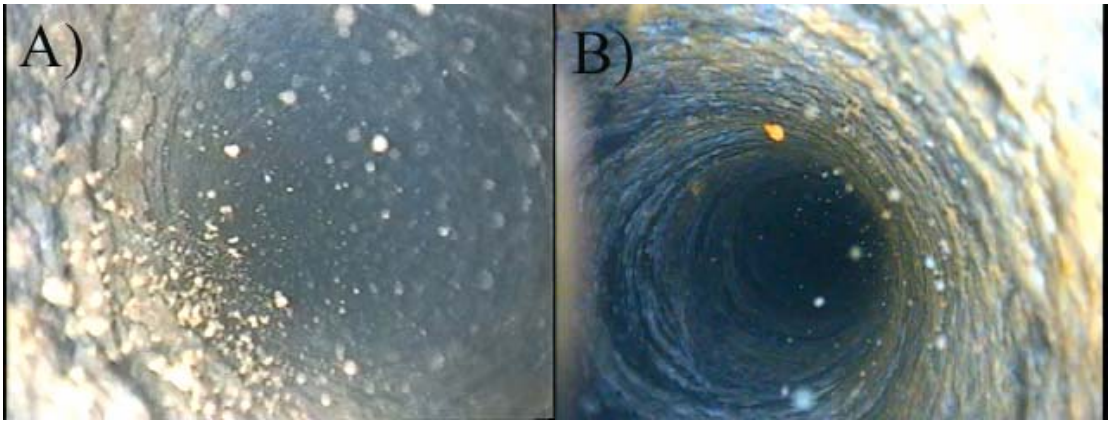

Figure C- 4: Screen captures of WWFS. A) Biofilm present all over wellbore at 29.3mbtoc, B) Cleaned wellbore at 29.3 mbtoc.

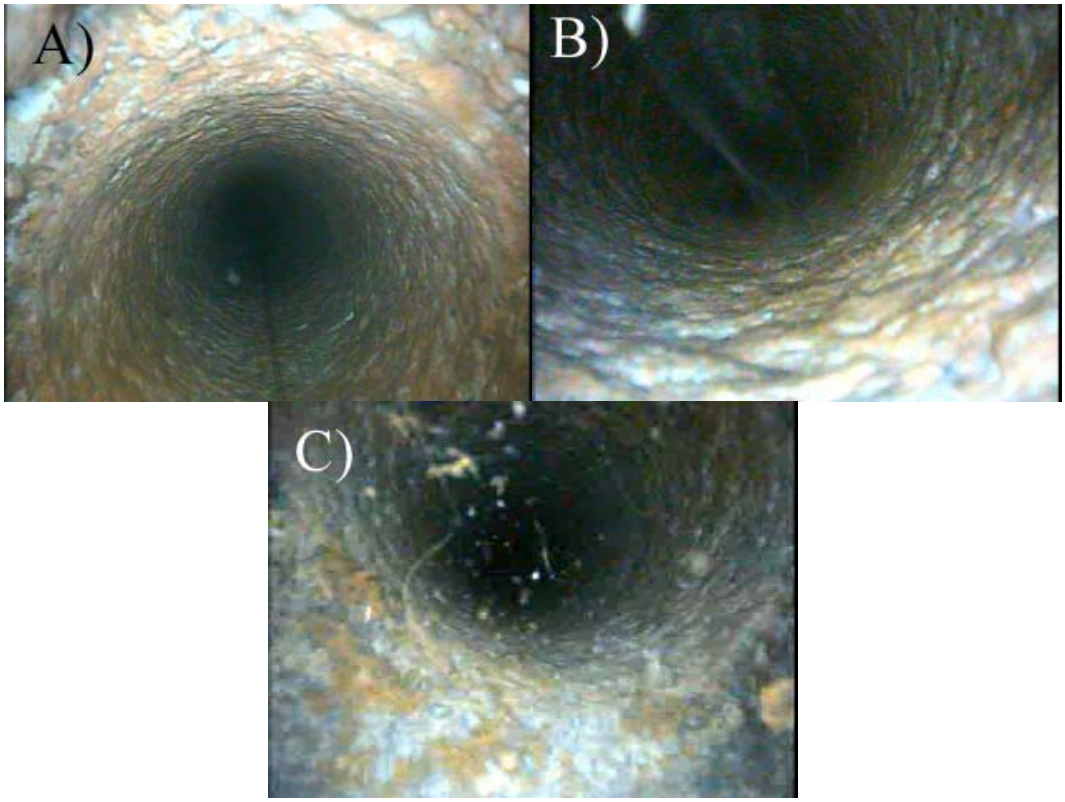

Figure C- 5: Screen captures of TW8. A) Presence of biofouling at 10.7 mbtoc, B) Biofouling presence at 19.81 mbtoc, C) biofouling presence at 34.7 mbtoc.

Appendix D

Positive reactions in BART™ systems from groundwater samples collected from wells at all three field sites. Groundwater chemistry results for each well are presented.

Figure D- 1: BART™ systems showing positive reactions for the presence of indicated bacteria and the lag time between sample water addition and first positive reaction.

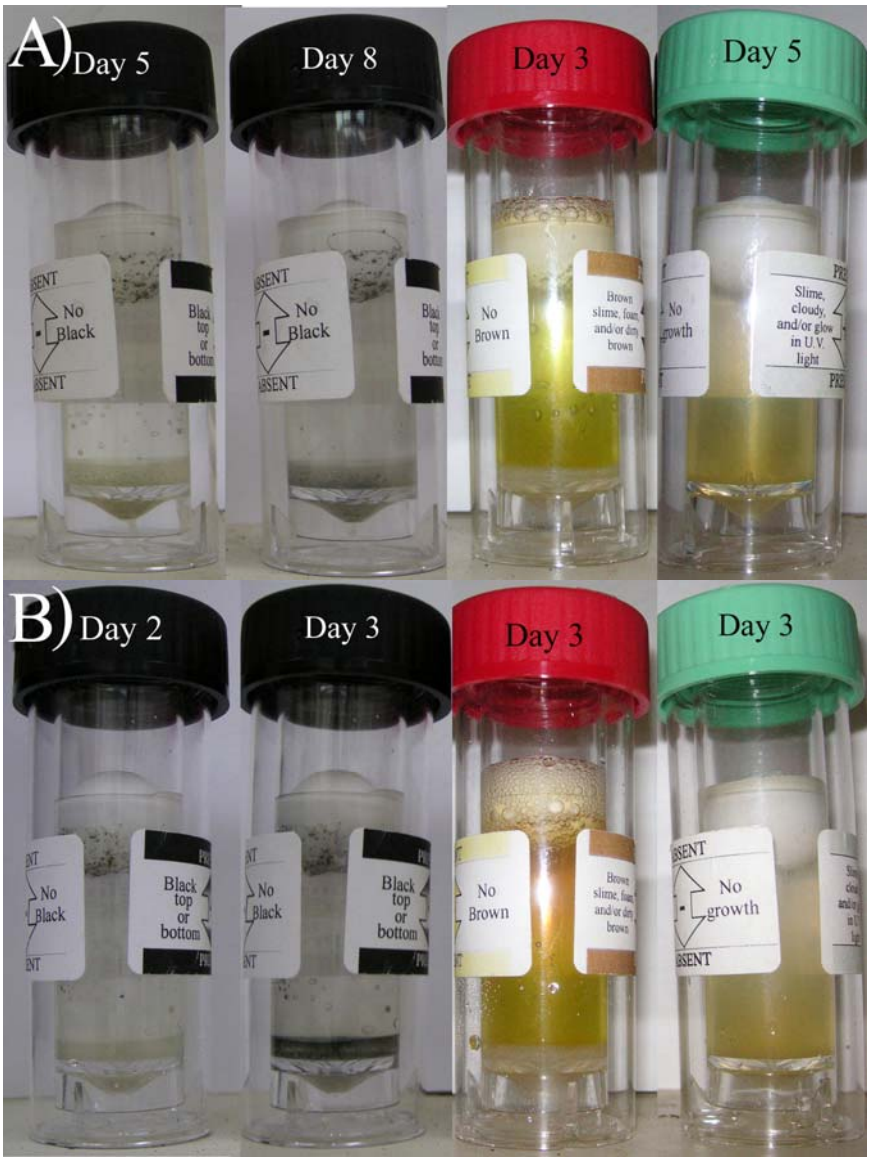

Figure D- 2: SRB, IRB and SLYM BART™ systems showing positive signs of bacteria present, and the time lag from sampling until the positive result. A) Sample water from WWCH, B) Sample water from WWFS.

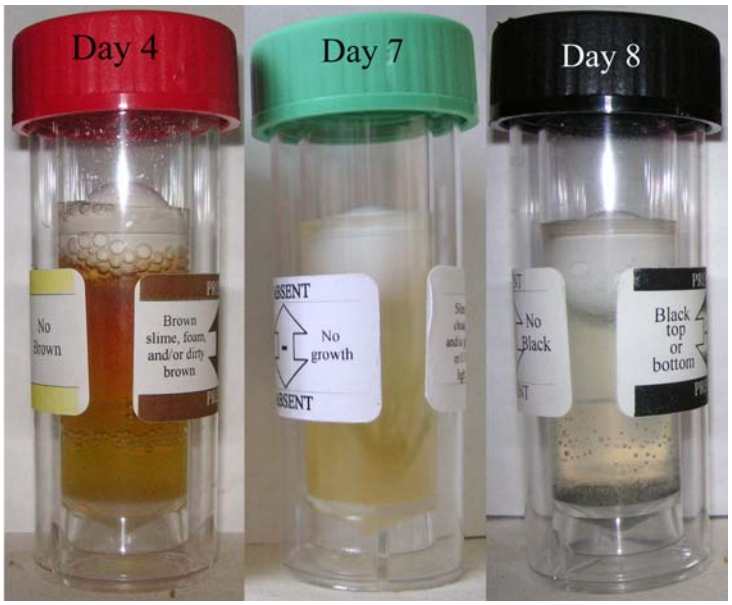

Figure D- 3: Photos of groundwater from TW7 showing a positive reaction in IRB, SLYM and SRB BART™.

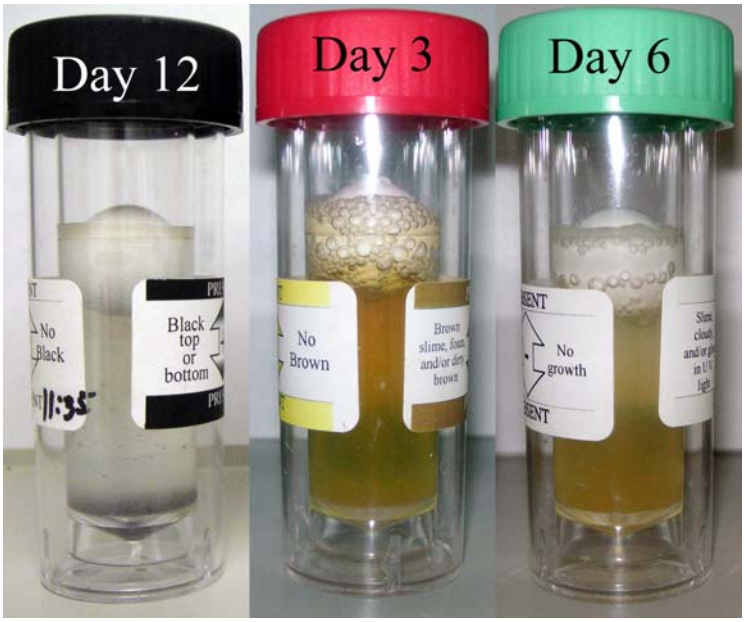

Figure D- 4: Positive results in BARTs™ with sample water from TW8.

Table D- 1: Groundwater chemistry results from the Portland field site. The wells used in this study are located in between wells P2 and P3 and would have similar results.

Well	Sampling Dates	Temperature (C)	DO (mg/L)	pH
P2-D	2/22/2007	6.65	1.76	7.27
P2-M	2/22/2007	7.3	1.97	6.97
P2-S	2/22/2007	4.21	2.21	7.09
P3-D	2/22/2007	8	2.05	6.98
P3-M	2/22/2007	8.2	1.61	6.96
P3-S	2/22/2007	6.79	2.33	7.3
P2-D	3/28/2007	9.95	0.35	7.62
P2-M	3/28/2007	9.49	0.39	6.96
P2-S	3/28/2007	8.94	0.65	7
P3-D	3/28/2007	10.38	0.21	6.81
P3-M	3/28/2007	10.66	0.09	6.88
P3-S	3/28/2007	9.59	0.94	7.5
P2-D	4/4/2007	8.95	0.27	7.64
P2-M	4/4/2007	9.9	0.29	6.97
P2-S	4/4/2007	8.93	0.47	7.01
P3-D	4/4/2007	10.09	0.15	6.89
P3-M	4/4/2007	10.3	0.16	6.91
P3-S	4/4/2007	9.61	2.14	6.99
P2-D	5/3/2007	9.06	0.11	7.68
P2-M	5/3/2007	10.02	0.46	7.05
P2-S	5/3/2007	9	0.11	7.1
P3-D	5/3/2007	10.42	0.22	6.97
P3-M	5/3/2007	10.8	0.3	7.05
P3-S	5/3/2007	10.49	0.49	7.25
P2-D	7/19/2007	11.01	0.37	7.84
P2-M	7/19/2007	9.93	0.31	7.13
P2-S	7/19/2007	9.44	0.32	7.14
P3-D	7/19/2007	10.55	0.12	7.04
P3-M	7/19/2007	11.06	0.14	7.13
P3-S	7/19/2007	11.41	0.13	7.65

Table D- 2: Groundwater chemistry results from the Cambridge field site. The wells used in this study were sampled directly.

Sampled May 15, 2007				
Parameter		**MW7**	**MW8**	**MW9**
pH		7.1	6.93	6.88
Temp.	^{o}C	7.45	9.1	7.72
Alk.(as $CaCO_3$)	ppm	292.7	295.1	289.4
DOC	ppm	1.238	1.2775	1.183
SO_4	ppm	13.07	15.745	13.04
Total P	ppm	0.0209	0.0066	0.0114
Ca	ppm	1016	1002	1027.5
Fe	ppm	<0.05	<0.05	<0.05
K	ppm	7.79	7.52	5.835
Mg	ppm	465	478	461
Na	ppm	35.4	28.7	30.2
S	ppm	65.5	75.65	65.45

Table D- 3: Groundwater chemistry results from the Perth field site. Well TW7 was sampled, located 15 m from TW8, thus the results should be similar.

	Temp	**pH**
TW7S	7.4305	6.720667

Dissolved Oxygen Results						
Well	**7/18/2006**	**8/16/2006**	**9/19/2006**	**10/5/2006**	**11/1/2006**	**12/4/2006**
	mg/L	mg/L	mg/L	mg/L	mg/L	mg/L
TW7S	2.5	3.57	3.82	4.16	4.77	6.72
TW7M	7.0	7.39	6.25	8.05	4.77	6.10
TW7D	6.0	6.50	5.25	6.32	4.82	7.22

Well	Ca	Mg	Na	K	Cl	SO4	NO3	HCO3	TDS
TW7S	32.50	5.80	2.20	1.40	4.00	10.73	0.20	40.00	110.00
TW7M	86.90	22.00	5.00	3.10	26.50	17.87	0.50	258.00	330.00
TW7D	81.60	20.80	4.90	2.50	23.10	14.15	0.90	244.00	310.00

Appendix E

Drawdown versus elapsed time data for the fouled pumping tests, diagrams of type curve matching, corresponding values of transmissivity and storativity from the computer program AQTESOLV, and recovery data from the pumping tests for wells MW7, MW8 and MW9 at the Cambridge field site.

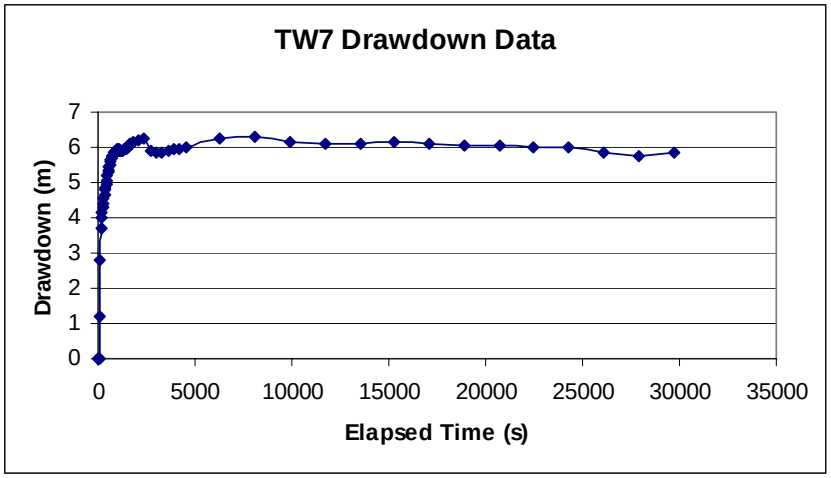

Figure E- 1: Drawdown curve from MW7 pumping test.

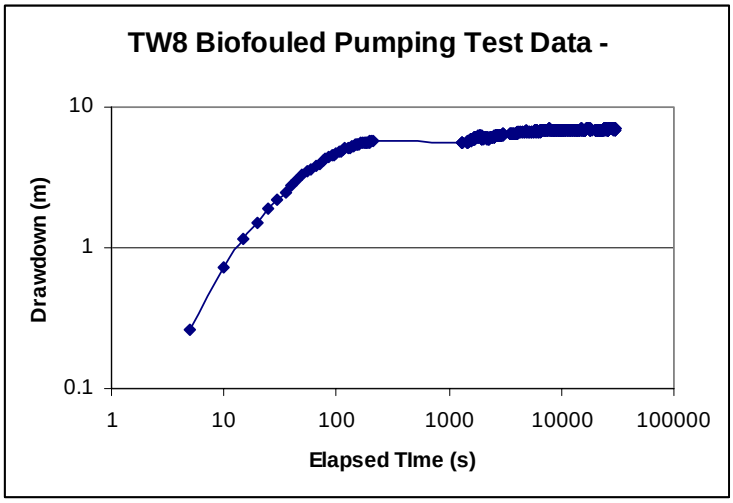

Figure E- 2: Drawdown curve from MW8 pumping test.

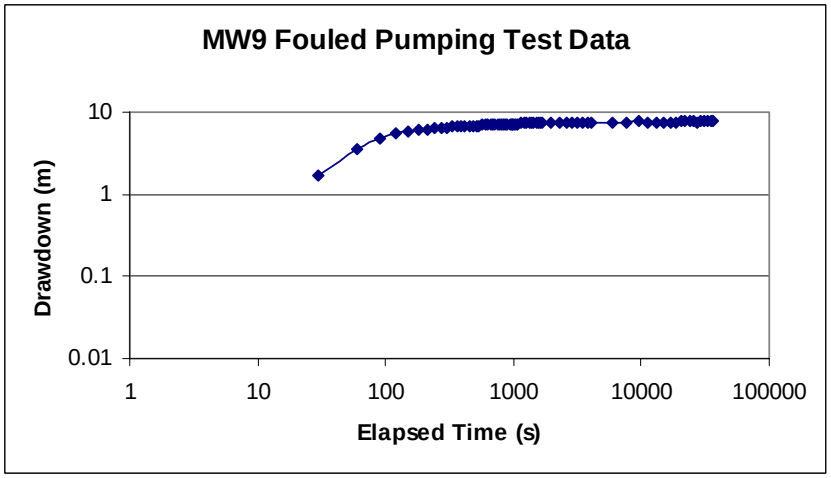

Figure E- 3: Drawdown curve from MW9 pumping test.

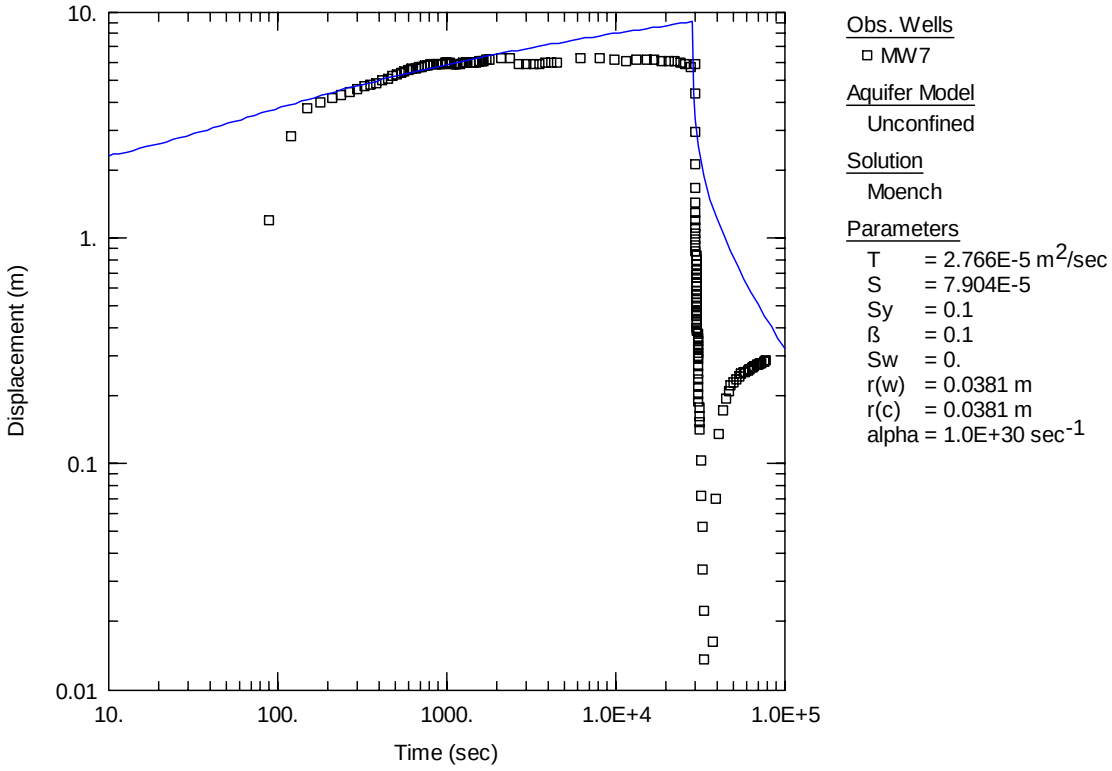

Figure E- 4: Moench (1997) curve matching to MW7 pumping test data with recovery. Theoretical solutions are represented by thin lines and the collected data by data points.

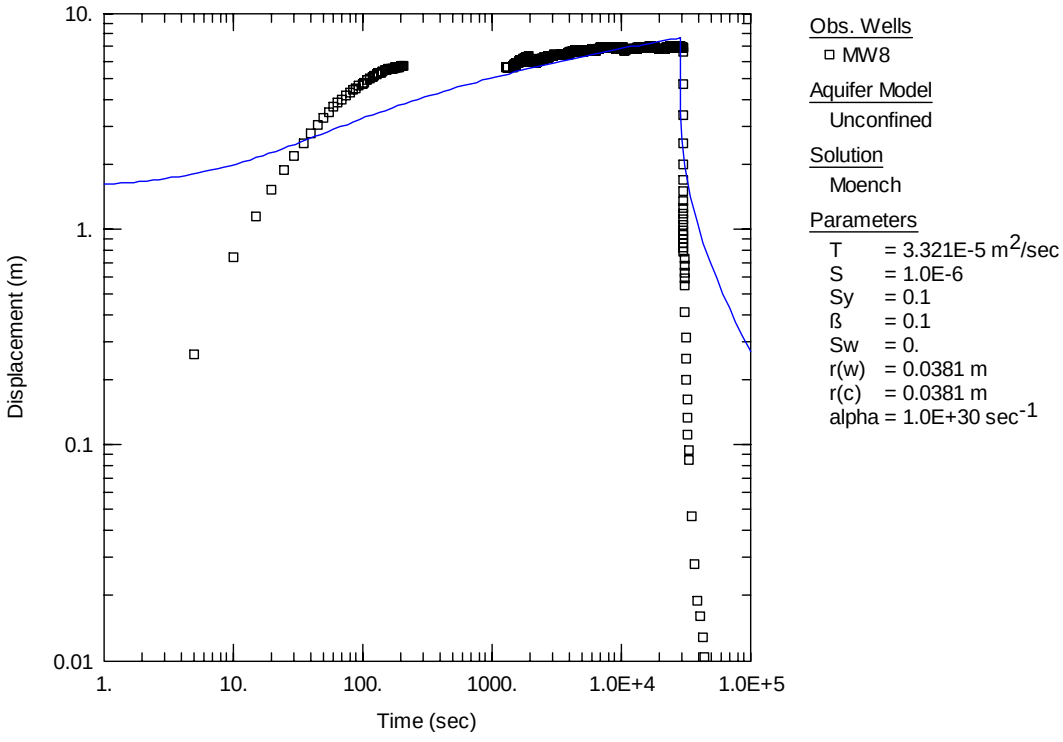

Figure E- 5: Moench (1997) curve matching to MW8 pumping test data with recovery. Theoretical solutions are represented by thin lines and the collected data by data points.

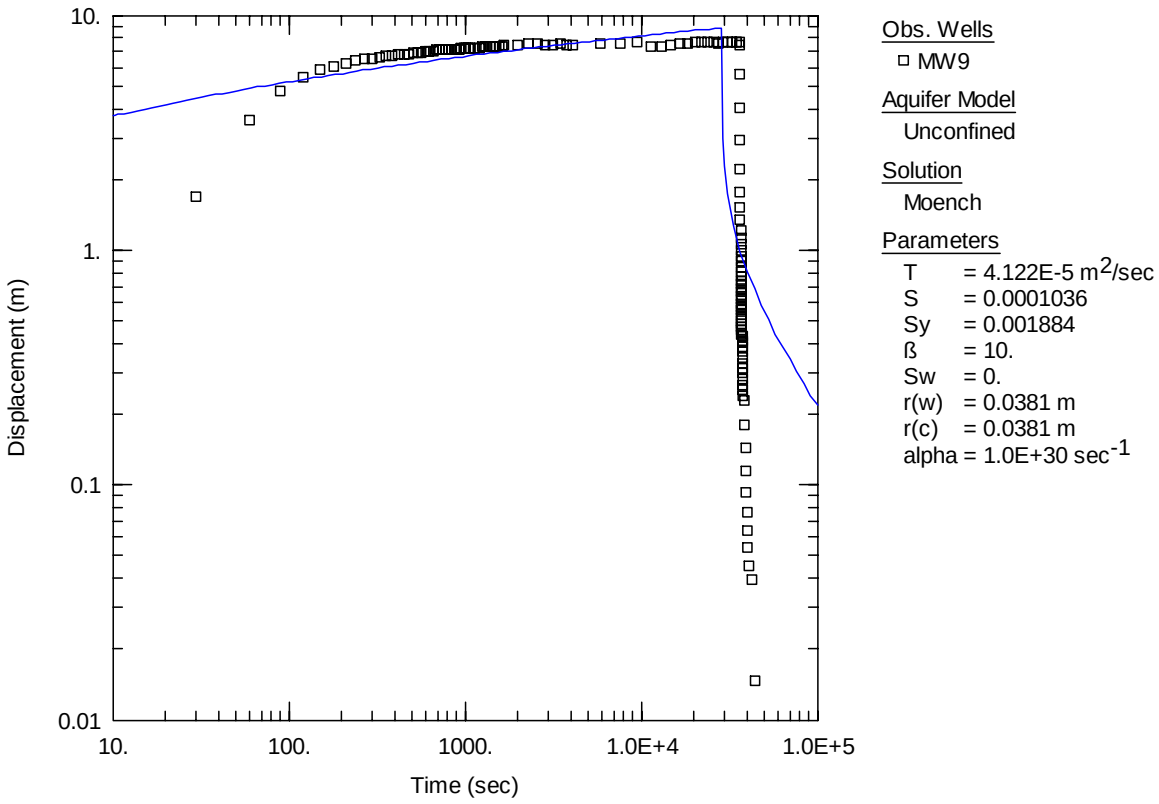

Figure E- 6: Moench (1997) curve matching to MW9 pumping test data with recovery. Theoretical solutions are represented by thin lines and the collected data by data points.

A)

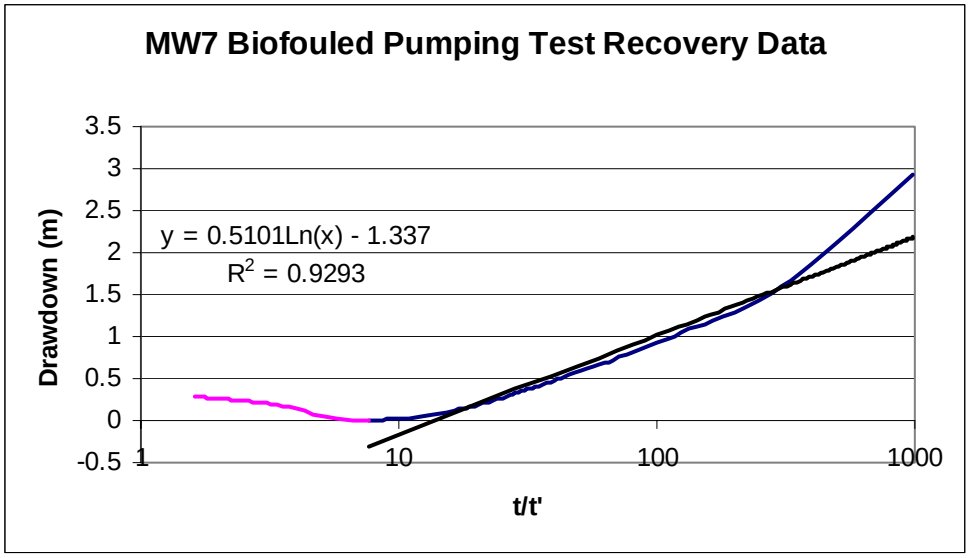

B)

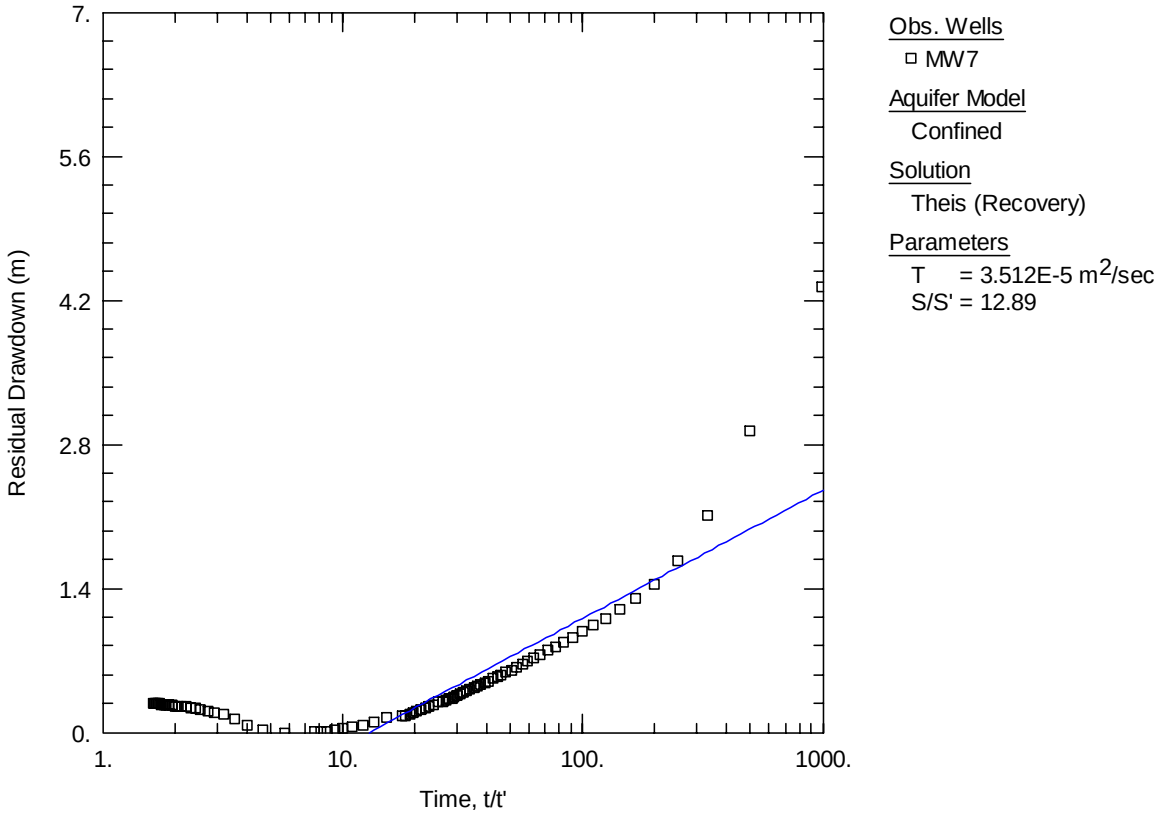

Figure E- 7: Theis Recovery Analysis of MW7 recovery data. A) Linear approximations, B) AQTESOLV solutions. Theoretical solutions are represented by thin lines and the collected data by data points.

A)

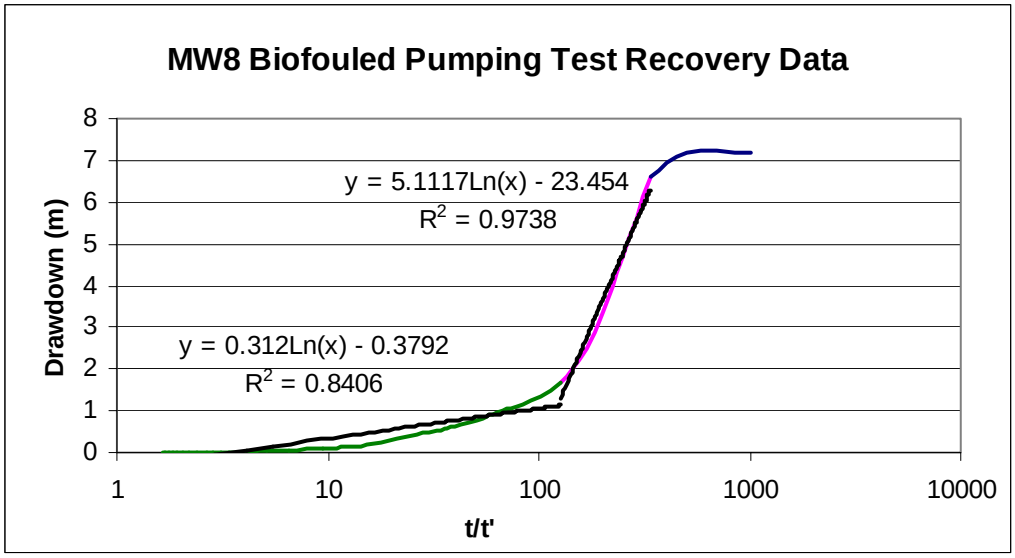

B)

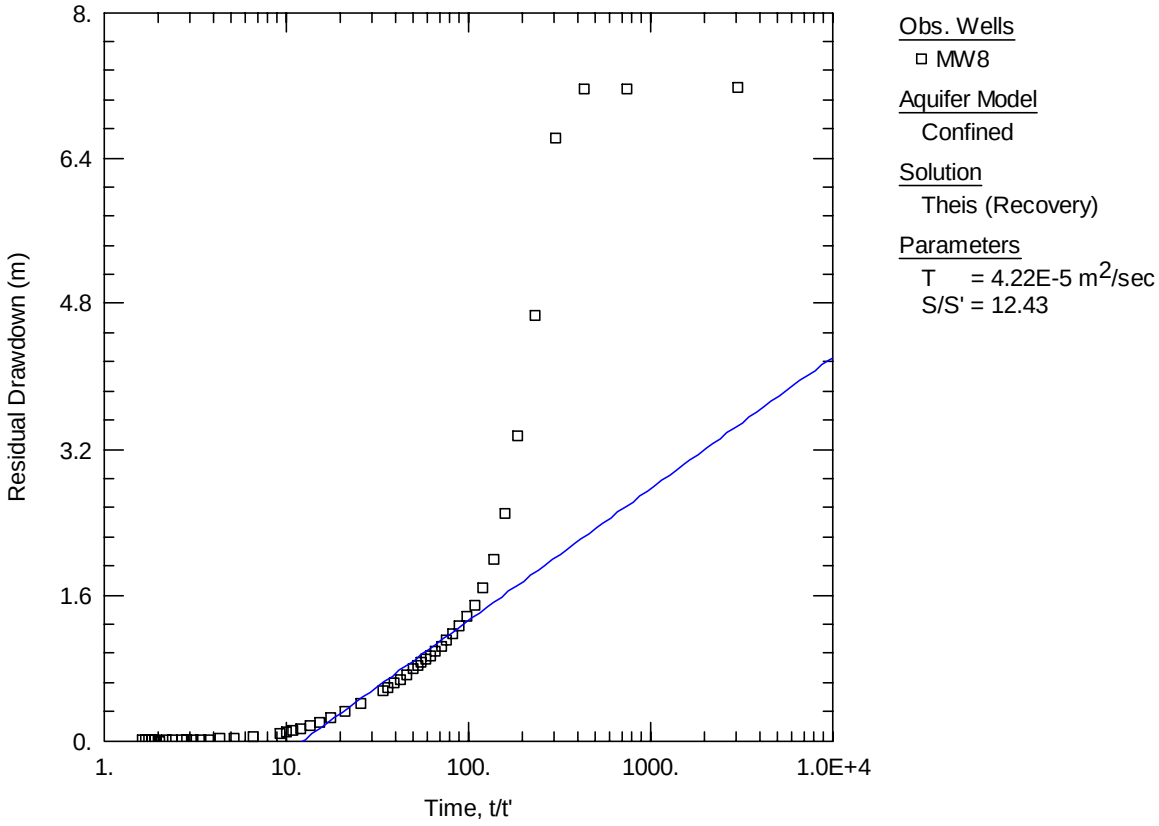

Figure E- 8: Theis recovery analysis of MW8 recovery data. A) Linear approximations, B) AQTESOLV solutions. Theoretical solutions are represented by thin lines and the collected data by data points.

A)

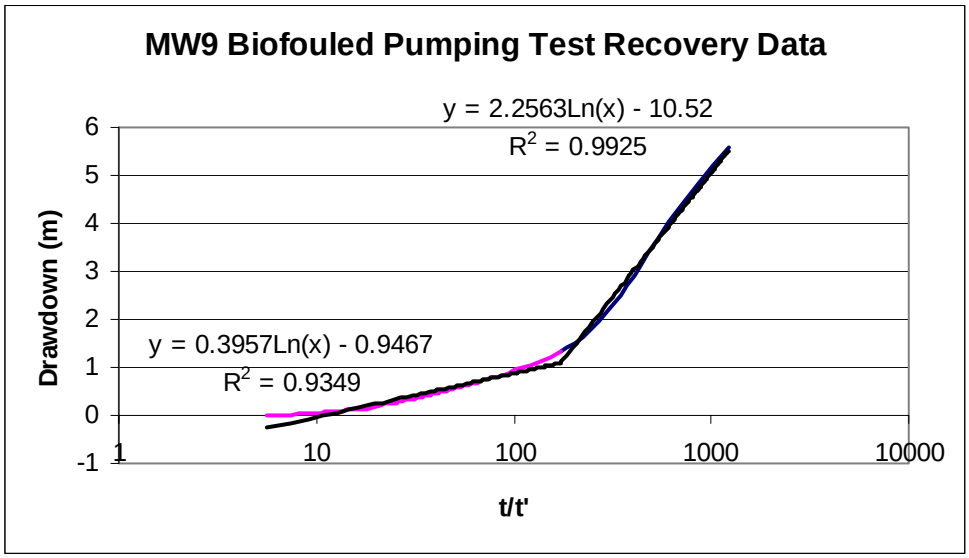

B)

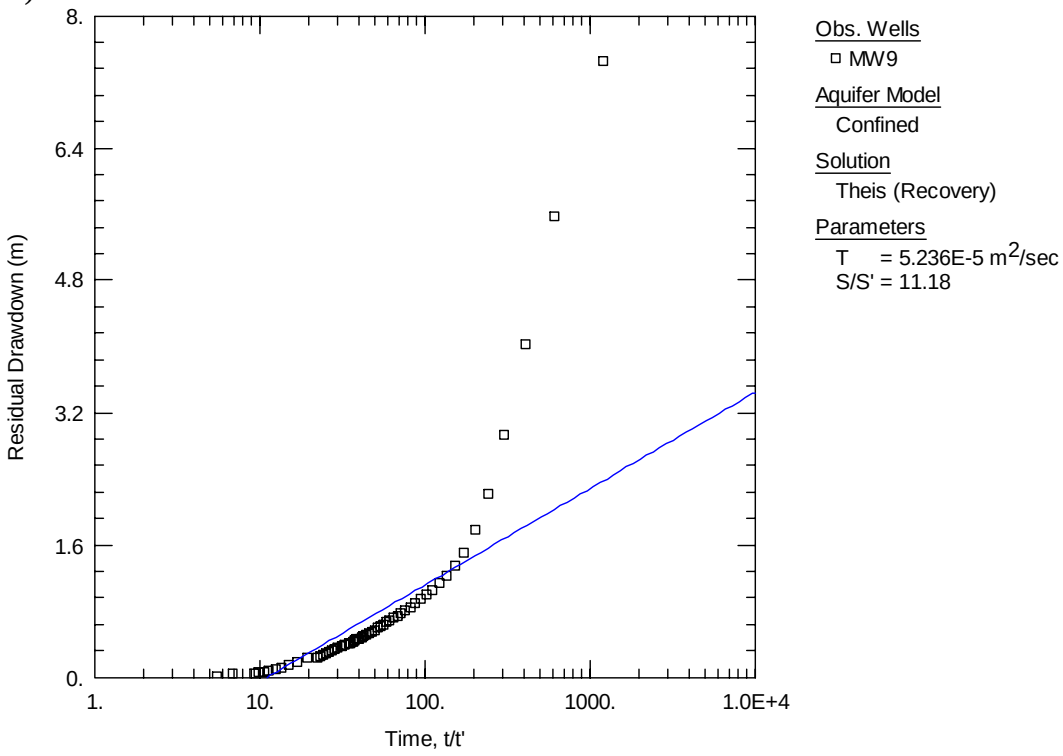

Figure E- 9: Theis recovery analysis of MW9 recovery data. A) Linear approximations, B) AQTESOLV solutions. Theoretical solutions are represented by thin lines and the collected data by data points.

Appendix F

Graphs displaying Moench(1997) method and Theis (1935) method for curve matching for pumping test results for WWCH and WWFS in the cleaned state. Recovery plots for WWCH in the biofouled state and cleaned states to determine skin effects.

A)

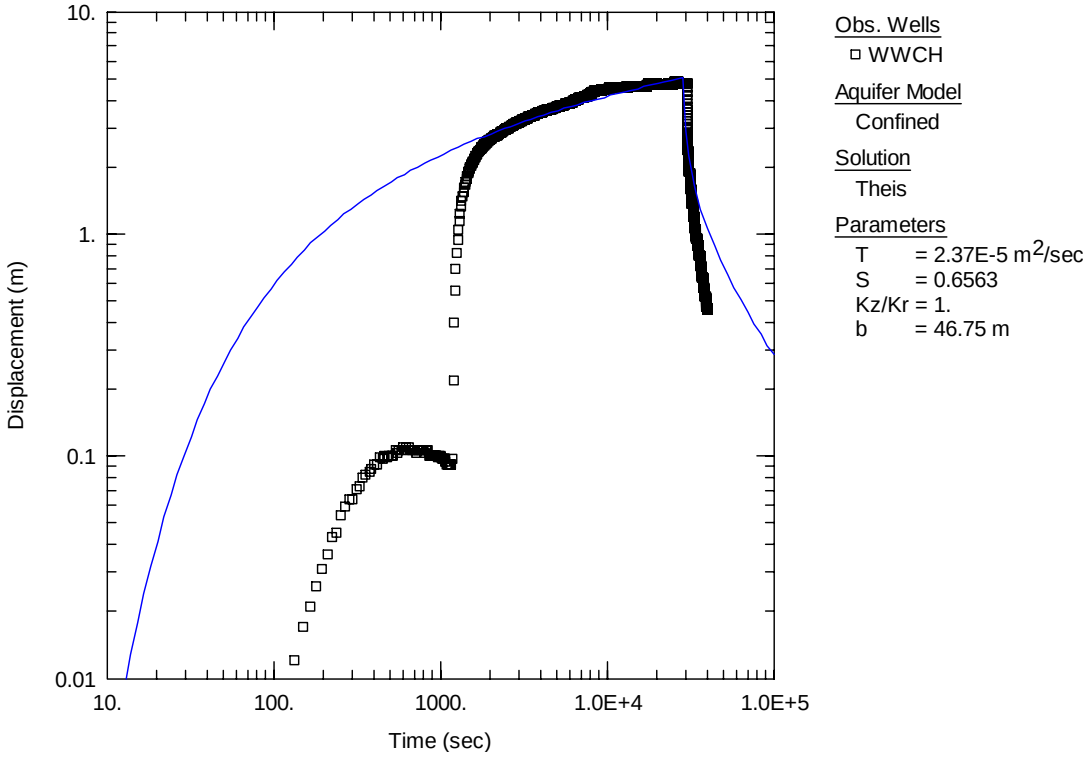

B)

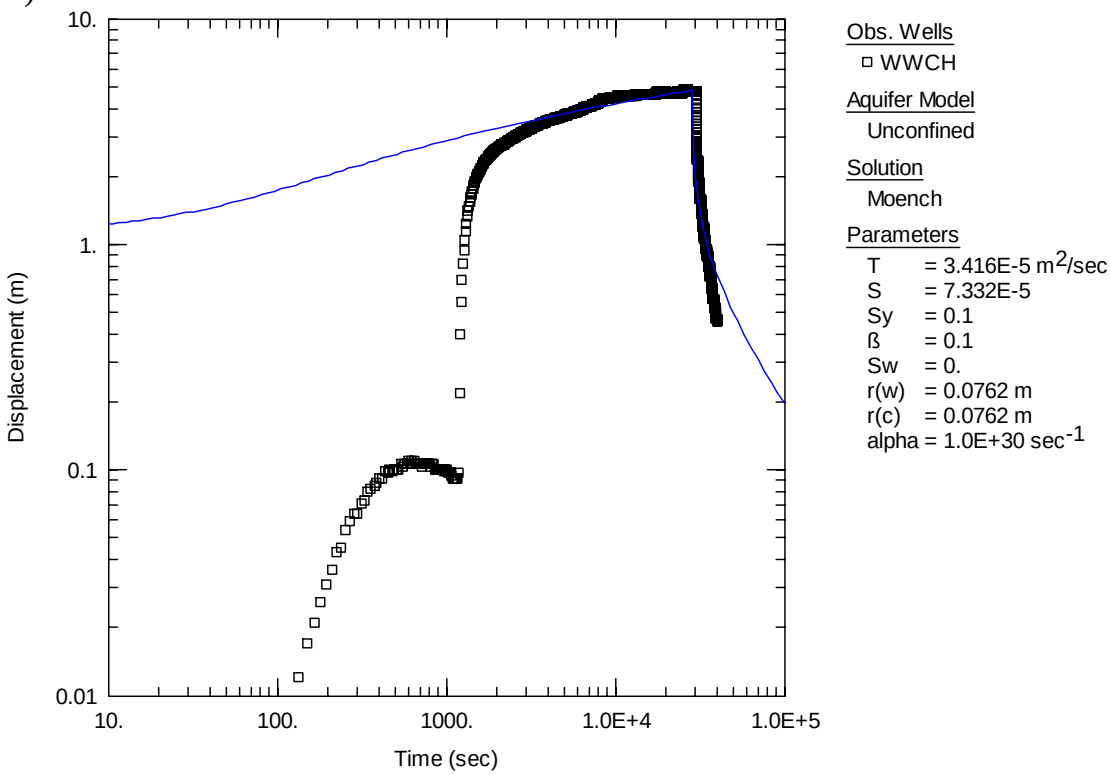

Figure F- 1: Curve match of WWCH cleaned state pumping test data with Theis (1935) solution. B) Curve match of WWCH cleaned state pumping test data with Moench (1997) solution. Theoretical solutions are represented by thin lines and the collected data by data points.

A)

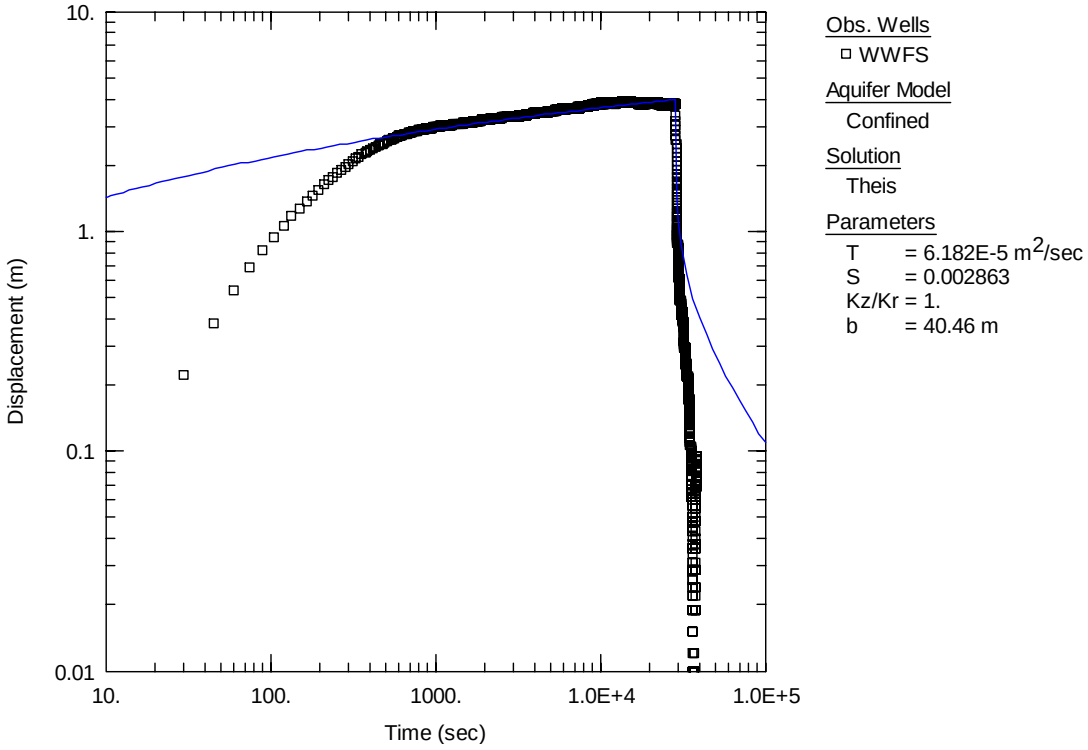

B)

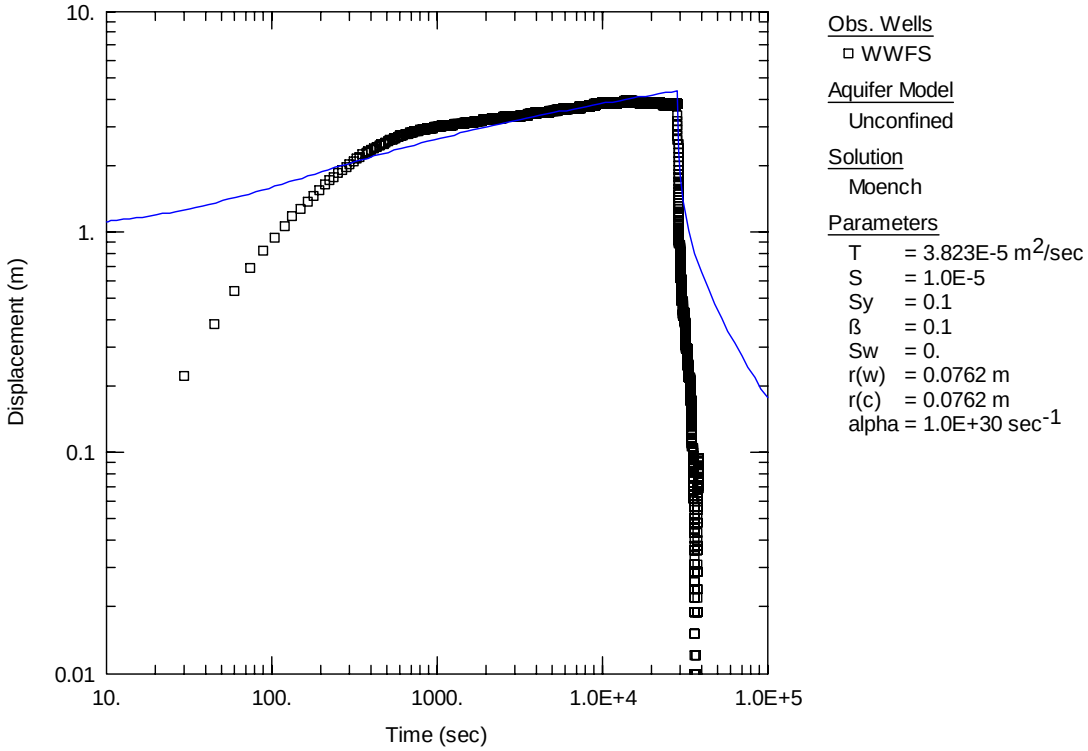

Figure F- 2: A) Curve match of WWFS cleaned state pumping test data with Theis (1935) solution. B) Curve match of WWFS cleaned state pumping test data with Moench (1997) solution. Theoretical solutions are represented by thin lines and the collected data by data points.

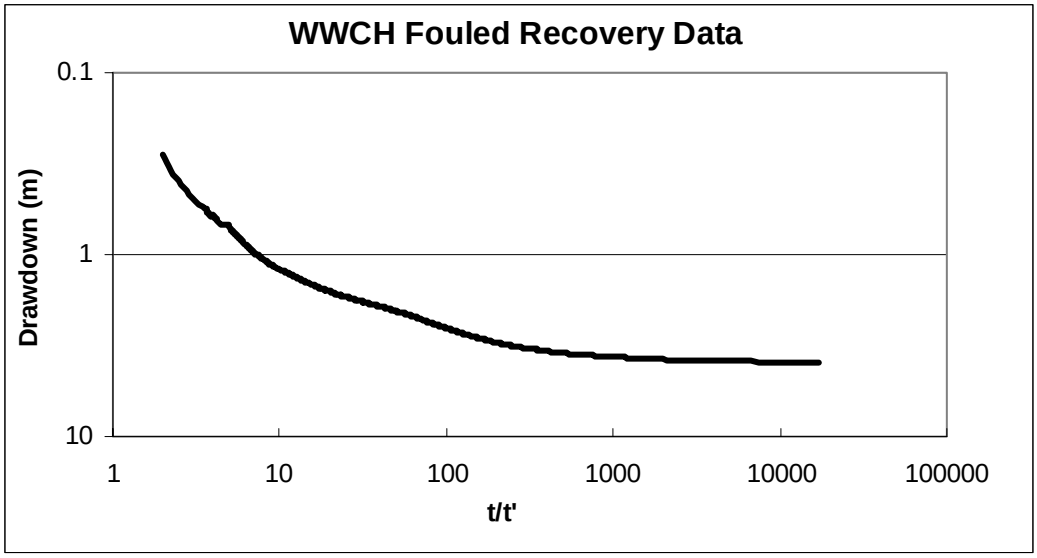

Figure F- 3: Recovery data from the WWCH biofouled pumping test.

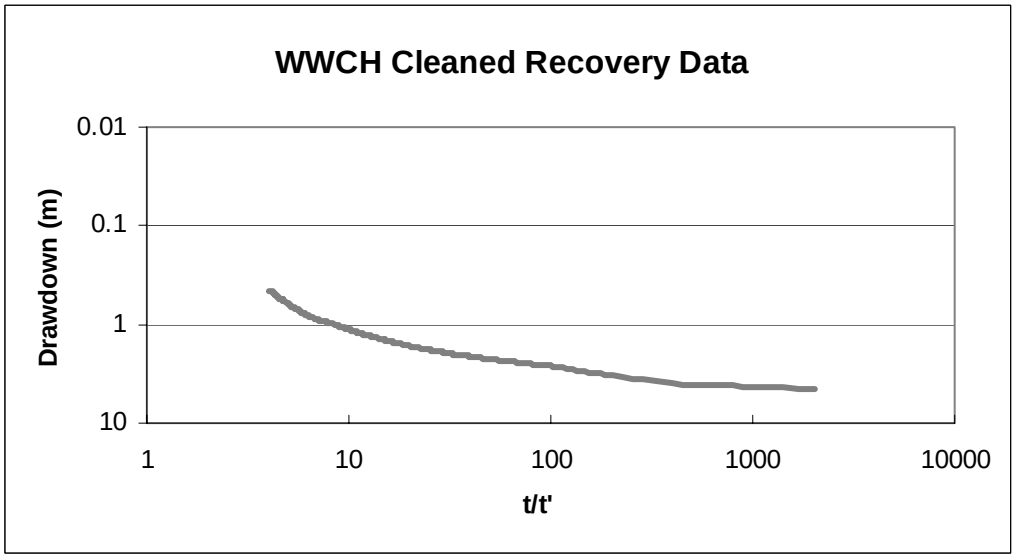

Figure F- 4: Recovery Data from the WWCH cleaned pumping test.

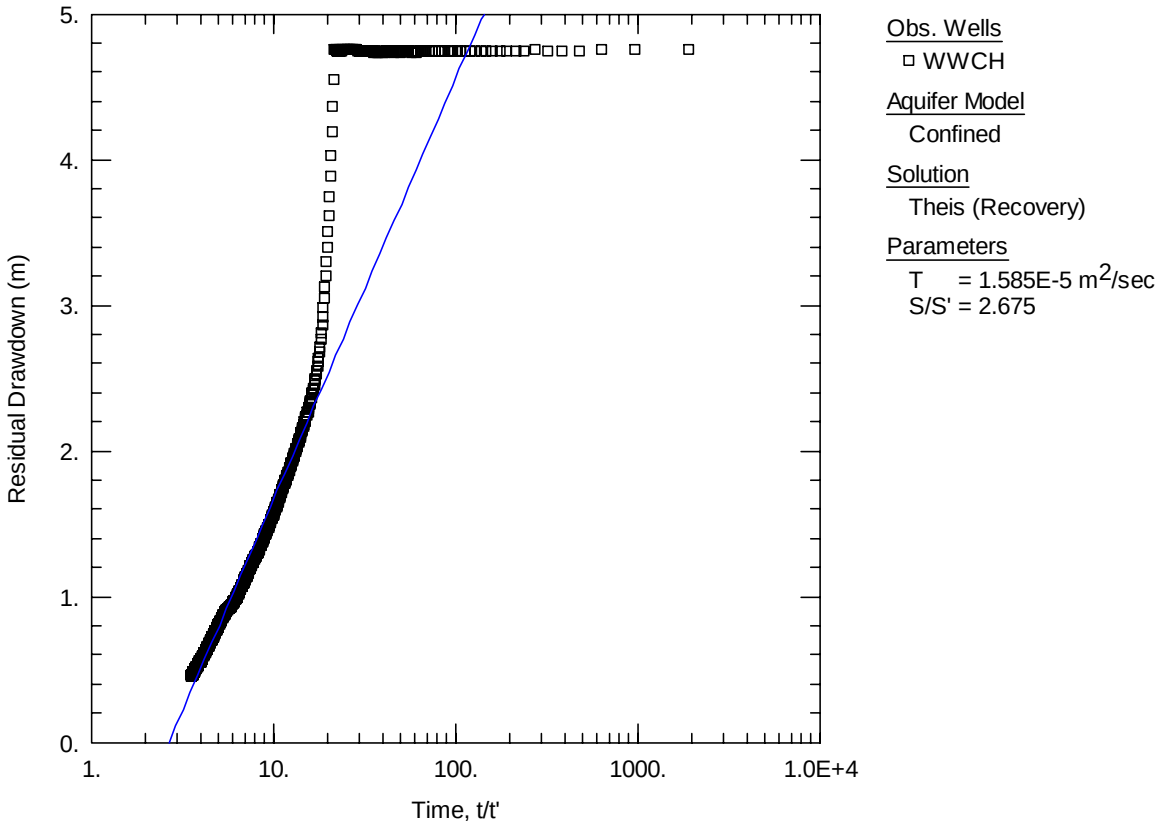

Figure F- 5: Recovery data from WWCH pumping test in the cleaned state with Theis (1935) recovery method approximation. Theoretical solutions are represented by thin lines and the collected data by data points.

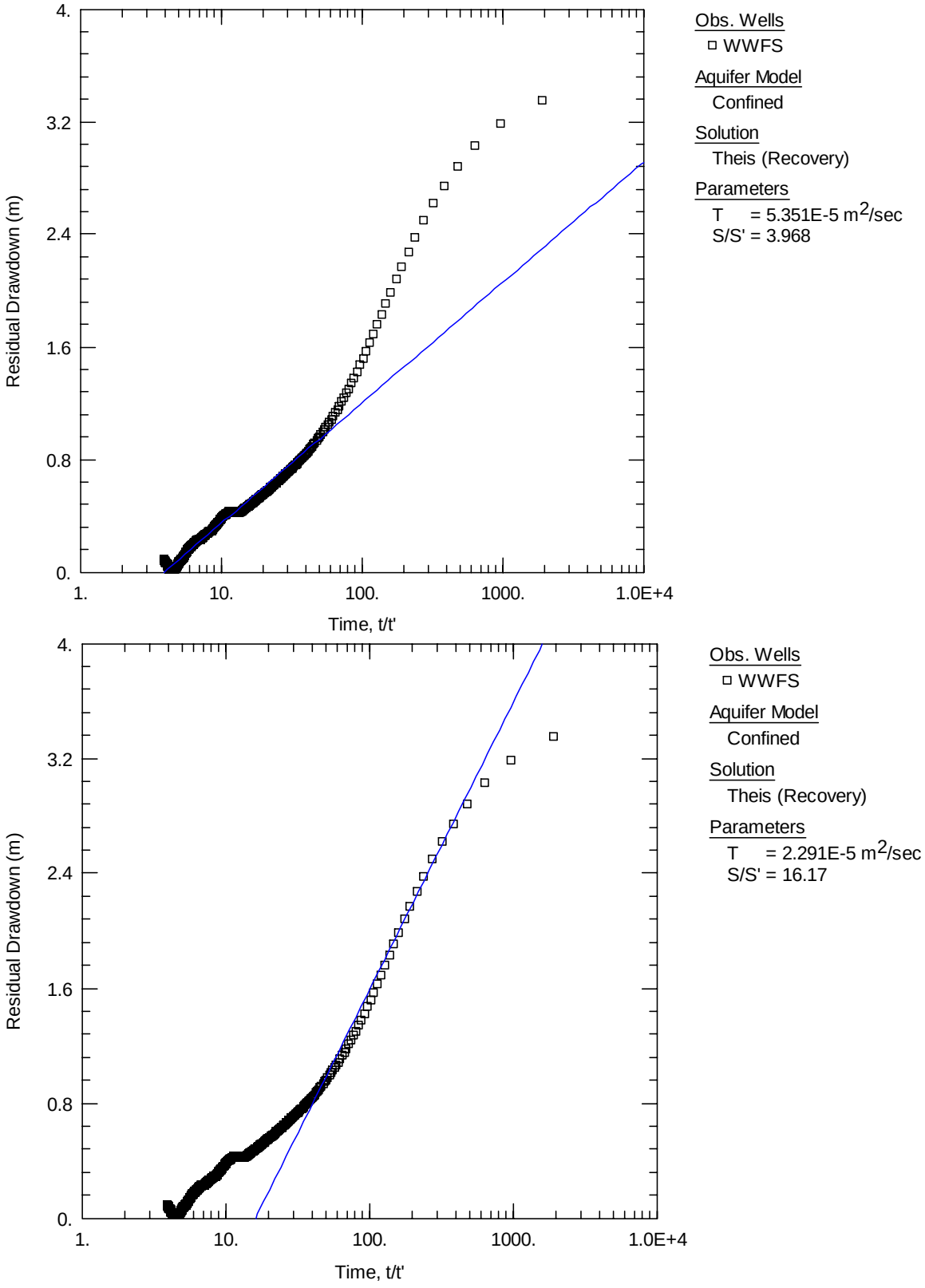

Figure F- 6: Two attempts with recovery data from WWFS pumping test in the cleaned state with Theis (1935) recovery method approximation. Theoretical solutions are represented by thin lines and the collected data by data points.

Appendix G

Transmissivity-depth profiles obtained from straddle packer tests of constant head injection test and slug tests. Profiles for wells MW8 and MW9 from the Cambridge field site and wells WWCH and WWFS from the Portland field site.

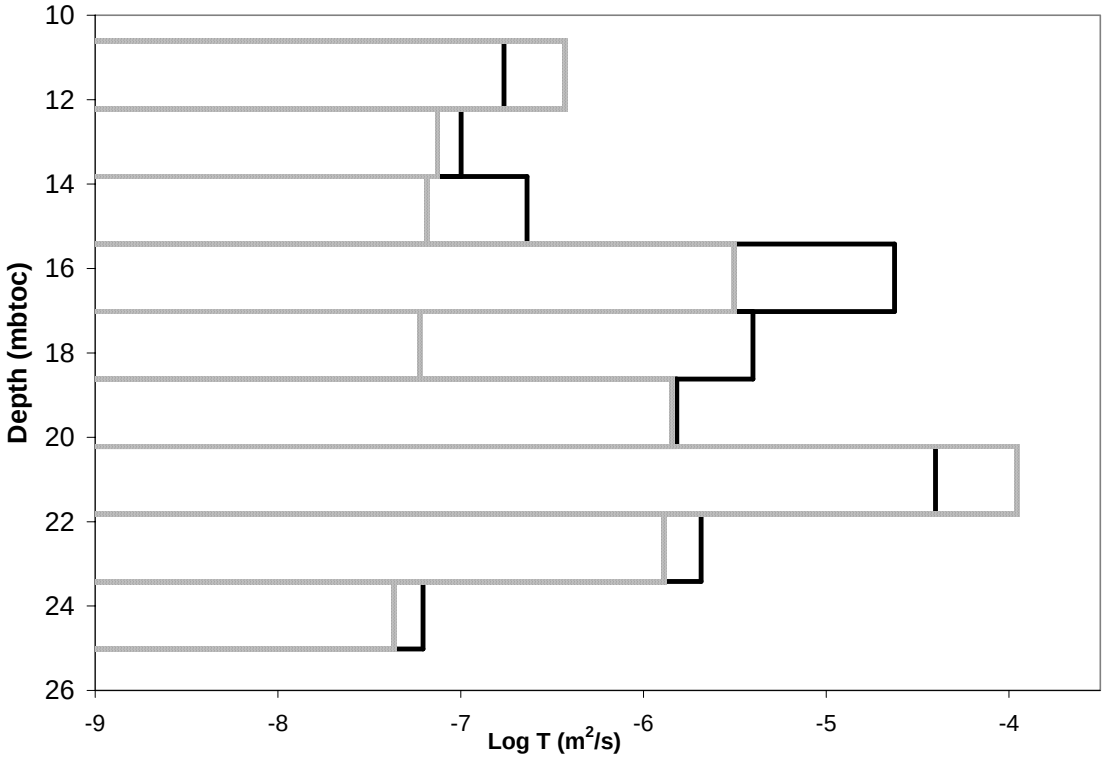

Figure G- 1: Transmissivity – depth profile for MW8. Grey lines represent biofouled values and black lines represent cleaned values.

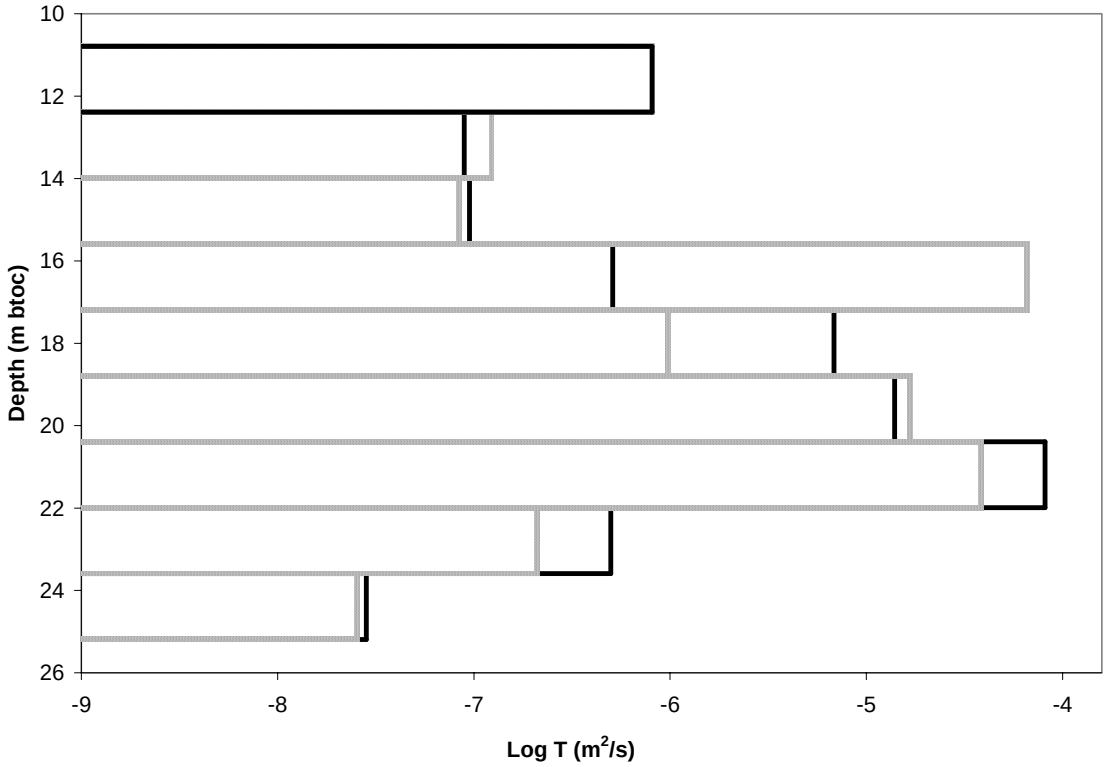

Figure G- 2: Transmissivity- depth profile for MW9. Grey lines represent biofouled values and black lines represent cleaned values.

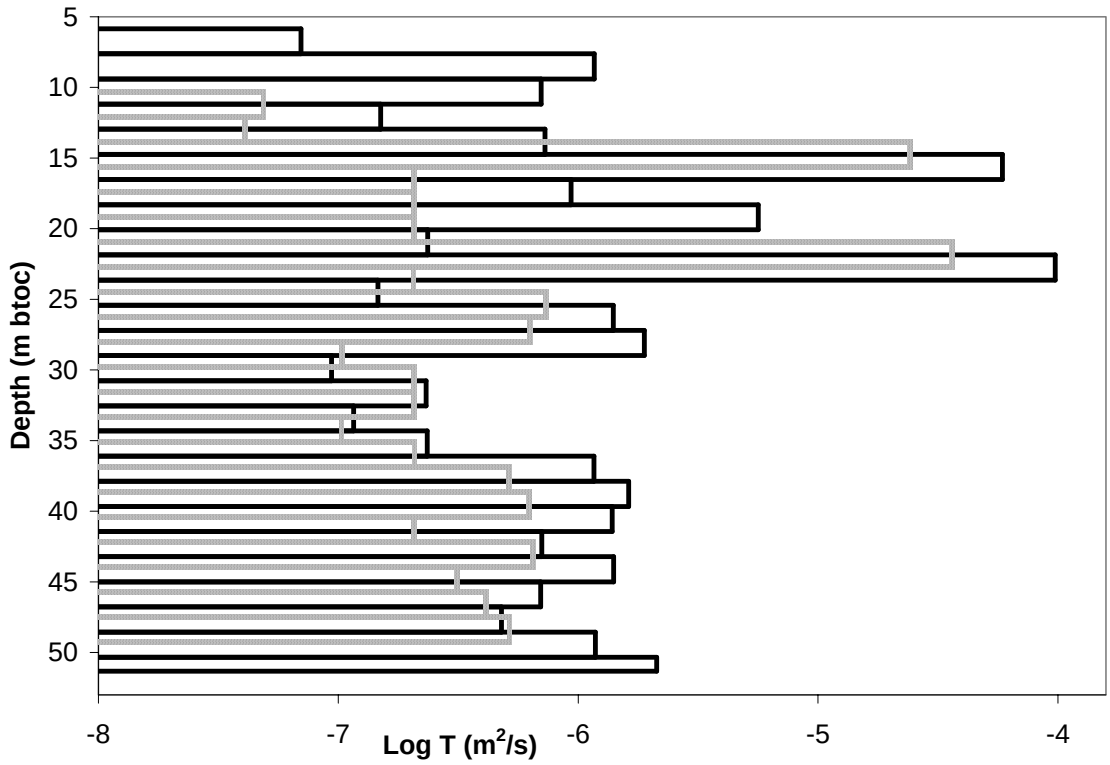

Figure G- 3: Transmissivity-depth profile for WWCH. Grey lines represent biofouled values and black lines represent cleaned values.

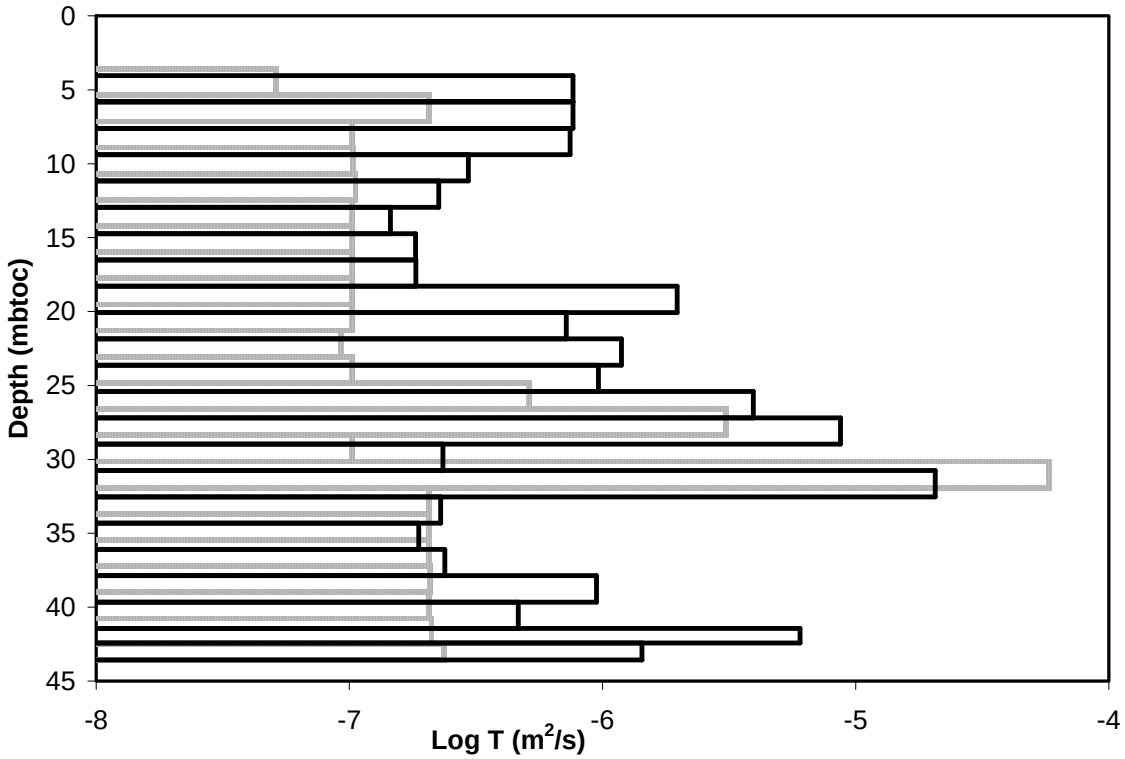

Figure G- 4: Transmissivity-depth profile for WWFS. Grey lines represent biofouled values and black lines represent cleaned values.

Appendix H

Geometric mean calculations of the hydraulic testing using packers for each well in the two states examined. Geometric means of the entire well and of only the low transmissivity values are summarized. Histograms of the transmissivity values are presented.

Table H- 1: Geometric mean values of MW7 transmissivity in both states examined, and of the low transmissivity zones.

Biofouled				Cleaned		
Interval	T (m2/s)	T (m2/s)		Interval	T (m2/s)	T (m2/s)
1	2.8E-05	2.8E-05		1	1.8E-08	1.8E-08
2	6.1E-07	6.1E-07		2	4.1E-08	4.1E-08
3	1.8E-07	1.8E-07		3	1.6E-04	
4	3.7E-04			4	2.8E-06	2.8E-06
5	1.3E-05	1.3E-05		5	7.1E-08	7.1E-08
6	9.9E-07	9.9E-07		6	1.1E-04	
7	5.6E-05	5.6E-05		7	1.6E-07	1.6E-07
8	1.6E-08	1.6E-08		8	6.3E-06	6.3E-06
Geometric Mean	3.3E-06	1.7E-06		Geometric Mean	1.1E-06	2.3E-07
Arithmetic Mean	5.9E-05	1.4E-05		Arithmetic Mean	3.4E-05	1.6E-06
Harmonic Mean	1.1E-07	9.6E-08		Harmonic Mean	7.8E-08	5.9E-08

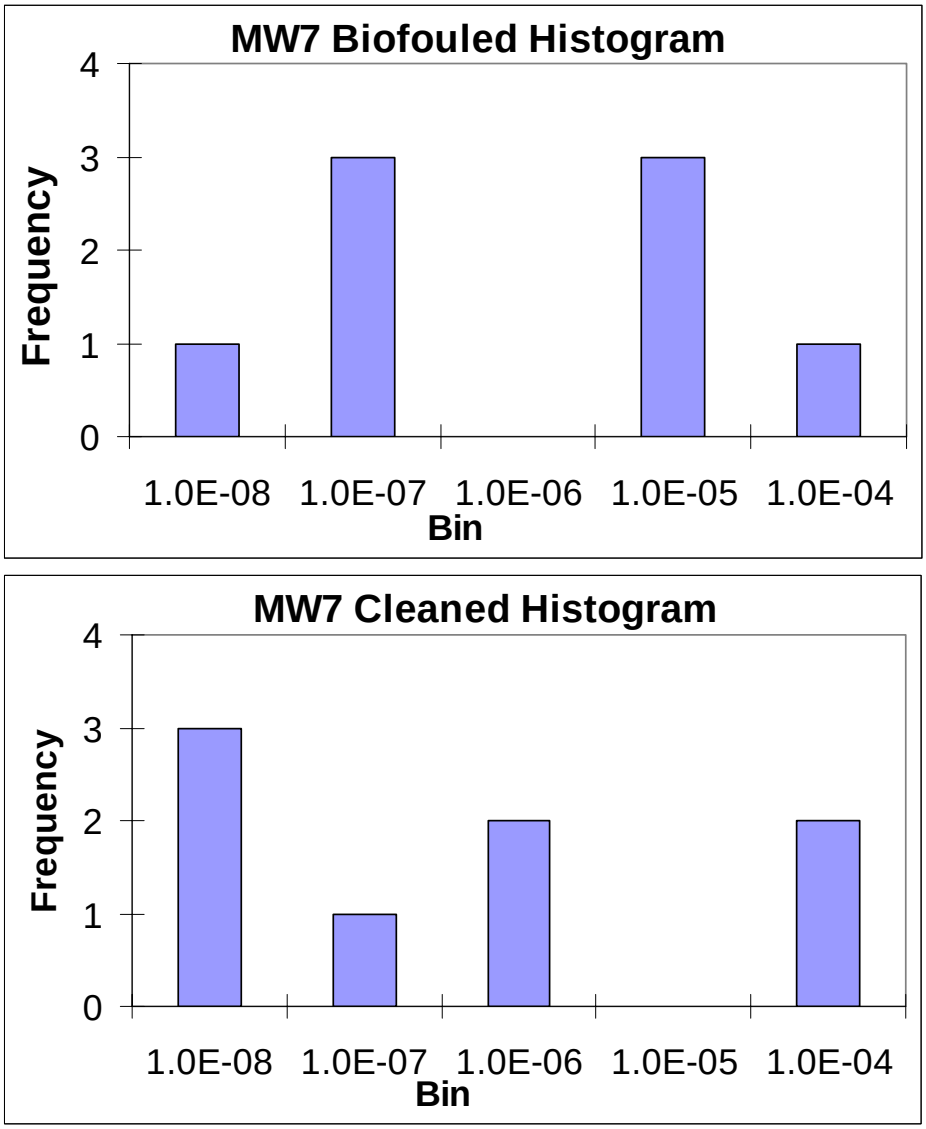

Figure H - 1: Histograms of the transmissivity data collected through hydraulic testing using packers.

Table H- 2: Geometric mean values of MW8 transmissivity in both states examined, and of the low transmissivity zones.

Biofouled				Cleaned		
Interval	T (m2/s)	T (m2/s)		Interval	T (m2/s)	T (m2/s)
1	3.7E-07	3.7E-07		1	1.7E-07	1.7E-07
2	7.4E-08	7.4E-08		2	1.0E-07	1.0E-07
3	6.5E-08	6.5E-08		3	2.3E-07	2.3E-07
4	3.1E-06	3.1E-06		4	2.4E-05	
5	6.0E-08	6.0E-08		5	4.0E-06	4.0E-06
6	1.4E-06	1.4E-06		6	1.5E-06	1.5E-06
7	1.1E-04			7	4.0E-05	
8	1.3E-06	1.3E-06		8	2.1E-06	2.1E-06
9	4.3E-08	4.3E-08		9	6.2E-08	6.2E-08
Geometric Mean	5.2E-07	2.7E-07		Geometric Mean	1.1E-06	4.4E-07
Arithmetic Mean	1.3E-05	8.1E-07		Arithmetic Mean	7.9E-06	1.2E-06
Harmonic Mean	1.2E-07	1.1E-07		Harmonic Mean	2.4E-07	1.9E-07

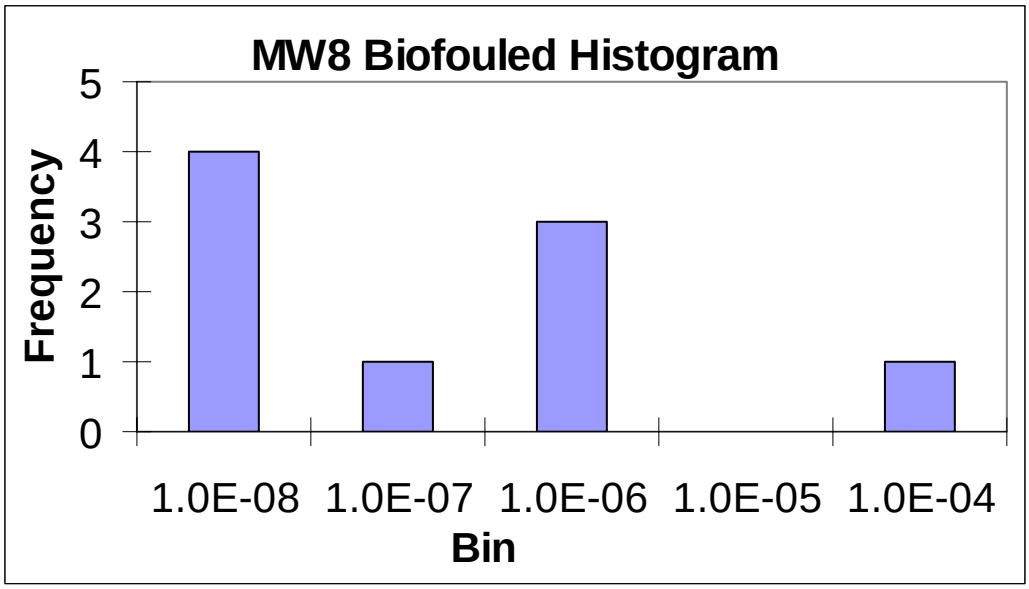

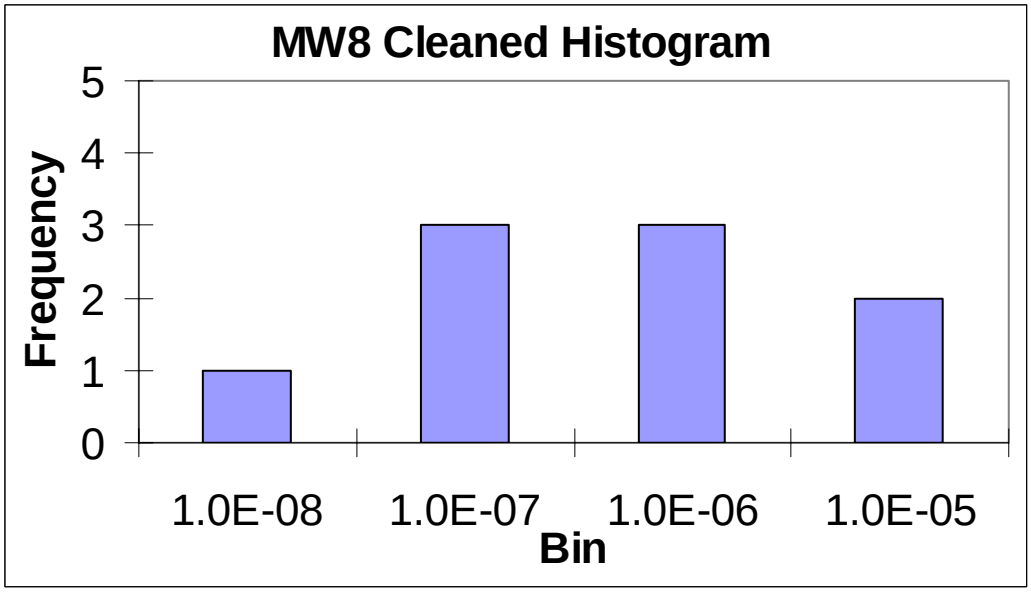

Figure H - 2: Histograms of the transmissivity data collected through hydraulic testing using packers.

Table H- 3: Geometric mean values of MW9 transmissivity in both states examined, and of the low transmissivity zones.

Biofouled				Cleaned		
Interval	T (m2/s)	T (m2/s)		Interval	T (m2/s)	T (m2/s)
1	8.1E-07	8.1E-07		1	8.1E-07	8.1E-07
2	1.2E-07	1.2E-07		2	8.9E-08	8.9E-08
3	8.4E-08	8.4E-08		3	9.5E-08	9.5E-08
4	6.6E-05			4	5.1E-07	5.1E-07
5	9.7E-07	9.7E-07		5	6.8E-06	6.8E-06
6	1.7E-05			6	1.4E-05	
7	3.9E-05			7	8.1E-05	
8	2.1E-07	2.1E-07		8	5.0E-07	5.0E-07
9	2.5E-08	2.5E-08		9	2.8E-08	2.8E-08
Geometric Mean	1.1E-06	1.9E-07		Geometric Mean	9.0E-07	3.2E-07
Arithmetic Mean	1.4E-05	3.7E-07		Arithmetic Mean	1.2E-05	1.3E-06
Harmonic Mean	1.4E-07	9.0E-08		Harmonic Mean	1.4E-07	1.1E-07

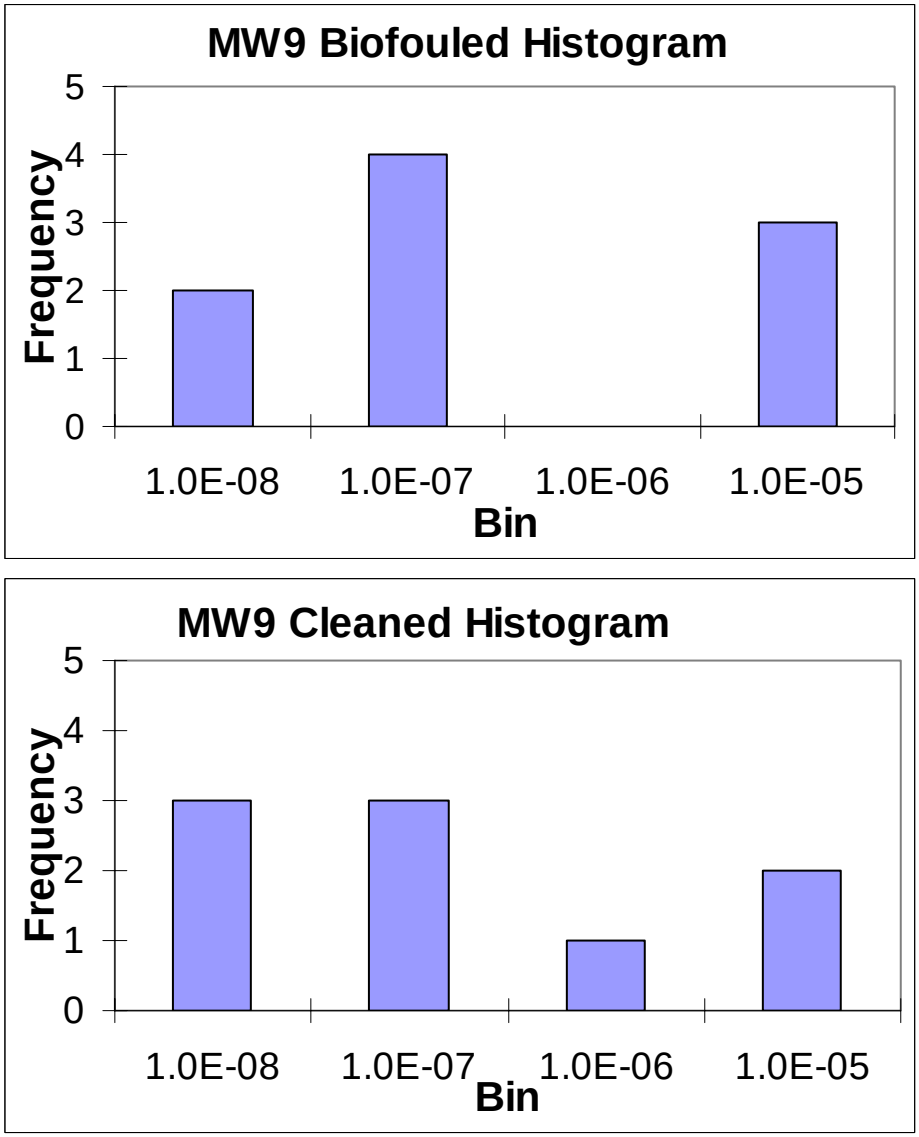

Figure H - 3: Histograms of the transmissivity data collected through hydraulic testing using packers.

Table H- 4: Geometric mean values of WWCH transmissivity in both states examined, and of the low transmissivity zones.

Biofouled				Cleaned		
Interval	T (m2/s)	T (m2/s)		Interval	T (m2/s)	T (m2/s)
1	1.2E-06	1.2E-06		1	2.1E-06	2.1E-06
2	5.2E-07	5.2E-07		2	1.2E-06	1.2E-06
3	4.1E-07	4.1E-07		3	4.8E-07	4.8E-07
4	3.1E-07	3.1E-07		4	7.0E-07	7.0E-07
5	6.5E-07	6.5E-07		5	1.4E-06	1.4E-06
6	2.1E-07	2.1E-07		6	7.1E-07	7.1E-07
7	6.3E-07	6.3E-07		7	1.4E-06	1.4E-06
8	5.2E-07	5.2E-07		8	1.6E-06	1.6E-06
9	2.1E-07	2.1E-07		9	1.2E-06	1.2E-06
10	1.0E-07	1.0E-07		10	2.3E-07	2.3E-07
11	2.1E-07	2.1E-07		11	1.2E-07	1.2E-07
12	2.1E-07	2.1E-07		12	2.3E-07	2.3E-07
13	1.0E-07	1.0E-07		13	9.4E-08	9.4E-08
14	6.3E-07	6.3E-07		14	1.9E-06	1.9E-06
15	7.4E-07	7.4E-07		15	1.4E-06	1.4E-06
16	2.1E-07	2.1E-07		16	1.5E-07	1.5E-07
17	3.6E-05			17	9.7E-05	
18	2.1E-07	2.1E-07		18	2.4E-07	2.4E-07
19	2.1E-07	2.1E-07		19	5.6E-06	5.6E-06
20	2.1E-07	2.1E-07		20	9.4E-07	9.4E-07
21	2.4E-05			21	5.9E-05	
22	4.1E-08	4.1E-08		22	7.3E-07	7.3E-07
23	4.9E-08	4.9E-08		23	1.5E-07	1.5E-07
				24	7.0E-07	7.0E-07
				25	1.2E-06	1.2E-06
				26	7.0E-08	7.0E-08
Geometric Mean	3.9E-07	2.6E-07		Geometric Mean	8.6E-07	5.9E-07
Arithmetic Mean	3.0E-06	3.2E-07		Arithmetic Mean	6.9E-06	1.0E-06
Harmonic Mean	1.9E-07	1.7E-07		Harmonic Mean	3.5E-07	3.2E-07

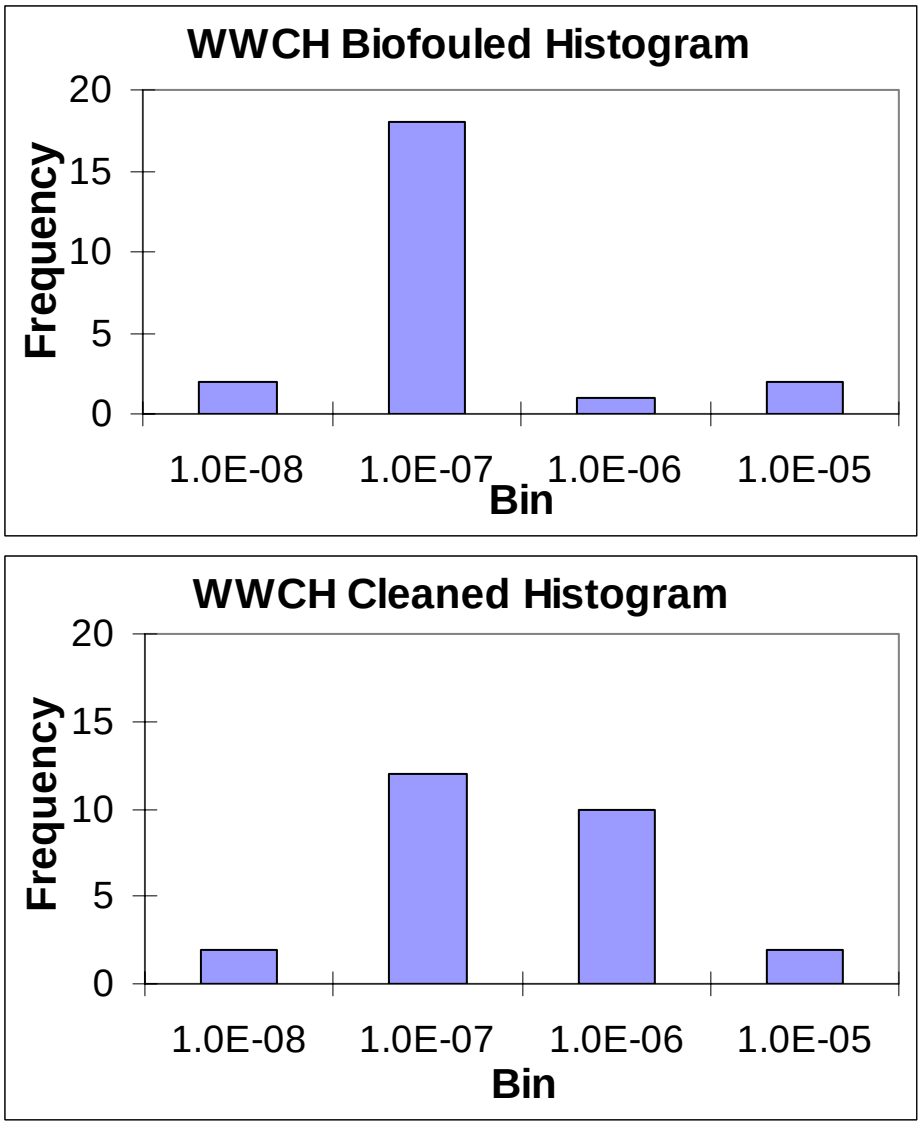

Figure H - 4: Histograms of the transmissivity data collected through hydraulic testing using packers.

Table H- 5: Geometric mean values of WWFS transmissivity in both states examined, and of the low transmissivity zones.

Biofouled				Cleaned		
Interval	T (m2/s)	T (m2/s)		Interval	T (m2/s)	T (m2/s)
1	2.4E-07	2.4E-07		1	6.0E-06	6.0E-06
2	2.1E-07	2.1E-07		2	4.6E-07	4.6E-07
3	2.1E-07	2.1E-07		3	9.5E-07	9.5E-07
4	2.1E-07	2.1E-07		4	2.4E-07	2.4E-07
5	2.1E-07	2.1E-07		5	1.9E-07	1.9E-07
6	2.1E-07	2.1E-07		6	2.3E-07	2.3E-07
7	2.1E-07	2.1E-07		7	2.1E-05	
8	5.8E-05			8	2.3E-07	2.3E-07
9	1.0E-07	1.0E-07		9	8.7E-06	8.7E-06
10	3.1E-06	3.1E-06		10	3.9E-06	3.9E-06
11	5.1E-07	5.1E-07		11	9.6E-07	9.6E-07
12	1.0E-07	1.0E-07		12	1.2E-06	1.2E-06
13	9.3E-08	9.3E-08		13	7.2E-07	7.2E-07
14	1.0E-07	1.0E-07		14	2.0E-06	2.0E-06
15	1.0E-07	1.0E-07		15	1.8E-07	1.8E-07
16	1.0E-07	1.0E-07		16	1.8E-07	1.8E-07
17	1.0E-07	1.0E-07		17	1.5E-07	1.5E-07
18	1.0E-07	1.0E-07		18	2.3E-07	2.3E-07
19	1.1E-07	1.1E-07		19	3.0E-07	3.0E-07
20	1.0E-07	1.0E-07		20	7.4E-07	7.4E-07
21	1.0E-07	1.0E-07		21	7.6E-07	7.6E-07
22	2.1E-07	2.1E-07		22	7.6E-07	7.6E-07
23	5.1E-08	5.1E-08		23	1.4E-06	1.4E-06
Geometric Mean	2.1E-07	1.6E-07		Geometric Mean	7.5E-07	6.5E-07
Arithmetic Mean	2.8E-06	2.9E-07		Arithmetic Mean	2.2E-06	1.4E-06
Harmonic Mean	1.4E-07	1.3E-07		Harmonic Mean	4.1E-07	3.9E-07

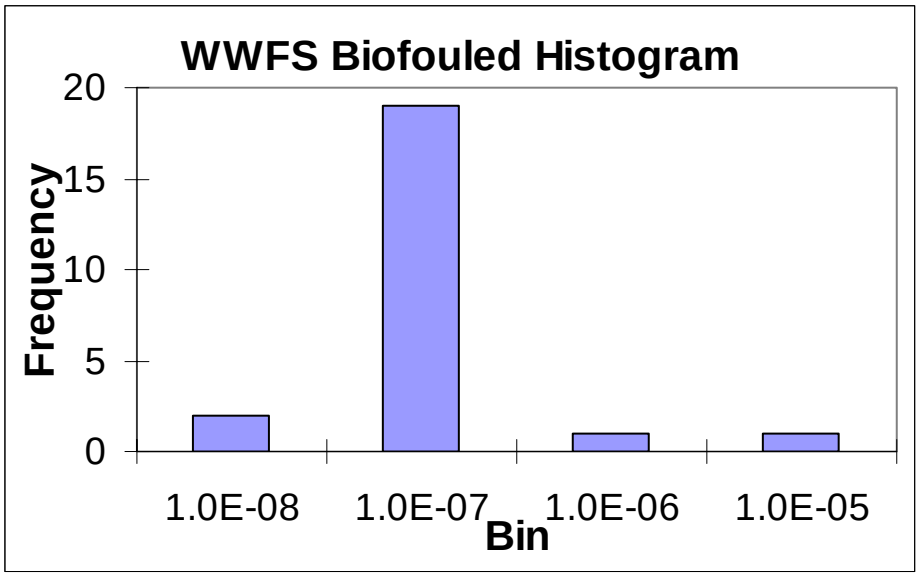

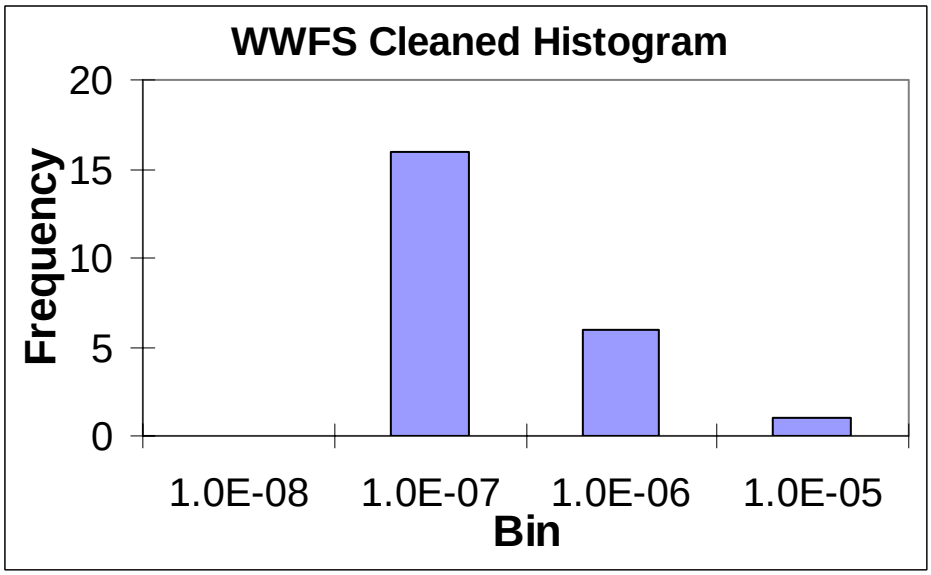

Figure H - 5: Histograms of the transmissivity data collected through hydraulic testing using packers.

Table H- 6: Geometric mean values of TW8 transmissivity in both states examined, and of the low transmissivity zones.

Drilled		Low T zones		Biofouled		Low T zones
Zone	T (m^2/s)	T (m^2/s)		Zone	T (m^2/s)	T (m^2/s)
1	1.6E-05			21	1.5E-05	
2	3.8E-06	3.8E-06		20	1.3E-05	
3	2.9E-07	2.9E-07		19	3.3E-06	3.3E-06
4	1.7E-03			18	6.4E-06	6.4E-06
5	2.0E-03			17	1.7E-03	
6	1.3E-03			16	3.9E-04	
7	1.1E-06	1.1E-06		15	4.8E-07	4.8E-07
8	7.3E-06	7.3E-06		14	4.8E-07	4.8E-07
9	2.9E-06	2.9E-06		13	2.3E-05	
10	3.7E-03			12	2.0E-03	
11	1.2E-04			11	6.9E-05	
12	1.1E-06	1.1E-06		10	6.1E-06	6.1E-06
14	1.8E-06	1.8E-06		9	4.8E-07	4.8E-07
15	3.7E-07	3.7E-07		8	7.2E-07	7.2E-07
16	1.3E-06	1.3E-06		7	7.4E-07	7.4E-07
17	5.3E-06	5.3E-06		6	9.6E-07	9.6E-07
18	1.1E-06	1.1E-06		5	2.4E-07	2.4E-07
19	7.3E-07	7.3E-07		4	2.1E-07	2.1E-07
20	5.4E-04			3	4.0E-04	
21	5.3E-06	5.3E-06		2	1.9E-06	1.9E-06
22	1.1E-06	1.1E-06		1	1.9E-06	1.9E-06
Geometric Mean	1.1E-05	1.6E-06		Geometric Mean	6.7E-06	1.0E-06
Arithmetic Mean	4.5E-04	2.4E-06		Arithmetic Mean	2.2E-04	1.8E-06
Harmonic Mean	1.5E-06	1.0E-06		Harmonic Mean	1.0E-06	6.3E-07

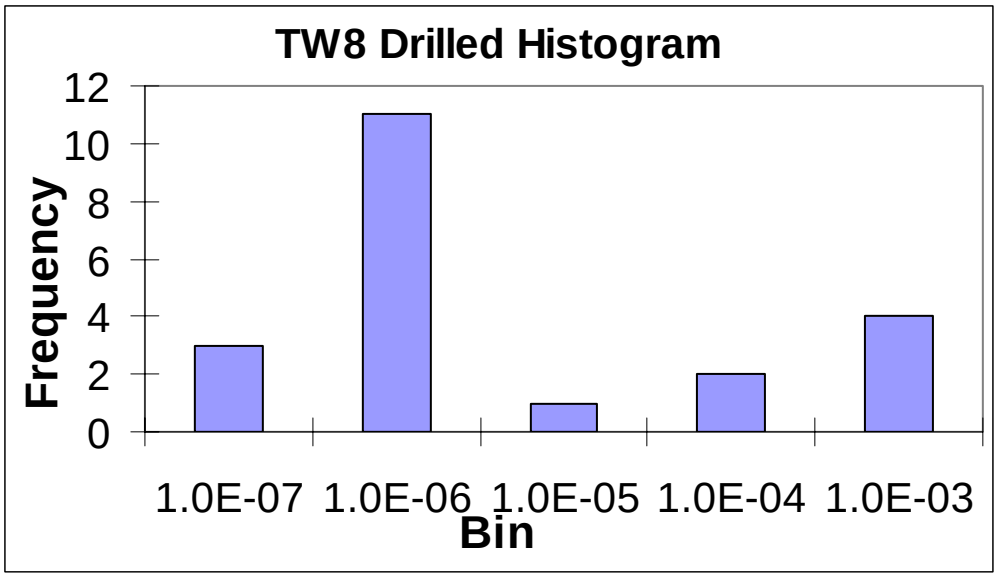

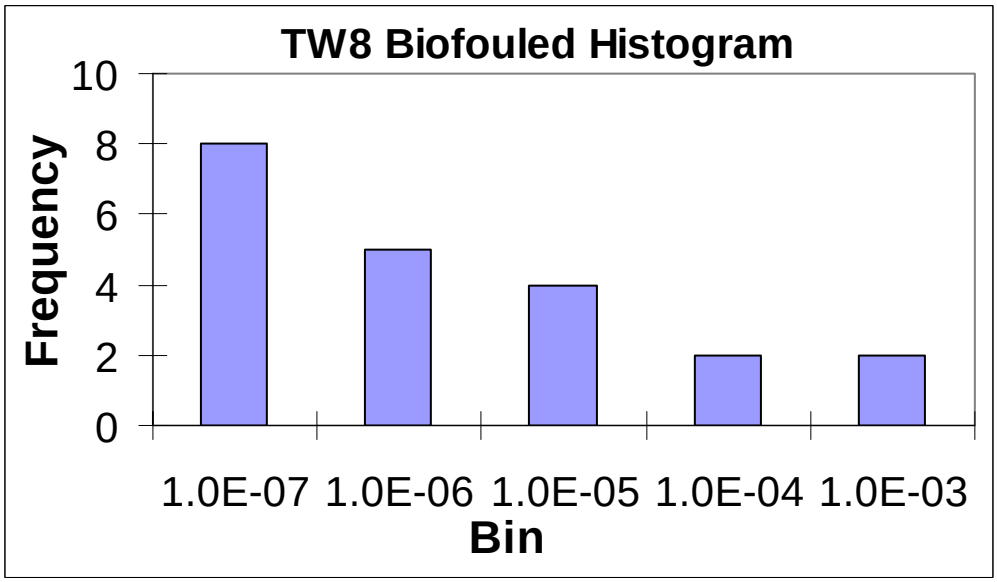

Figure H - 6: Histograms of the transmissivity data collected through hydraulic testing using packers.

Appendix I

Results from the biofilm growth laboratory experiment. Contains glucose concentrations determined from the modified Dubois et al. (1956) method.

During three rounds of nutrient addition in the laboratory, a combination of nutrients was determined to encourage biofilm growth in TW8 sample water. Visual identification of bacteria present indicated that aerobic slime forming bacteria, mixed aerobic and anaerobic iron related bacteria and sulfate reducing bacteria were common in the wells at all the Perth field site. Since iron related bacteria can produce copious amount of slime in addition to the slime forming bacteria the iron related bacteria were targeted as the bacterial community to grow. The resulting glucose concentration, which represents the presence of a biofilm, for the first round of nutrient addition to groundwater from neighboring well TW7 is presented in Figure I- 1. With a glucose concentration of approximately 98 µg/mL the sample with Difco beef peptone nutrient was the highest whereas the control sample from the shallow section of the well was the lowest, with a glucose concentration of 0.61 µg/mL.

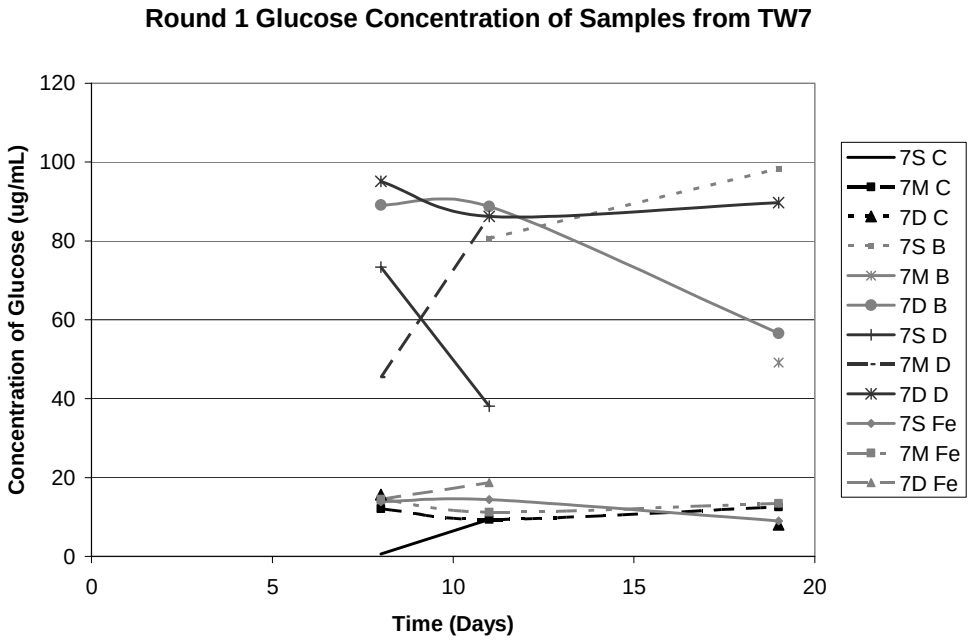

Figure I- 1: Concentration of glucose found on glass slides at the bottom of each TW7 groundwater sample-nutrient concoction. The control samples are marked as C, samples with iron filings added as Fe, Samples with Dextrose as D and samples with beef peptone as B.

Based on these results, sample water from TW8 was mixed with two nutrients and the addition of iron. The highest amount of glucose detected was from a combination of the Difco beef peptone nutrient and iron filings at approximately 83 µg/mL after four days. The lowest glucose concentration was the control sample, which contained only groundwater, at 18 µg/mL. A plot of the glucose concentrations for these samples is shown in Figure I- 2.

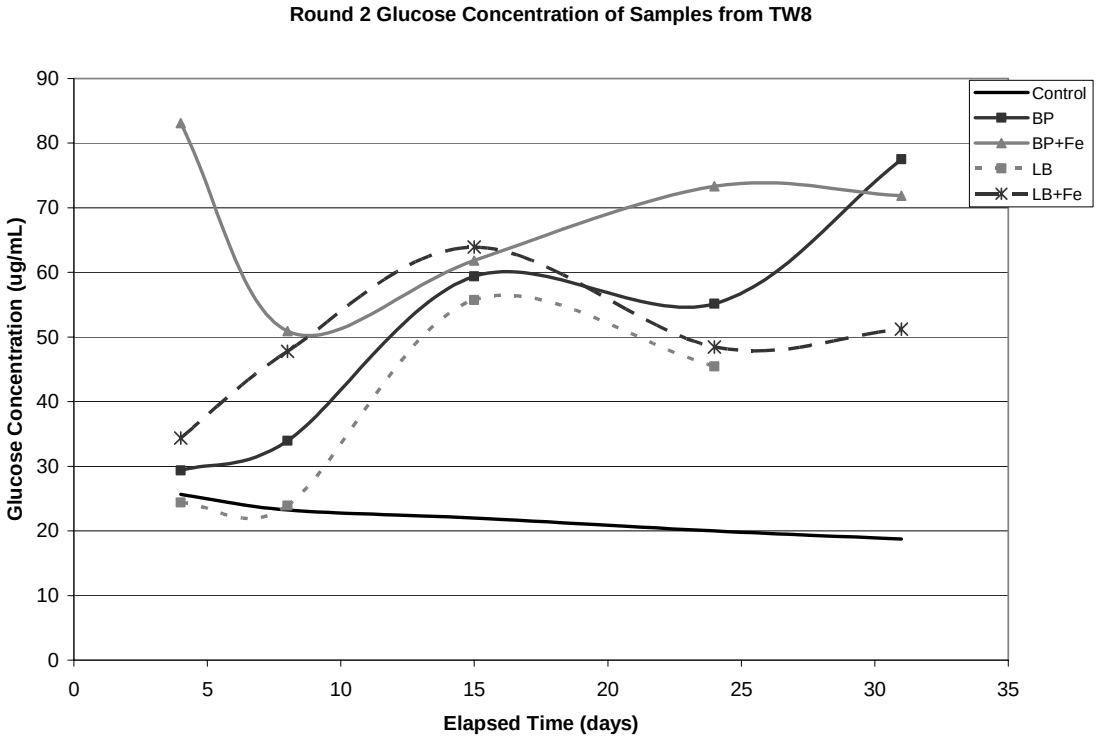

Figure I- 2: Concentration of glucose found on glass slides removed from the bottom of each TW8 groundwater sample with Difco beef peptone and LB broth and iron filings. The samples containing beef peptone are marked as BP, those with LB broth as LB and the samples with iron filings as Fe.

With steel wool replacing the iron filings, a third round of glucose concentrations were collected. Using the nutrient with the highest glucose concentrations to that point (Difco beef peptone) and three grades of commercially-bought steel wool, glucose concentrations of 206 µg/mL to 5.5 µg/mL were observed. A plot of the glucose

concentrations with respect to the number of elapsed days is shown in Figure I- 3**Error! Reference source not found.**.

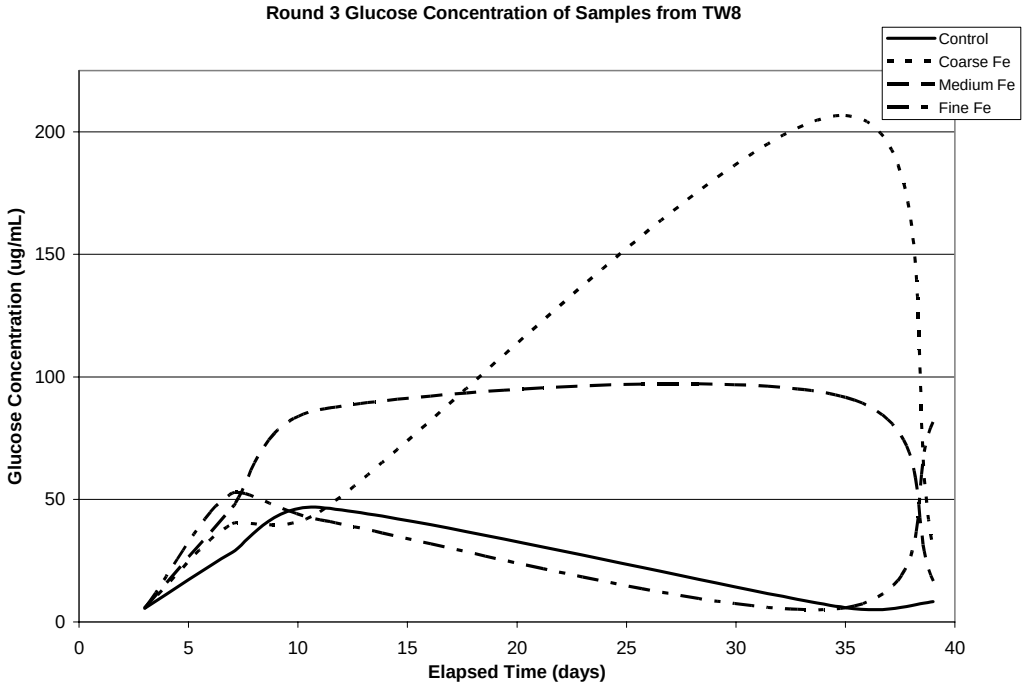

Figure I- 3: Concentration of glucose found on glass slides removed from the bottom of each TW8 groundwater sample with beef peptone nutrient and steel wool bundles.

Addition of floating steel wool increased the amount of iron available to the bacteria and increased the production of biofilm, as demonstrated by the largest glucose concentrations of more than 200µg/mL in the lab experiments. As shown in Figure I- 2 and Figure I- 3 the glucose concentrations increased from the first sampling day. This increase in glucose concentrations indicates an increase in biofilm growth on the glass slides. The glucose concentrations decrease at the end of the third round (Figure I- 3**Error! Reference source not found.**) is due to debris falling off the floating steel wool mass and coating the slides.

Appendix J

Pumping test data, curve matching data using the Theis (1935) solution and the Moench (1997) solution for well TW8 from the Perth field site.

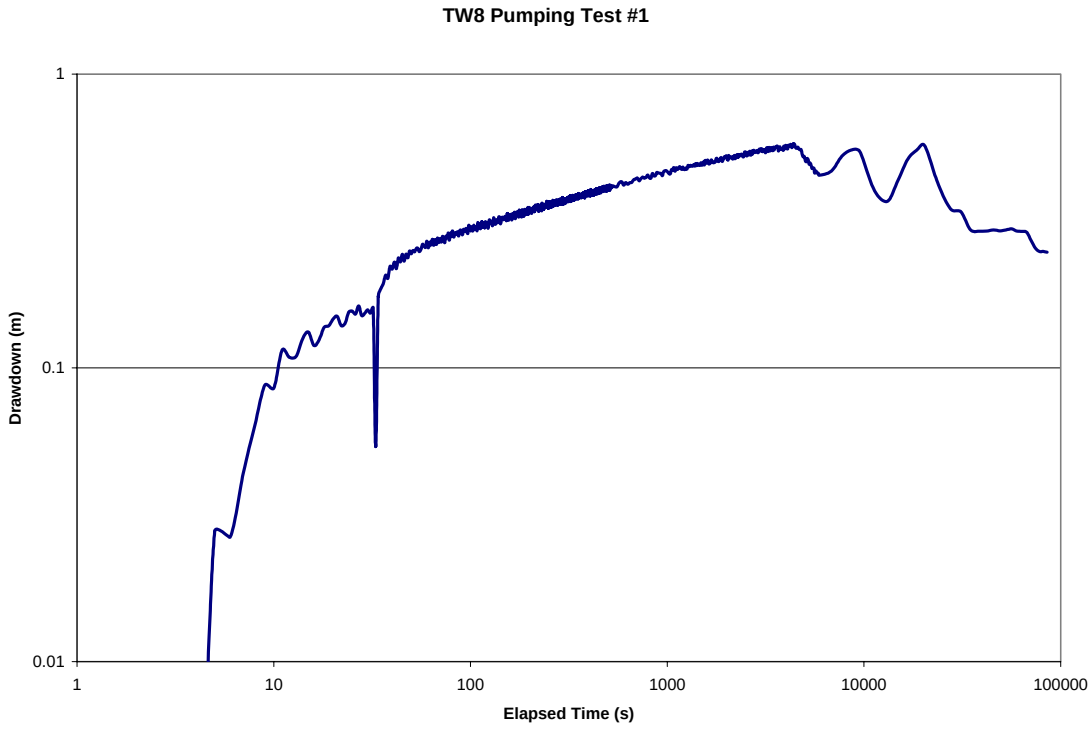

Figure J- 1: Drawdown- time curve for pumping test #1 at the Perth field site.

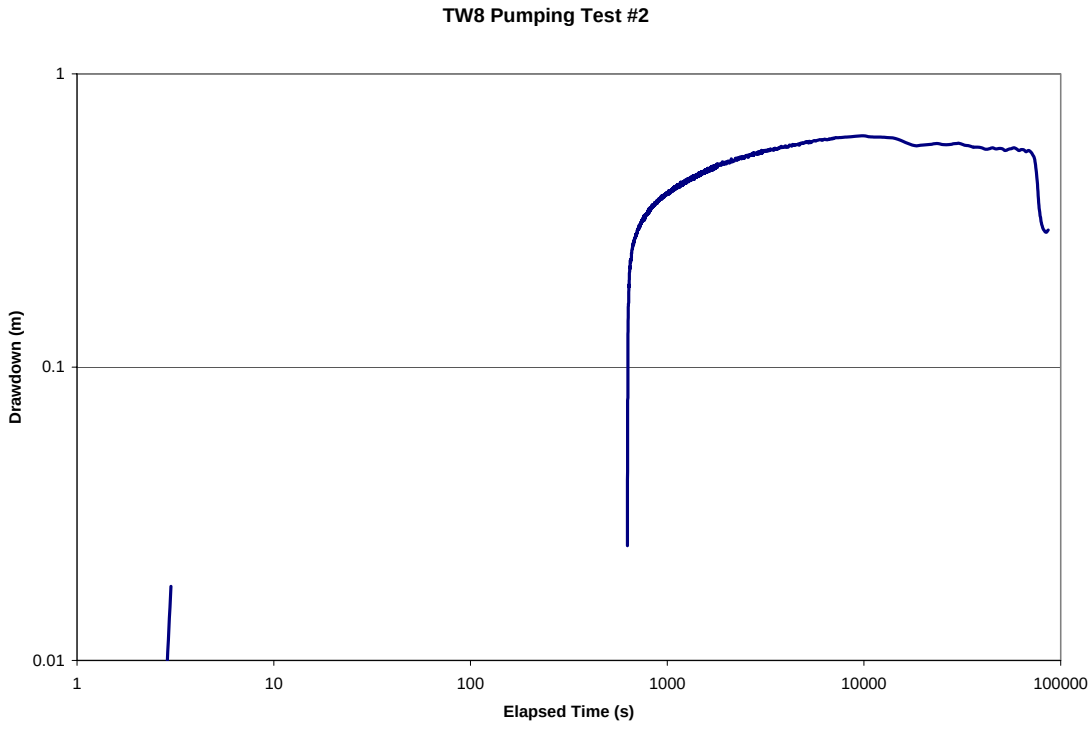

Figure J- 2: Drawdown- time curve for pumping test # 2 in TW8 at the Perth Field site.

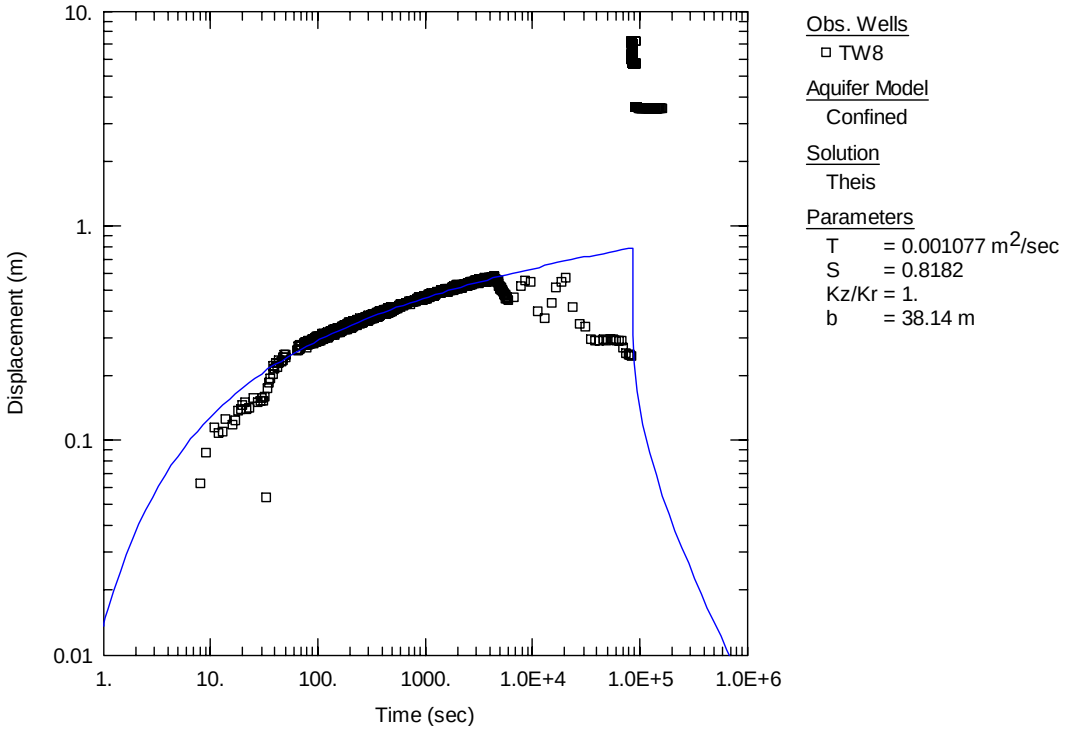

Figure J- 3: Theis (1935) type curve matching to the TW8 pumping test #1 data. Theoretical solutions are represented by thin lines and the collected data by data points.

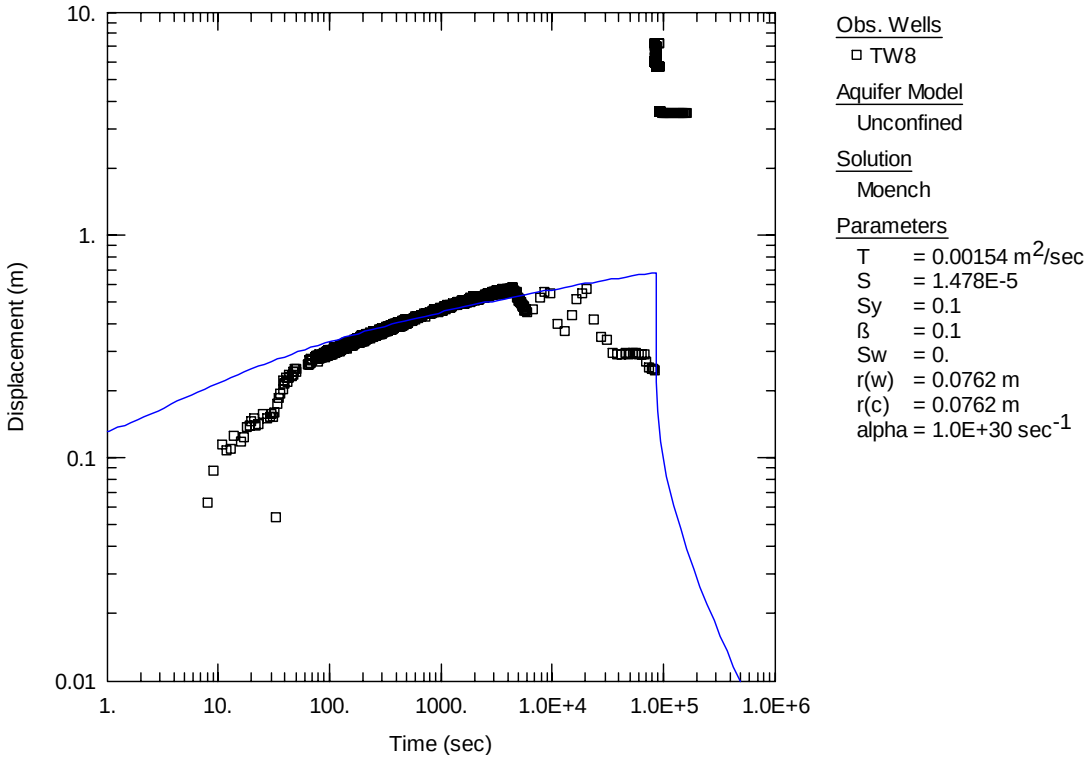

Figure J- 4: Moench (1997) curve matching to the TW8 pumping Test #1 data. Theoretical solutions are represented by thin lines and the collected data by data points.

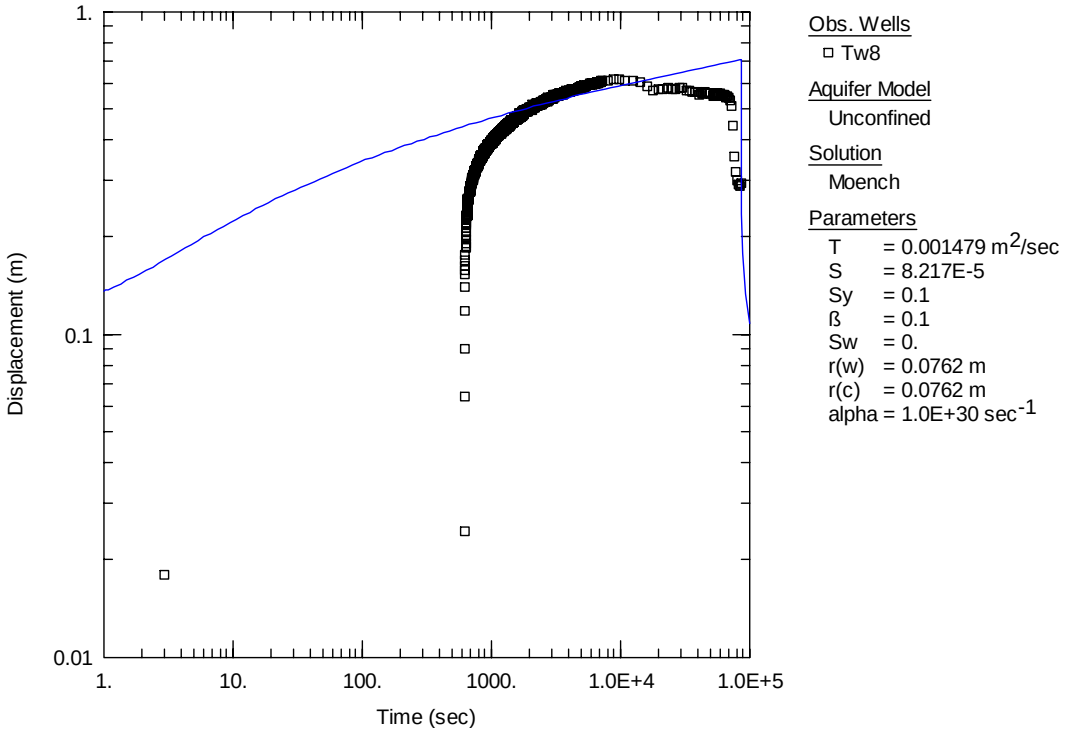

Figure J- 5: Moench (1997) curve matching to the TW8 pumping test #2 data. Theoretical solutions are represented by thin lines and the collected data by data points.